EPFL

Thèse n° 8393

Enhancing T-cell response in cancer immunotherapy using nanoparticles

Présentée le 9 juillet 2021

Faculté des sciences et techniques de l'ingénieur
Laboratoire des polymères
Programme doctoral en science et génie des matériaux

pour l'obtention du grade de Docteur ès Sciences

par

Cristiana BERTI

Acceptée sur proposition du jury

Prof. M. Ceriotti, président du jury
Prof. H.-A. Klok, directeur de thèse
Prof. A. Fink, rapporteuse
Dr A. Harari, rapporteur
Prof. F. Stellacci, rapporteur

École
polytechnique
fédérale
de Lausanne

2021

The work described in this Thesis has been performed at the École Polytechnique Fédérale de Lausanne from November 2016 until June 2021 under the supervision of Prof. Harm-Anton Klok.

This work was financially supported by the ISREC Foundation, made possible by a donation from the Biltema Foundation.

Acknowledgments

This work would not have been possible without the continuous supervision and support of my thesis director, Prof. Harm-Anton Klok, who gave me the possibility to carry out this work and guided me all along my PhD. A huge thank you for making me a better scientist.

Special thanks goes to my thesis jury members, Prof. Alke Fink, Dr. Alexandre Harari, Prof. Francesco Stellacci and to the president of the jury, Prof. Michele Ceriotti for their time and the discussions they opened. I would particularly like to thank our collaborator Prof. Kandalaft for providing a different perspective on my project.

All my gratitude goes to the whole Laboratory of Polymers, starting with Cindy and Susanne for always being there with a smile and a solution. Thank you Eva for the good atmosphere that you can always bring to the lab and in our LP parties. A special *merci* to Philippe, not only for your practical help but also for the chats, more and less serious, that we had during my years in the lab. It is so precious to work with someone who is always so positive and cheerful. I will always remember and miss our moments together! A huge *merci* also to Jacques, our *factotum* and most of all good friend. Thank you for always being there to help me and everyone you know. You really deserve the best! A great thank you to the growing female part of the lab, starting from my office mate Tanja. I am so glad we ended up sharing the lab and the office, I always enjoyed talking to you and you have been so helpful and understanding in difficult moments. I don't know what I would have done without you! *Merci* to Lisa, our orders master, *chef de patisserie* and most importantly a huge help and support for most of my PhD. Alice, *grazie mille* for your contagious good mood and smile, the chats and gossiping in the office and during the journeys to Italy. Thank you of course also for your precious help with my project and your scientific advice! Thank you so much Kuljeet for your suggestions and your help with the revision of the Thesis Introduction. Thank you to all the old and new girls in the lab: Claudia, Ioana, Sophia, Maria, Sabrina, Anna-Lena, Frieda and Zhao. I am so glad that you were part of the group, it really changes the atmosphere and I am sure it will positively impact the group in the years to come. Thank you to Corey, a.k.a. our Master of Ceremonies, for always being there to help and to give precious suggestions for our projects. Thank you to all the other LP members that shared lunches, meetings, barbecues, coffee breaks and evenings: Maxime, Alex, Justin, Julian, Markus, Michael, Mark, Piotr, Jian, Xiaobin, Fei, Ghezae and Yann. Although

we did not work directly together you always helped to create a great environment in the lab and it is a pleasure seeing little by little everyone following their own path and career.

Thank you also to my “adoptive” lab from Agora, starting from Michele, who followed me step-by-step from the beginning and taught me a lot. Thank you for your infinite patience and continuous help! Rita, bella mia, you have become one of my closest friends and I hope I can keep you in my life for the next years. You are genuinely an amazing person and scientist and I wish all the best in your personal and working life. I look forward to try new brunch spots with you! Thank you Hajer for your kindness and especially for keeping me company during late evening experiments, making them much funnier! Thank you to Cheryl, Anne-Laure and Chakri for always being so nice and helpful with all the *in vivo* experiments.

Thank you to the EPFL friends that I have met during these years. Alice, *grazie mille* for all the hikes and coffee breaks. Good luck for finishing successfully your PhD, it has been great having you as a support and in the meantime following your personal growth. *Grazie* Simone for sharing the struggles of life at the end of PhD! Thank you to my first supervisor, Ale, and to all the people that helped me during these years in Lausanne: Giuseppe and Marcela, Lisa and Yann, Simon, Vanessa and Kaycie. A great thank you to my fellow yogini Fausto, Ceci, Julien, William, Daniela, Tarek and Jackie for the nice time on and off the mat!

A huge thank you to my forever friends: Nani, Betta, Melissa, Elena, Tommy, Giacomo, Massimo, Filippo and Laura, Mattia, Giulia, Poppi, Simone e Davide. A great thank you to my continuous support, Virginia. Thank you for the vocal messages, the eternal Skype calls and for always being there. You are an amazing person and researcher and I know we will be always there for each other! Also a special thank you to Nicola and all his friends and family for brightening up my last year of PhD. I feel so lucky and grateful to have you in my life right now.

Finally, I would not be here without the support of my close family who have always been there for me. This work is all for you, Mom, Papi, Matte, Nonni and all the big family. Thank you for putting up with me during this last 29 years!

Table of contents

Summary

Cancer vaccines have been studied for the last two decades as a promising therapy in oncology for their high specificity and reduced side effects compared to common chemotherapy and radiotherapy. In clinical setting, the only approved cancer vaccine is dendritic cell-based, a complex and cumbersome procedure where patients' dendritic cells (DCs) are extracted and *ex vivo* pulsed with the antigen before reinfusion in the patient.

An easier solution would be to encapsulate tumor antigens in nanoparticles that could be directly injected in the patient. Cancer vaccines based on nanoparticulate systems would offer a biocompatible strategy for efficient protection, targeted delivery and controlled release of tumor antigens to DCs. So far, however, limited results have been obtained when translating nanoparticles in clinical setting. The limiting factors are mainly (i) the heterogeneity of tumors and patients and (ii) the difficulty in predicting the response of human DCs due to the application of nanoparticles for cancer vaccination on human immortalized cell lines or murine primary cells.

The overall aim of this Thesis is to contribute to make progress towards overcoming the limitations mentioned above. First, to help address the challenges with regards to the heterogeneity of human tumors, this Thesis explores whole tumor lysate as the antigen source. The use of whole tumor lysate-based vaccines has the advantage that it allows to challenge the immune system with a broad spectrum of tumor-related epitopes. The tumor lysate used in this Thesis is referred to as oxidized tumor lysate and has been obtained from cancer cells that have been additionally treated with hypochlorous acid, which has been shown to further improve immunogenicity. To help bring tumor-lysate based cancer vaccines closer to the clinic, this Thesis has explored the potential of nanoparticles to transport and deliver tumor lysate antigen and investigated the efficacy of these nanoformulations *in vitro* and *in vivo*, also using human donor derived dendritic cells and T lymphocytes. This Thesis consists of three parts:

Chapter 1 provides an overview of the current strategies in cancer immunotherapy with a focus on cancer vaccines. Nanoparticles and their properties will be discussed in depth, considering their interaction with the

immune system and the latest research strategies for enhancing their uptake by DCs.

Chapter 2 describes the development and testing on human primary cells of poly(ethylene glycol)-b-poly(lactic-co-glycolic) (PEG-PLGA) block copolymer nanoparticles loaded with oxidized tumor lysate. Poly(lactic-co-glycolic) acid (PLGA) is one of the most widely studied and used polymers for the generation of nanoparticle-based drug formulations and has also been granted approval by authorities for use in clinical practice. This work will focus on studying antigen uptake and downstream immune response of human donor derived dendritic cells that have been presented with either free oxidized tumor lysate or the corresponding PEG-PLGA based nanoparticle formulation. This Chapter will investigate by flow cytometry the autologous T cell populations generated and their specific apoptotic activity on cancer cells. Additionally, mice models of melanoma B16F10 have been used to test the effect of oxidized tumor lysate-loaded nanoparticles on tumor growth and survival in a therapeutic vaccination setting.

Chapter 3 explores a new nanoparticle platform for the delivery of protein antigens. Rather than encapsulating the antigen in a synthetic polymer particle, **Chapter 3** explores nanoparticles that are obtained by self-crosslinking of protein-based antigens. This has the great advantage of essentially quantitative protein encapsulation and allows to generate reduction sensitive protein nanogels that undergo accelerated intracellular disassembly and antigen release. **Chapter 3** first explores these nanogels using ovalbumin as a proof-of-concept and then extends this work to oxidized tumor lysate. Both human and murine primary cells are employed for toxicity and uptake experiments by flow cytometry and confocal microscopy. This work shows that antigen uptake by human dendritic cells is enhanced when oxidized tumor lysate based nanogels are employed as compared to free oxidized tumor lysate.

Keywords: cancer vaccines, nanoparticles, oxidized tumor lysate, antigen uptake, PEG-PLGA, delivery of protein antigens, protein nanogels, antigen release.

Riassunto

I vaccini contro il cancro sono stati studiati negli ultimi due decenni come una promettente terapia in oncologia per la loro specificità e per i ridotti effetti collaterali rispetto al comune utilizzo di chemioterapia e radioterapia. In ambito clinico, l'unico vaccino contro il cancro approvato è basato sulle cellule dendritiche, seguendo una procedura complessa e onerosa dove le cellule dendritiche dei pazienti sono estratte *ex-vivo* e stimolate con l'antigene prima di essere reinfuse nel paziente.

Una soluzione più semplice consiste nell'incapsulare gli antigeni tumorali in nanoparticelle da iniettare direttamente nel paziente. I vaccini per il cancro basati su sistemi nanoparticolati offrono una strategia biocompatibile per una protezione efficiente, una somministrazione specifica e unl rilascio controllato di antigeni tumorali alle cellule dendritiche. Fino ad ora, tuttavia, l'utilizzo delle nanoparticelle in ambito clinico ha portato a risultati modesti. I fattori limitanti sono principalmente (i) l'eterogeneità dei tumori e dei pazienti e (ii) la difficoltà nel predire le risposte delle cellule dendritiche umane, dato che la sperimentazione di nanoparticelle nei vaccini per il cancro si basa perlopiù su linee cellulari umane immortalizzate o su cellule murine primarie.

Lo scopo finale di questa Tesi è di contribuire al superamento dei sopracitati fattori limitanti. In primo luogo, per affrontare il problema dell'eterogeneità dei tumori umani, questa Tesi impiega il lisato tumorale come fonte di antigeni. L'utilizzo di vaccini basati sul lisato tumorale presenta il vantaggio di stimolare il sistema immunitario con un'ampia gamma di epitopi tumorali. Il lisato tumorale studiato in questa Tesi è un lisato tumorale ossidato maggiormente immunogenico, ottenuto da cellule tumorali trattate con acido ipocloroso. Per promuovere l'utilizzo dei vaccini contro il cancro basati sul lisato tumorale all'applicazione clinica, questa Tesi ha investigato il potenziale delle nanoparticelle per trasportare e somministrare il lisato tumorale e l'efficacia di queste nanoparticelle *in vitro* e *in vivo*, impiegando inoltre cellule dendritiche e linfociti T ottenuti da donatori umani. Questa Tesi è composta di tre parti:

Il **Capitolo 1** offre un quadro generale delle strategie attuali nell'immunoterapia oncologica, focalizzandosi sui vaccini per il cancro. Sono

discusse in dettaglio le nanoparticelle e le loro proprietà, considerando le loro interazioni con il sistema immunitario e le strategie messe in atto nella ricerca per aumentare la loro assimilazione nelle cellule dendritiche.

Il **Capitolo 2** descrive lo sviluppo e la sperimentazione su cellule umane primarie di nanoparticelle basate su un copolimero a blocchi, composto da glicole polietilenico e acido poli(lattico-co-glicolico) (PEG-PLGA), per somministrare il lisato tumorale ossidato. L'acido poli(lattico-co-glicolico) (PLGA) è un polimero tra i più studiati ed usati per generare formulazioni di medicinali basati su nanoparticelle e ha inoltre ottenuto l'approvazione delle agenzie del farmaco per l'utilizzo nella clinica. L'obiettivo di questo progetto è studiare la cattura dell'antigene nelle cellule dendrtitiche ottenute da donatori umani e la conseguente risposta immunitaria. Queste cellule dendritiche sono state stimolate con il lisato tumorale ossidato solubile o la corrispondente formulazione in nanoparticelle di PEG-PLGA. In questo Capitolo viene utilizzata la citometria di flusso per studiare le popolazioni di cellule T autologhe generate e la loro specifica attività apoptotica sulle cellule tumorali. Inoltre, modelli murini di melanoma (B16F10) sono stati usati per testare l'effetto delle nanoparticelle con lisato tumorale ossidato sulla crescita tumorale e la sopravvivenza degli animali in seguito a vaccinazione terapeutica.

Il Capitolo 3 esplora una nuova tipologia di nanoparticelle per la somministrazione di proteine antigeniche. Anziché incapsulare l'antigene in una particella di polimeri sintetici, il **Capitolo 3** esplora l'utilizzo di nanoparticelle ottenute dal cross-linking spontaneo di proteine antigeniche. Questa strategia ha il vantaggio di incapsulare in modo quantitativo le proteine e permette di generare nanogels proteici reattivi, che in ambienti riduttivisi degradano e rilasciano l'antigene nello spazio intracellulare. Il **Capitolo 3** inizialmente esplora questi nanogels impiegando l'ovalbumina per uno studio preliminare e in seguito estende questo lavoro al lisato tumorale ossidato. Linee cellulari primarie, sia umane che murine, sono state studiate per valutare la citotossicità e la cattura dell'antigene con citometria di flusso e microscopia confocale. Questo progetto dimostra che la cattura dell'antigene da parte di cellule dendritiche umane migliora quando vengono somministrati nanogels formati da lisato tumorale ossidato, rispetto alla soministrazione di lisato tumorale ossidato solubile.

Parole chiave: vaccini per il cancro, nanoparticelle, lisato tumorale ossidato, cattura dell'antigene, PEG-PLGA, somministrazione di antigeni proteici, nanogels proteici, rilascio dell'antigene

1. Nanoparticles Formulations for Improving Efficiency of Cancer Vaccines

1.1. Introduction

Cancer has been defined as a dynamic disease, showing variations between different patients affected by the same type of tumor (intertumoral heterogeneity) or within the tumor of a single patient (intratumoral heterogeneity), where additional spatial and temporal differences can also develop. This variability and evolution of cancer translates into failure of classical anticancer approaches such as surgery, chemotherapy, radiotherapy and targeted molecules.[1] In particular, the last ones can be the source of a selective pressure that induces *de novo* cancer resistance.[2] There is therefore a greater need for a different and personalized approach that could respond to the changing faces of cancer. For this reason, recent years have seen the advance of immunotherapy, which aims at driving the immune system against cancer in a specific manner, inducing a memory response.

1.2. Cancer immunotherapy

Cancer immunotherapy is a type of cancer treatment that (re)awakens the patients' immune system to eliminate cancer cells. Wilhelm K.D. Busch and Friedrich Fehleisen initially suggested the association between immune system and cancer progression in the Nineteenth Century.[3] Based on their studies, William Coley demonstrated that patients with melanoma had better prognosis after infection with heat-inactivated *Streptococcus pyogenes* and *Serratia marcescens*.[4] Similarly, in 1929, a reduced number of cases of cancer was noticed in tuberculosis patients.[5] Thanks to mice models, in 1950s Lloyd Old could demonstrate that mice infected with BCG (Bacillus Calmette-Guerin) had better resistance to tumor challenge, demonstrating a relationship

between immune response to infection and cancer.[5] It was later discovered that the immune system, both innate and adaptive, plays a role in tumor recognition and elimination, followed by a phase of equilibrium that may evolve in two directions: either cancer eradication or eventually escape of cancer cells from immune surveillance and further tumor growth.[6] The recent recognition of the importance of this interaction between immune cells and cancer added two additional hallmarks of cancer cells to the six already established by the seminal study of Weinberg and Hanahan in 2000.[7] First, the ability to alter cancer cell metabolism to promote neoplastic proliferation, and second, the evolution of mechanisms of resistance to the fight of the immune system against cancer.[8]

Among the cells of the immune system, Dendritic Cells (DCs) were identified as professional Antigen Presenting Cells (APCs) due to their ability to capture, internalize and process extracellular elements. In their role of phagocytosis of cells and debris in the body, DCs are able to uptake apoptotic cancer cells and present their components (antigens) on their cell surface, loaded onto major histocompatibility complexes (MHC) I or II. Following antigen presentation, DCs can migrate to secondary lymphoid organs and activate antigen-specific T cells through the direct interaction of MHC complexes with clone-specific T-cell receptors (TCRs), together with a series of co-stimulatory surface signals (CD80, CD86, CD40, ICOSL) and secreted pro-inflammatory cytokines (IL-12, IL-15, IL-6, TNF-α), which will shape the type of T cell response.[9,10] After this combination of stimuli, the selected $CD8^+$ cytotoxic T cells with the tumor specific TCRs will undergo clonal expansion under stimulation by IL-2 and IFN-γ, recognize the cancer cells and kill them, mainly by granzyme-perforin mediated apoptosis.[11,12] This cancer immunity cycle is described **Figure 1**. In contrast, surface molecules can inhibit the activity of T cells: CTLA-4, which binds receptor B7.1/2 on DCs, and PD-1, which binds PD-1L on DCs and cancer cells. [13,14,15]

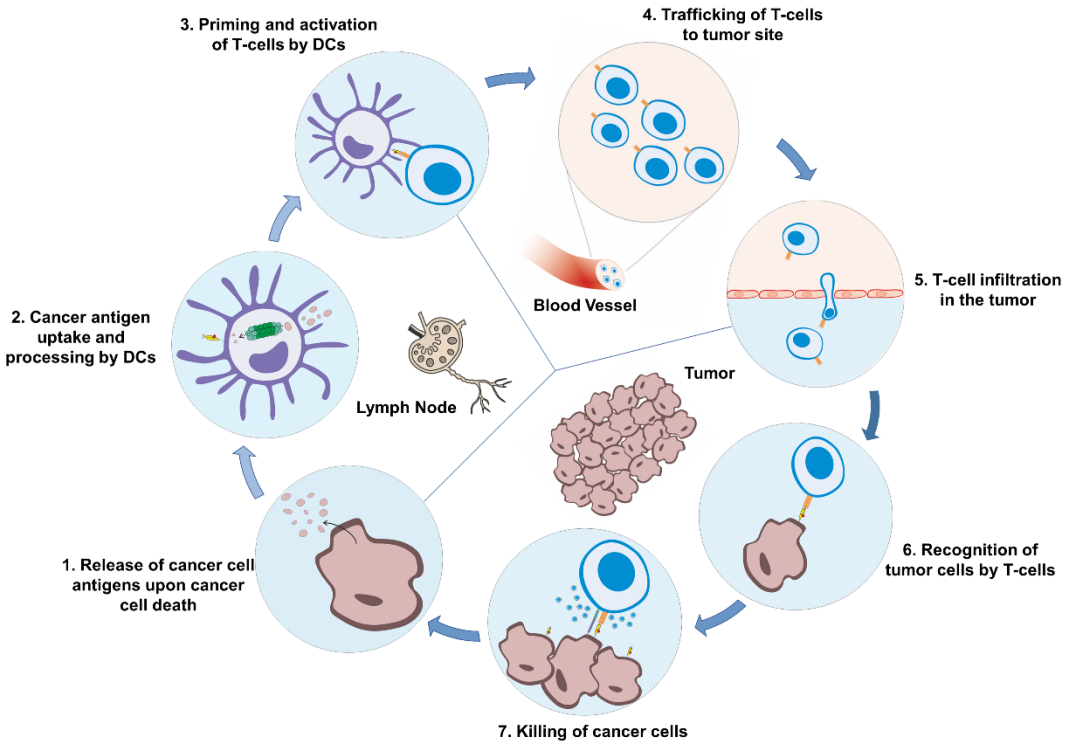

Figure 1. Schematic overview of the cancer immunity cycle described in seven steps. Adapted from [16].

The interaction between cancer and the immune system is well studied for both therapy and prognosis and is described according to the level of immune cell infiltration in the tumor. Immune desert or "cold" tumors are the ones with worse prognosis and response to therapies, where there is no T cell priming due to lack of antigen presentation or tolerance. Immune-excluded tumors present immune cells, but only in the tumor periphery or stroma, and therefore have limited response to immunotherapy. Finally, "hot" tumors are the ones where immune cells can infiltrate and are characterized by the presence of pro-inflammatory cytokines. It has been shown for example that infiltration of $CD3^+$ and effector memory $CD3^+CD8^+$ T cell in the tumor are often a predictor of positive prognosis.[17] The aim of cancer immunotherapy is to turn cold tumors into hot ones; among the strategies tested in pre-clinical and clinical settings, the most important are immunomodulatory drugs, adoptive cell therapy (ACT) and cancer vaccines.

1.2.1. Immunomodulatory drugs

The main regulators of T cells activation are cytokines and immune checkpoint blockade inhibitors (ICBIs). Acting on these molecules could therefore enhance T cell proliferation and activation. Amongst cytokines, interferon alpha (IFN-α) and IL-2 are

the only ones clinically approved as a monotherapy, although they need high doses to induce a proper anticancer response, thereby increasing their systemic side effects. While IFN-α exerts a direct anti-angiogenic and anti-cancer effect, IL-2 is mainly secreted by $CD4^+$ helper T cells (paracrine production) and to some extent by $CD8^+$ T cells (autocrine production), sustaining $CD8^+$ T cells expansion, contraction, and memory generation.[18] However, IL-2 in therapy is limited by its short half-life and systemic side-effects, such as capillary leakage in a sepsis-like syndrome which can lead to multiorgan failure.[19,20] To improve the circulation half-life and reduce their toxicity, both cytokines have been modified with different molecules (polyethylene glycol, apolipoprotein A-I , Fc or target-specific domain of immunoglobulins) or engineered to reduce their affinity to the receptor.[21]

ICBIs are the most advanced strategies that target the immune system. In cancer therapy, ICBIs have reshaped the treatment of certain type of malignancies such as metastatic melanoma, renal cell cancer, colorectal cancer and non-small-lung cancer.[22,23] However, they are limited in efficacy to “hot” tumors, where there is an infiltration of immune cells in the tumor. Additionally, due to their broad spectrum effect on T cell functionality, ICBIs can induce autoimmune and inflammatory side effects, probably caused by the activation of T cells also in normal tissues and the production of pro-inflammatory cytokines.[20,24] To avoid these side effects and select patients that could effectively responds to ICIBs, there are predictive -omic biomarkers, but these require time and cost expensive tools.[25] For these reasons, there is still the need for novel immunotherapies that activate specific antitumor T-cells and that generate a long-lasting memory against cancer, such as Adoptive Cell Therapies and Cancer Vaccines.[26]

1.2.2. Adoptive Cell Therapy (ACT)

Cell-therapies are based on autologous strategies to isolate and expand tumor-specific T cells. Endogenous T cell therapies (ETC) sort and expand *ex vivo* antigen-reactive T cells from peripheral blood. The main advantage of this strategy is that the T cell selected can each be adapted to patient’s specific antigens or neoantigens and, being autologous, poses little safety concerns. However, patients need pre-conditioning through lymphodepletion and IL-2 stimulation, both bringing various toxicities. Moreover, the technique is limited by various *in vitro* steps to identify the most promising epitope, then expand *ex vivo* the candidate T cells and reinfuse them in the

patient. The efficacy of the procedure in terms of number of cells recovered and their activity, once reinfused, varies highly between patients. All these steps require cost and time expensive resources and processes that limit ETC therapies.[27] Selecting T cells that infiltrate the tumor would avoid the sorting and selection of T cells from peripheral blood, exploiting natural selection in the tumor. These cells are called Tumor Infiltrating Lymphocytes (TILs) and, however promising, they are limited by the toxicity of therapies for patient pre-conditioning, the variable yield and activity of TILs following *ex vivo* manipulation, the risk of developing tolerogenicity, the complexity and high cost.[13]

Genetically engineering T cells could expand the applicability of ETC for different tumors. The TCR can be engineered to recognize a specific intracellular or extracellular antigen but present similar manufacturing limitations of ECTs and TILs. In engineered chimeric antigen receptor (CAR) T-cells, the intracellular TCR domain derived from the CD3ζ is conserved while the extracellular domain consists in the single-chain fragment (scFv) from an antibody sequence that recognizes non HLA-restricted extracellular antigens.[28] The advantage is to bypass HLA restriction of antigen presentation, activating the effector cells directly.[29] CAR T-cell therapies have advanced in the last decade with the FDA approval of Kymriah in 2017, for the treatment of B-cell acute lymphoblastic leukaemia (ALL), and Yescarta in 2018, for the treatment of adult patients with relapsed or refractory large B-cell lymphoma. The exceptional results obtained by these therapies are counterbalanced by the related toxicities (cytokine release syndrome, CRS, and immune effector cell-associated neurotoxicity syndrome, ICANS) and the few tumors targeted. Therefore, only a limited number of patients could benefit from the therapy, and multi-specific CARs or other combination therapies are required to avoid tumor relapse.[30] To reduce CAR T-cell toxicities, a recent work proposed the combination of an on/off switch system that respond to the addition of a small-molecule drug to be combined with the CAR system. The resulting STOP-CAR T cells can be blocked by adding the drug to reduce their side effects.[31] Furthermore, CAR technology is now extending to other immune cell types such as NK cells and macrophages.[30]

1.2.3. Cancer Vaccines

ACT and ICBIs are limited by the fact that their efficacy depends on the tumor burden and type, previous T cell infiltration, immune cell exhaustion and tumor escape mechanisms (nonresponse to immunotherapy or cancer progression after initial response).[32] An alternative strategy would be to target APCs, such as DCs, that can be antigen-stimulated *ex vivo* or *in vivo* and generate cancer vaccines, which will be described in more detail in Paragraph 1.3. Antigens stimulate DCs to activate T cells offering different advantages such as avoiding the need for T cell selection, expansion and TCR engineering, reducing costs and times for the procedure and decreasing risk of tolerogenicity and exhaustion.[27] However, different barriers affect therapeutic activity of cancer vaccination: the choice of the antigen, interactions with different cells localized in various tissues, defects in antigen processing and presentation by APCs, tumor heterogeneity, impaired functionality of T cells due to the immune suppressive microenvironment, adaptive immune resistance, identification of optimal combination therapies and vaccination regimen.[26,33]

1.2.4. Limitations of cancer immunotherapies

Approved cancer immunotherapies are limited to specific tumors (for example CAR T cell therapies Kymriah, for recurrent or refractory B-cell acute lymphoblastic leukaemia, and Yescarta, for relapsed or refractory adult large B-cell lymphoma), show heavy side effects and lack efficacy in solid tumors (except for ICBIs, which however is generally not effective in solid but “cold” tumors).[20] Moreover, various factors influence the outcome of these therapies, such as the immune landscape of the tumor, low predictability of neoantigens and tumor mutational burden.[34] Also in some immune infiltrated tumors, T cells fail in recognizing and killing cancer cells. The reasons are different and reside in the complexity of the tumor microenvironment (TME), that affects the response to cancer immunotherapy.[35] Thus, the common promise of immunotherapy as specific and side effect-free therapy compared to chemotherapy and radiotherapy is still far from clinical reality.

1.3. Cancer Vaccines

The mechanism of vaccination was recognized already in 430 B.C., when Athenian historian Thucydides observed that subjects recovering from the Plague could not get infected a second time.[36] In modern times, the first vaccination reported was against smallpox, performed by Edward Jenner in 1796, when the mechanisms of the immune system were still unknown. Patients that were inoculated with the pus extracted from patients suffering from cowpox (a similar but milder disease compared to smallpox) developed a resistance to the subsequent infections from smallpox. It was in the end of the nineteenth century that antibodies were identified as elements of the immune system that are able to recognize and neutralize microorganisms. Then, Paul Ehrlich suggested a correlation between antibodies and pathogen related molecules, named antigens.[37] Similar to pathogens, cancer cells are characterized by specific antigens that can be recognized by the immune system and that have been used in cancer vaccination, either for pulsing *ex vivo* the DCs (DC-based cancer vaccines) or injected in various formulations directly *in vivo* (peptide-based and tumor-lysate based cancer vaccines).

1.3.1. DC-based cancer vaccines

In DC-based vaccination, DCs are isolated from the patient's blood via leukapheresis, cultured *ex vivo* with a specific cocktail of cytokines, pulsed with specific tumour antigens, and reinfused into the patient. Reinfused DCs will then boost the patient's own immune response against their own tumour and, due to their autologous origin, pose a low risk of toxicity.[38] Sipuleucel-T (Provenge) is the first FDA approved DC-based vaccine for hormone-refractory prostate cancer patients who do not respond to androgen-deprivation therapy or chemotherapy. In Sipuleucel-T treatment, DCs are obtained from the blood of selected patients and stimulated *ex vivo* with GM-CSF and prostatic acid phosphatase (PAP) antigen. After four days, cells are reinfused in the patients in three doses at two weeks intervals. Results show increased median patient survival with well-tolerated adverse effects in both treatment and placebo groups. However, compared to standard care chemotherapy in use, Sipuleucel-T is twice as expensive and requires specialized manufacturing facilities.[39] Various other DC-based vaccines that use whole tumor cells are under clinical evaluation (GVAX, Vigil) while others rely on different antigen sources for *ex vivo* DC pulsing, such as tumor specific

antigens (MART-1 vaccine), autologous oxidized tumor lysate or autologous tumor lysate loaded on yeast cell wall particles.[40] Recently, naturally circulating DCs were also employed for DC-based vaccines production.[41] Although lower in number compared to classical monocyte-derived DCs, they would require easier *ex vivo* culture, thus preserving their functionality. This might be a potential solution for increasing efficacy of DC-based cancer vaccines, that are currently limited in their anticancer properties in the clinic.[42] Additionally, the need for engaging multiple DC subsets to enhance immunity, together with the demand to investigate the optimal antigen sources, loading strategy, combination approaches and vaccine delivery strategies are required for improving efficacy of DC-based cancer vaccines.[43]

1.3.2. Peptide-based cancer vaccines

The previous paragraph has underlined how DC-vaccination efficacy is limited by DC functionality after *ex vivo* culture, suggesting that an alternative and easier manufacturing approach is needed, such as direct injection of the antigen for DC targeting. Tumor antigens are typical molecules (mostly proteins)[44,45] identified in the tumors that can be directly injected in patients to induce a specific immune response. Recently, two clinical phase I trials in advanced melanoma patients treated with personalized peptide-based vaccines showed promising results, but the approach needs to be tested in a larger cohort. Moreover, there is still room for improvement in the vaccination strategy (adjuvants, peptides or mRNA, combination therapies, injection site, vaccination timing and dosage) and most importantly which antigen to target, to obtain a long-lasting effect.[46] Antigens used for cancer vaccine formulation are mainly Tumor Associated Antigens (TAAs), Tumor Specific Antigens (TSAs), neoantigens and whole tumor lysates. TAAs are overexpressed molecules in tumor tissues (involved in tissue differentiation and proliferation that are found in healthy tissues as well) and are expressed in various types of cancers.[47] A few well-studied TAAs that are overexpressed in tumor tissues are human epidermal growth factor 2 (HER2), human telomerase reverse transcriptase (TERT), antiapoptotic proteins (such as survivin), mucin 1 (MUC1) and tissue differentiation antigens such as prostate specific antigen (PSA), melanoma antigen recognized by T cells 1 (MART-1) and tyrosinase.[48] However, they are also expressed in healthy tissues; therefore T cells either do not recognize these antigens as immunogenic or break immunological tolerance due to their overexpression. Some other antigens such as cancer testis antigens such as NY-ESO-1, melanoma

associated antigen family (MAGE1) and oncofetal antigens are TAAs specific to tumors and not expressed in normal adult tissues. Tumor Specific Antigens (TSAs) originate either from an oncogenic mutation or from oncogenic viral antigens (human papillomavirus-associated cervical cancer, hepatitis B virus-associated hepatocellular carcinoma and human herpesvirus 8-associated Kaposi sarcoma). Being shared among patients of the same tumor type, their targeting can be achieved in the same patient population.[33] Neoantigens are a subset of TSAs that derive from genetic mutations, originating in a certain type or subtype of cancer that result in a unique peptide sequence and hence high specificity. Although on the one hand high tumor specificity induces increased immunoreactivity and avoid off-target reactions, on the other hand, cancer-specific or patient-specific neoantigens have to be identified by complicated, long and expensive prediction tools.

Different other factors also affect the outcome of peptide-based cancer vaccination. First of all, every person has a different HLA where the neoantigen will be loaded and surface presented by APCs (HLA-restricted presentation), with variable efficiency due also to mechanisms of immune evasion. Secondly, vaccination with TAAs/TSAs might not be an effective treatment for cancers with low numbers of mutations due to a non-sufficient immune response.[49] Lastly, MHC I-associated antigens have been mainly considered until now, but there is emerging evidence that long peptides (13-18 residues) instead of short ones (8-11 residues) should be preferred since they could induce both $CD4^+$ and $CD8^+$ responses.[47] It had already been claimed that a reason for the clinical inefficacy of cancer vaccines is also the type of tumor antigens, as short peptides can be loaded directly on DC surface without co-stimulation and because they would not induce the supportive role on $CD4^+$ T cells.[50] Additionally, recent findings, carried out in tumor biopsies from 32 melanoma patients, underlined the important role of a subset of $CD4^+$ T cells with similar cytolytic activities as $CD8^+$ ones. Upon recognition of the antigen, $CD4^+$ T cells of cytolytic subtype could kill melanoma cells in a Granzyme-dependent way, redefining the role of $CD4^+$ T in cancer immunotherapy.[51] A solution to stimulate both $CD4^+$ and $CD8^+$ T cell response and to avoid tumor immune escape would be to use cancer vaccines that target multiple peptides, such as whole tumor lysate ones.

1.3.3. Tumor lysate-based cancer vaccines

A different approach would be to consider only the "antigenic essence" for cancer vaccination, where a purified protease recovers only surface proteins from living cancer cells, assuming that all intracellular components should be neglected.[29] Alternatively, using whole cancer cells lysates offer a highly personalized source of tumor antigens with the advantage of presenting a large plethora of tumor antigens without the need to identify them and offering a solution to immune escape mechanisms and to haplotype restriction.[52] Among the antigens in the tumor lysate there would be therefore both $CD8^+$ and $CD4^+$ T cell stimulating epitopes.[53] These arguments are supported by an increased objective response in patients receiving whole tumor lysate vaccines than the ones receiving molecularly defined antigens.[54,55]

Additionally, oxidation of tumor lysate (oxTL) with hypochloric acid (HOCl) has shown to increase its immunogenicity. Addition of HOCl converts amines into aldehydes and these into carboxylic acids. This event alters protein conformation and allows access to previously hidden residues for antigen presentation and to proteolytic sites for alternative antigen processing. When tested with model proteins such as OVA, Trp2, or cancer cell line SKOV-3, HOCl oxidation facilitated uptake by bone marrow-derived dendritic cells (BMDCs), and processing and presentation mediated by MHC I and II.[56,57] Analysis of human monocyte derived DCs (mo-DCs) response to oxTL has shown increased human leukocyte antigen (HLA) II surface presentation and oxTL-unique HLA II restricted antigens compared to TL pulsed mo-DCs.[58] Furthermore, oxidized tumor lysate was used to pulse monocyte-derived DCs generated from patients and induced a downstream T-cell response, suggesting its translational potential.[59] In a following Phase I clinical trial in patients affected by recurring ovarian cancer, vaccination of DC *ex vivo* with autologous oxTL (OCDC) increased overall survival without serious adverse events in combination with Bevacizumab and Cyclophosphamide (OCDC/Bev/Cy). Studying the $CD8^+$ T cell response, interestingly showed that OCDC vaccination could stimulate T cells against previously unrecognized neoepitopes and increased T-cell avidity against previously recognized neoepitopes.[60] Further addition of low-dose IL-2 and Aspirin to OCDC/Bev/Cy prolonged time-to-progression and overall survival compared to OCDC/Bev/Cy alone.[61] This supports the idea that vaccination with whole tumor lysate could be an easy, safe and effective

approach to target neoantigens while bypassing the complex bioinformatic predictions tools.[52,60]

1.4. The journey of nanoparticles in cancer vaccination

Cancer vaccines are powerful tools in the fight against tumors, showing the promise of a targeted therapy with little adverse effects. However, clinical data on their efficacy as monotherapy is not encouraging. In a recent Review, analysing clinical trials on breast cancer and ovarian cancer vaccination therapies conducted between 2000 and 2019, there was no statistical significance in overall response rate when comparing various types of vaccines (the trials were based on DC, protein, peptides, whole tumor cell, engineered virus or *Listeria monocytogenes* injections), probably due to the vaccine formulation itself, the route of administration and the need to co-deliver ICBIs or anti-angiogenesis drugs.[62] In this context, nanoparticles could offer various advantages, mainly because their particulate nature (size, shape, surface) is similar to those of pathogens, which facilitate delivery to lymphoid tissues without the need for reinjection, recognition and uptake by APCs.[63] Nanoparticles for use in oncology therapeutic and diagnostic are among the most represented and have been approved by FDA and EMA, since they are generally associated with less systemic toxicity compared to classical formulations.[64] Nanoparticles play a role of protecting the cargo before intracellular delivery, increasing uptake of antigen by DCs *in vitro* and *in vivo*, controlling intracellular antigen release, having intrinsic immunogenicity based on the chosen material and enabling co-delivery of adjuvants and drugs. Additionally, nanoparticles injection *in vivo* would circumvent the cumbersome and long process of DCs *ex vivo* generation currently in practice in DC-based vaccines.[65,66] The following paragraphs will more precisely define the role of nanoparticles for the delivery of cancer antigens from injection and trafficking to lymph nodes, to targeting and uptake by DC, considering the following intracellular controlled release of antigens and the co-delivery of adjuvants and drugs.

1.4.1. Nanoparticles draining to lymph nodes following vaccination

DCs are defined as the bridge between innate and adaptive immunity. They originate from the bone marrow mainly from myeloid precursors during haematopoiesis.

Immature DCs then move to peripheral tissues where they recognize and uptake antigens.[67] Upon maturation they migrate through the lymph to secondary lymphoid organs where they interact with $CD8^+$ T cells and present the antigen in complex with MHC I through cross-presentation.[68] The first challenge faced by the antigen material contained in vaccines is to effectively reach and be up taken by DCs in the lymph nodes (LNs), where T-cells also reside. Nanoparticle properties can be tuned to passively target DCs in lymph nodes upon subcutaneous or intradermal injection *in vivo*. For example, nanoparticles below 200 nm have been associated with LN-resident DCs, while bigger particles were up taken by DCs at the injection site in mice. This suggests that smaller nanoparticles can passively target the LNs, with the advantage of directly reaching the site where naïve T-cells reside and cross-presentation occurs.[69] When comparing different sizes of (poly-γ-glycolic acid) γ-PGA-Phe nanoparticles, it was shown that 40 nm nanoparticles drained faster to lymph nodes after subcutaneous administration in mice compared to 100 or 200 nm ones, confirming previous assumptions. It was also found that large nanoparticles (100-200 nm) were more effective at delivering higher cargo (antigen) loads than small nanoparticles (40 nm), although small nanoparticles were up taken in larger numbers by DCs. From this observation it was suggested that large sized nanoparticles should be preferred since the final amount of antigen delivered to DCs is higher.[70]

1.4.2. Uptake of nanoparticles by DCs

Once nanoparticles are injected and enter the epithelial tissue or drain to secondary lymphoid organs, they have to be up taken by DCs for antigen processing and presentation. The uptake mechanism can generate both intracellular (TLR4-MyD88 signalling and oxidative stress) and extracellular (generation of exosomes) immune response.[71] Most importantly, different nanoparticle characteristics like size, surface charge, hydrophobicity, shape, elasticity, surface targeting moieties and chemical composition affect the efficiency of uptake and the immune response that will be generated. The effects of nanoparticles characteristics on DC uptake and activation are discussed below in detail.

Size. DCs can actively uptake antigens in different ways: phagocytosis, receptor-mediated endocytosis or pinocytosis.[72] Phagocytosis is derived from ancient Greek and literally means “cell eating” (“phagein” means “to eat”; “kytos” means

"cell"). Upon interaction with the cell membrane, materials are engulfed by a phagosome and internalized in the cell. The phagosome fuses with lysosomes, intracellular vesicles where the content of the membrane will be degraded by hydrolytic enzymes. Pinocytosis means "cell drinking" ("pino" means "to drink") and is observed in vesicles smaller than the ones generated from phagocytosis (few to hundreds of nanometres) which uptake fluids. Macropinocytosis, clathrin and caveolae mediated pathways or independent endocytosis all fall under pinocytosis mechanisms.[73] Soluble antigens are mainly up taken by immature DCs via micropinocytosis, while particulate material such as particles are up taken by phagocytosis and macropinocytosis (size > 500 nm or smaller particles that tend to aggregate or be opsonized) or endocytosis for smaller particles.[74,75] Endocytosis can be mediated by clathrin or caveolae dependent pathways, generating 50-60 nm vesicles for up taking extracellular material, or by clathrin and caveolin independent endocytosis.[66,74] As a general rule, nanoparticles up to 200 nm in size are up taken by clathrin-mediated endocytosis while bigger nanoparticles follow the caveolin-mediated endocytosis, although the uptake mechanism also depends on the cell type and the nanoparticles material.[73] After testing particles of different size *in vitro* it was reported that, at parity of zeta-potential and antigen loading, 200 nm nanoparticles could induce better uptake by DCs and downstream immune response compared to 700 nm ones, probably because the endocytic pathway, related to MHC-I antigen presentation, was favoured.[76] In another work, testing uptake of OVA-based nanoparticles of sizes ranging from 50 nm to 500 nm showed no significant difference in the uptake mechanism by JAWS II murine DCs, which happened mainly through clathrin-mediated endocytosis.[77] This had been observed in a previous study on BMDCs, where it was also proven that after 24 hours incubation there was no increase in uptake, defining this time point as the last useful one to detect differences in uptake *in vitro*.[78] In a recent work, 100 nm PLGA nanoparticles with slightly negative zeta potential were used to co-encapsulate OVA, the immune modulating agent Imiquimod (R837) and apolipoprotein E3 (ApoE3). These nanoparticles were up taken by BMDCs *in vitro* mainly by micropinocytosis and to a less extent by caveolae- and clathrin-mediated endocytosis.[79] The main claim of this study was that it is mainly the material rather than the size that dictates the destiny of antigen uptake mechanism. In fact, mannose receptor mediated endocytosis delivers the antigen towards less acidic endosomes and MHC-I presentation. In contrast, antigens up taken by pinocytosis and scavenger-receptor

endocytosis target the antigen to highly acidic lysosomes, where antigens would be subjected to MHC-II mediated surface presentation.[80]

Surface Charge. Like nanoparticle size, surface charge has also been studied to understand the preferential uptake by cells. Generally, charged nanoparticles and especially the ones with a positive charge, are better up taken by the cells.[81] However, due to the overall negative charge on the cell membrane, there is a trade-off between increased uptake and higher toxicity of cationic particles.[73] For example, gelatin nanoparticles were tested for OVA delivery, where OVA was either linked on the surface (S-NP) or encapsulated within the particles coated with Dextran (Dex-NP). Cationic S-NP clearly showed a concentration dependent cytotoxicity compared to anionic Dex-NP. [82] Surface charge might also play a role in the immune response to nanoparticles, since cationic superparamagnetic iron oxide (γFe_2O_3/APTS) particles could enhance cellular uptake and increase antigen cross-presentation in Mutu DC immortalized murine APCs compared to their anionic counterparts (γFe_2O_3/DMSA). However, no information on cytotoxicity was provided.[83]

Hydrophobicity. Nanoparticles with hydrophobic surfaces tend to interact with the hydrophobic core of the membrane bilayer and undergo direct cell penetration, whereas hydrophilic nanoparticles enter the cells by embedding within the vescicles.[73] The direct interaction of hydrophobic nanoparticles with cell membranes reflects in increased activation of DCs.[71] This has been shown in chitosan nanoparticles incubated with human fibrosarcoma cells (HT1080) and in polyglutamic acid (PGA) nanoparticles incubated with BMDCs, where increasing hydrophobicity had a direct correlation with increased uptake.[84] In PGA nanoparticles this also reflected in increased activation of BMDCs.[85]

Shape. The effects of nanoparticle shape on their uptake are less clearly understood as the shape also affects nanoparticles size and charge. Some papers report better internalization of rod-like nanoparticles compared to spherical ones, while others report the opposite.[73] Alternatively, needle-like LV@HPA/PEI particles, where OVA was surface absorbed, showed low cytotoxicity and could improve OVA uptake in murine DCs.[86] BMDCs were also incubated with differently shaped DNA nanoparticles (DN) with sizes between 50-80 nm and a similar mass, showing that more compact DN (block shaped compared to hollowed ones) were preferentially uptaken.[87] When

comparing uptake of rod or ellipsoid *versus* spherical nanoparticles by macrophages, results have also been contradictory, with some works reporting better uptake of spheres, while others better uptake of rods and ellipsoidal particles.[88,89,90]

Elasticity. Nanoparticle shape becomes an issue when considering soft nanoparticles, as their shape can change from spherical to ellipsoidal upon interaction with the cell membrane.[91] Elasticity is therefore an element that needs consideration in nanoparticle-cell interactions; however, its contribution to cellular uptake has also raised different opinions. It is unclear whether stiffer or softer nanoparticles are preferred for uptake by DCs. For example, an experiment using PEG-based nanoparticles (200 nm in size) with varying elastic moduli (0.255 to 3000 kPa) confirmed that in macrophage murine cell line J774, *in vitro* uptake of stiffer nanoparticles was faster and in higher numbers compared to soft nanoparticles. However, upon intravenous *in vivo* administration in mice, nanoparticles that are more elastic showed longer distribution and elimination half-life, especially at earlier time points. Therefore, softer nanoparticles were retained in organs which received higher blood output and would offer prolonged drug distribution *in vivo*.[92] Recently it has been observed that elastic properties also influence the uptake mechanism: harder nanoparticles usually rely on uptake by endocytosis, while softer ones on micropinocytosis.[91] This would explain why in some works nanoparticles with intermediate elasticity show overall better uptake, since they would employ both pathways for immune cell internalization.[93] Additionally, the type of cell targeted and the combination of the other properties of nanoparticles influence uptake mechanisms and efficiency.[73]

Surface Targeting Moieties. Surface receptors specific to DCs have been targeted for increased uptake *in vitro* and *in vivo*, avoiding off-target delivery and thus reducing the dose of vaccine administered. Moreover, it seems that certain surface receptors might enhance MHC-II presentation (DC-SIGN, DCIR2, Scavenger Receptor SRs) compared to MHC-I presentation (Mannose Receptor, MR and CD40L *in vitro* but not *in vivo*).[80,94] Therefore, surface modification of nanoparticles affect the uptake by DCs and this impacts antigen processing and the population of T cells that will be activated. The receptors chosen for targeting both human and mice DCs are usually integrin CD11c, C-type lectins (DEC-205, DC-SIGN and mannose receptors), CD40, MHC class II and FcγR.[95]

CD11c is expressed on the surface of murine and human DCs and targeting antigens to DCs via anti-CD11c antibodies has shown both downstream $CD4^+$ and $CD8^+$ T cell responses. DC-targeting with porous silica nanoparticles (pSiNP) modified with control isotype antibody or anti-CD11c antibody (CD11c-pSiNP) showed that murine DC preferentially uptake CD11c-pSiNP.[96] Similarly, inoculation of mice with a fusion protein of CD11c-specific variable single-chain fragment and HER2/neu tumor antigen extracellular domain mixed with CpG ($scFv^{CD11c}$-$HER2_{CpG}$) resulted in prolonged survival in tumor-bearing mice.[97]

C-type lectins, such as DEC-205 and DC-SIGN, can be targeted through functionalization of nanoparticles with specific antibodies or with mannose. DEC-205 has been shown to induce more potent cross-presentation *in vitro*, because upon internalization it is recycled in late endosomes and lysosomes, where antigen processing and presentation is mediated. For example, anti-DEC-205 antibodies can be used to functionalize nanoparticles, as was done with OVA-loaded PLGA nanoparticles. Increasing the density of anti-DEC-205 antibodies mimicked multivalent ligands and binding of apoptotic cells via DEC-205. This increases the expression of CD36, an immune enhancer, with a stimulating effect on both T helper cells (Th) 1 and 2, detected by increased cytokines production (both IL-12 and IL-10) *in vitro* and *in vivo*.[98] However, in humans, DEC-205 is also expressed by other cell types such as B cells, T cells, NK cells, monocytes and macrophages, which makes them less specific towards DCs. On the contrary, targeting DC-SIGN has the advantage of a more DC-specific response in humans.[99] For example, targeting the mannose receptor on BMDC, increased the uptake of cross-linked polymeric micelles. Tetra-O-acetyl-α-D-mannosylethyl acrylamide and poly(pentafluorophenyl) acrylate were synthetized via RAFT polymerization and self-assembled into micelles, further cross-linked via a pH sensible linker. Flow cytometry and confocal microscopy demonstrated that nanogels with higher grade of mannose modification could better interact with BMDCs overexpressing mannose receptors.[100]

CD40 belongs to the family of TNF-α receptors and is commonly overexpressed on DCs following maturation. An interesting work compared uptake by BMDCs of PLGA nanoparticles loaded with OVA, Poly I:C and R848, and surface modified with antibodies anti CD11c, DEC-205 or CD40. CD40 targeting showed a

significantly higher uptake compared to targeting other surface receptors or non-targeting. However, there was no difference on *in vitro* DC maturation, T cell activation and in *in vivo* immunological responses between nanoparticles targeted to different DC-specific receptors. There was a difference comparing targeted and non-targeted nanoparticles, underlying the importance of target strategies not only for reducing the dose of vaccines administered, but also to increase their efficacy.[101]

In a different work, murine DC-binding peptides were selected by phage display and then used to functionalize by acetylation mesoporous silica nanoparticles (MSN) carrying OVA and CpG. Peptide-modified MSN, compared to soluble OVA or non-modified MSN, could induce higher uptake and activation of BMDCs *in vitro* and DCs *in vivo*. Vaccination with peptide-modified MSN increased survival and reduced tumor growth in a mouse model of B16 melanoma, without significant toxicity.[102]

1.4.3. Materials and their use in cancer vaccination

Finally, the material of choice for particles production contributes greatly to the interaction with DCs. Ideally, the material should induce activation of the immune system without a systemic or cytotoxic effect. Among the materials investigated for nanoparticles formulation applied to cancer vaccination, research has focused on polysaccharides (chitosan, dextran, alginate, hyaluronic acid and pullulan), proteins (gelatin, virus-derived proteins, albumin), lipids, nucleic acids, synthetic polymers and inorganic materials. The main features of each material are described below and examples in cancer vaccination applications are summarized in **Table 1**. Almost all of the vaccines described in **Table 1** were tested in murine primary and immortalized cell lines.

Table 1. Overview of the materials employed in cancer vaccines formulation.

Materials	Examples in cancer vaccines formulations	References
Chitosan	Chitosan and poly(glutamic acid) NPs	103
	Chitosan and mannose-alginate NPs loaded with tumor cell lysate	104
	Chitosan NPs loaded with OVA	105
Dextran	Acetalated dextran NPs loaded with OVA	106
	OVA and murabutide-loaded Acetalated dextran microparticles	107
	Dextran-functionalized graphene oxide loaded with OVA	108
	Dextran nanoparticles to deliver covalently or non-covalently linked synthetic long peptides	109
Alginate	Mannose surface modified alginate NPs to deliver OVA	110
	Cationic poly(lysine) and sodium alginate NPs to deliver Bovine Serum Album	111
Hyaluronic Acid (HA)	HA coating of pH-responsive liposomes delivering OVA	112
	HA coating of 1,2-dioeleoyl-3-trimethylammonium-propane (DOTAP) and PLGA NPs loaded with OVA	113
Cholesteryl pullulan (CHP)	NY-ESO loaded on CHP nanogels	114, 115
Gelatin	Dextran coated gelatin NPs for the delivery of OVA	116
	Gelatin NPs modified with PEI and coated with polyI:C and OVA	117
Proteins	Nanocomplexes from albumin bound to maleimide-functionalized Evans blue dye reacted with thiol-modified CpG adjuvant or cysteine-modified antigens	118
	OVA cross-linked with genipin to produce NPs and coated with adjuvant CpG	119
	Virus-Like Particles (VLPs)	120, 121, 122
Lipids	DOTAP and 1,2-dioleoyl-sn-glycero-3-phosphocholine (DOPC) based cationic liposomes to encapsulate synthetic long peptides	123
	Anionic ganglioside liposomes containing MPLA and WT1or gp100	124
	Multilamellar particles formed by cationic liposomes interacting with negatively charged mRNA	125,126,127,128

Nucleic acids (NA)	NANPs to deliver mRNA, CpG, Poly I:C and cyclic dinucleotides	129,130
	Hybrid DNA-dsRNA single-stranded RNA origami to deliver PolyI:C	131
	Openable tubular origami for pH-responsive delivery of co-delivery of CpG, dsRNA and OVA, gp100 or Adpgk	132
	RNA structures coupled with CpG	133
Synthetic Polymers	PLGA NPs and MPs for delivery of whole tumor lysates	134,135,136,16,137,138
	PLGA NPs for delivery of tumor specific proteins, peptides and with differing DC-targeting moieties and TLRs	139,135,16,140,141
	PLGA NPs loaded with CpG coated with fusion DC-MC38 or fusion DC-GL261	142
	Polymeric hybrid micelles of PEG-PCL and PEI-PCL encapsulating CpG and antigen Trp2	143
Inorganic materials	Fe_3O_4 absorbed with model antigen OVA	144
	Extra-large silica mesopores loaded with OVA and coated with PEI	145
	Mesoporous silica forming metal organic framework to deliver OVA and PolyI:C	146
	Gold NPs coated with model antigen OVA or with a control pentapeptide	147
	Calcium carbonate MPs loaded with tumor lysate and coated with a conjugate of TLR7/8 agonist	148

Chitosan. Chitosan is a biodegradable and biocompatible cationic mucopolysaccharide derived from deacetylation of chitin. Deacetylation grade and molecular weight can be tuned to change its hydrophobicity, solubility, degradation rate, immune-stimulating properties and toxicity.[149] The presence of amine groups allows for easy functionalization of chitosan-derived nanoparticles, which can be prepared by different methods (cross-linking, reverse micellar method, precipitation, emulsion-droplet coalescence method) depending on the application and drug loaded.[150] Moreover, chitin and chitosan have immune stimulating properties.[120]

Dextran. Dextran is a FDA approved polysaccharide whose acetalation (Ac-DEX) increases its hydrophobicity and, based on the degree of acetalation, can change its degradation rates. Ac-DEX is an acid-sensible polymer and can be used to generate nanoparticles by emulsion. Due to its tuneable properties, it has been used to deliver small molecules, proteins, peptides, nucleotides, and inorganic molecules.[151]

Alginate. Alginate has been used since it is a biodegradable polyanionic polymer and can be easily synthetized through addition of divalent ions to form a hydrophilic network.[152]

Hyaluronic acid. Hyaluronic acid (HA) is a component of the extracellular matrix formed from repeating units of N-acetylglucosamine and glucuronic acid. This linear mucopolysaccharide offers various groups for modification (hydroxyl, carboxylic and N-acetyl groups) together with high biocompatibility. Various cancer cells express HA receptors, such as CD44. All these elements taken together enable the use of HA as a delivery platform to target cancer cells for the delivery of chemotherapeutic agents.[153,154,155] In cancer vaccination, HA has been used mostly to coat nanoparticles to increase their biocompatibility or, due to its high interaction with water molecules and presence in the extracellular matrix, to form cross-linked hydrogels.[113]

Cholesteryl pullulan. Pullulan is a biocompatible polysaccharide composed of repeating units of maltotriose trimers. In nature, it is produced from yeast-like fungus *Aureobasidium pullulans*. Modification of hydrophilic pullulan with hydrophobic cholesterol by acylation generates amphiphilic cholesteryl pullulan (CHP) that can assemble to generate CHP nanogels. Nanogels hydrophobicity, size and cargo release could be tuned by using different amount of cholesterol.[156] Amongst the cargo employed, cancer antigens (HER2, NY-ESO-1, MAGE-A4, synthetic long peptides) have been loaded to formulate CHP-based vaccines with applications in clinical trials.[157]

Gelatin. Similarly to HA, gelatin is derived from a component of the extracellular matrix, collagen, therefore offering high biocompatibility, higher encapsulation efficiency of protein-derived drugs, easy availability and manufacture. It is formed by repeating units of alanine, glycine and proline residues that offer abundant functionalities and both cationic and anionic groups. Gelatin nanoparticles can be prepared by two-step desolvation, coacervation, solvent evaporation, microemulsion or nanoprecipitation methods.[158]

Proteins. One of the main issues of the biopolymers cited above is that, although biocompatible, they often need to be surface modified to prolong their half-life or possess surface charges that can either inhibit their interaction with cells (anionic ones) or induce cytotoxicity (cationic ones). Proteins on the other side offer high biocompatibility and amino, carboxy and hydroxy groups for surface modification. For

example, albumin is a well-known protein widely used in drug delivery since it can prolong the blood circulation half-life of binding molecules. Albumin is the most abundant protein in the blood and can bind both endogenous and exogenous compounds. Most importantly, it offers different binding sites that allow for interaction and transport of molecules with various grades of hydrophobicity. This has made albumin the protein of choice for generation of nanoparticles *via* different methods: desolvation, emulsion, thermal gelation, nanospraying and self-assembly.[159] Although greatly used to target cancer cells for delivering chemotherapeutic agents, albumin has also been used to deliver immune-stimulating agents and antigens. Other proteins (ferritin, encapsulin, heat-shock proteins, E2 protein) have been used to deliver chemotherapeutic drugs, siRNA for gene delivery or cancer antigens, offering high biocompatibility and solubility.[160,161] Proteins are the monomeric building-block that self-assemble in nanocomplexes with the advantage of offering an interior cavity for diverse drug loading, characterized by easy self-assembly of repetitive units that increase surface avidity of binding on immune cells. Since their genetic sequence and protein tertiary structure is known, nanoparticles can be rationally designed and surface bioengineered to prolong their circulation half-life and cell targeting properties.[162] Belonging to the protein-based nanoparticles are also virus inspired ones, named virus-like particles (VLPs). The main advantages of using VLPs is that they are naturally immunogenic, have evolutionally developed to penetrate tissues, interact with and enter cells and, once cultured in the host cell, will replicate continuously, allowing inexpensive manufacturing. The recent development and approval by the European Medicinal Agency (EMA) of a COVID-19 vaccine based on a replication-deficient adenovirus as a vector for S-glycoprotein of SARS-Cov-2 has brought the attention on the efficacy and safety of virus-based vaccines.[163]

Lipids. Amphiphilic phospholipids (phosphatidylcholine, phosphatidylserine, sphingomyelin, cholesterol) have been used to assemble under hydrophobic interactions and form micelles or liposomes depending on the molecular shape and structure of the lipophilic chain. They can be loaded with both hydrophobic and hydrophilic cargos, can be surface modified, offer good compatibility and have been approved and used in the clinic.[164] They are also considered to have intrinsic adjuvant properties, such as immune stimulating complexes (ISCOMs) composed of saponins, cholesterol and phospholipids.[120] In recent history, lipid nanoparticles have been the first EMA approved

vaccines for the delivery of mRNA encoding for Sars-CoV-2 spike proteins, which could promote approval of liposomes for different applications of vaccination.[165,166]

Nucleic Acids. DNA and RNA offer a programmable and highly biocompatible biomaterial that can form nanocomplexes through self-assembly of the different nucleobases. Using long single strands of nucleic acids, different structures could be generated and their size controlled using different critical micellar concentrations (CMC) and temperatures (CMT). Modifications such as encapsulation, coating with cationic molecules, cross-linking and using non-natural nucleobases offer a strategy to enhance stability.[167,168] DNA and RNA can also be modified according to the application with lipids, polymers or hydrophobic molecules.[129] Nucleic acids have been used in cancer therapy for drug delivery and in immunotherapy for gene-regulating, gene-editing, as specific target-binding molecules (aptamers) and as immune stimulating agents.[169,170,171] Additionally, an on/off mechanism has been developed to deliver therapeutic NANP and its neutralizing NANP in case of side-effects.[172] Despite the increasing interest in nucleic acid based structures, their pharmacokinetics after *in vivo* administration is not clear, and, up to now, only six oligonucleotide-based drugs have been approved by FDA. Although biocompatible, nucleic acids have to be chemically modified to prevent their degradation by nucleases, raising the issue of self-toxicity that should be evaluated case-by-case.[129]

Synthetic polymers. The main advantage of using biopolymers and liposomes is that they derive from cellular or viral production and have high biocompatibility. However, in vaccination, a certain immune stimulating effect needs to be achieved, and this usually is obtained by co-delivery of adjuvants. Synthetic polymers would offer intrinsic adjuvant properties– being recognized as “foreign” by human bodies – and with the advantage of being synthetized with specific features depending on the application, especially regarding degradation rate and controlled intracellular release of the cargo.[173] Due to their low toxicity and degradation properties, various polymers have been tested for nanoparticles production, such as poly(lactic-co-glycolic acid) (PLGA), poly(methyl methacrylate) (PMMA), poly(caprolactone) (PCL), poly(ethylene glycol) (PEG), poly(ethylene imine) (PEI) and poly(propylene sulfide) (PPS).[174,134,175,176,177]

PLGA has been approved by FDA and EMA due to its high biocompatibility and degradation in lactic and glycolic acid, which are by-products of cellular

metabolism. Its degradation rate can be tuned by the ratio of lactic and glycolic acid, with PLGA 50:50 being the one with faster degradation rate. Degradation happens mainly by hydrolytic mechanism and is accelerated by the porosity of the particles and the content of glycolic acid. After intramuscular injection of PLGA microspheres with various PLA and PGA ratios, PLGA(50:50) based microspheres were the fastest degrading ones, while the slowest were PLA ones. For this reason, PLA could be a good candidate for implantable scaffolds but not for fast release particles.[178] PLGA particles can be synthetized by single (oil in water, O/W) or double (water in oil in water, W/O/W) emulsification-solvent evaporation technique and spray-drying. Nanoparticles based on PLGA have been used for delivering drugs for different diseases: neurological, cardiovascular, for diabetes, for infections and for cancer, in both chemotherapy and cancer vaccines.[179] To prolong PLGA circulation half-life, monomethoxy poly(ethylene glycol) (MePEG) has been conjugated to PLGA by ring-opening polymerization of the lactide and glycolide in presence of MePEG to produce the block co-polymer PEG-PLGA. Comparison of PLGA or PEG-PLGA biodistribution in rats after intravenous administration has shown prolonged blood circulation of PEG-PLGA nanoparticles after 12 hours and their reduced transport to elimination organs (spleen, liver and kidney).[180]

Inorganic Materials. Different inorganic materials (iron, silica, zinc, gold, calcium carbonate) have been used to deliver antigens in cancer vaccines due to their immune stimulating properties, control over chemophysical properties, ease of production and application for imaging and phototermal therapies (PTT). For example, iron oxide (Fe_3O_4) nanoparticles have been approved by FDA for MRI imaging but also as drug delivery carriers. Additionally, gold nanoparticles (GNPs) are among the inorganic nanoparticles that can be used in cancer therapy for anticancer drug delivery, PTT, imaging and immunotherapy.[181,182]

1.4.4. Nanoparticles inside the cell: endosomal escape strategies to improve cross-presentation

Anti-cancer specific immune response relies mainly on $CD8^+$ T-cell mediated killing, activated by antigen presentation on MHC-I complex by DCs. However, exogenous antigens up taken by pinocytosis are directed to the lysosome and presented

on MHC-II.[80] Exogenous antigens up taken by phagocytosis are directed from the phagosome to the Endoplasmic Reticulum (ER) and then loaded on the MHC-I. Alternatively, exogenous antigens up taken by marcopinocytosis or clathrin-mediated endocytosis, can be processed and loaded on MHC-I following a TAP-dependent or independent pathway (TAP is a protein responsible for molecules translocation from the cytosol to the ER). In the TAP-independent pathway, cytoplasmic antigens are directed to early endosomes for MHC-I loading and cell membrane presentation. In TAP-dependent mechanism, antigens in the cytosol are degraded by proteasomes and transferred in the ER through TAP for loading onto MHC-I. From the ER, MHC-I antigen complexes are directed to early endosomes and then to the cell membrane or directly to the cell membrane. Therefore, in both TAP-dependent and independent loading, antigens need to be localized in the cytosol and this happens via antigen escape from lysosomes into the cytosol. [94] For this reason, biomaterials have been engineered to respond to external (heat, light, magnetic field, electric field and ultrasound) or internal (pH, redox, tissue-specific enzymes and molecules) stimuli for cytosolic delivery.[183,184,185] Nanoparticles used in cancer vaccination are often injected subcutaneously or intradermally in *in vivo* models. After injection, they might be drained to lymph nodes or to elimination organs. Therefore, external-stimuli are not viable-mechanisms to control antigen release because there is no precise location to irradiate. Additionally, it is difficult to predict the location and presence of specific enzymes and molecules that could work as release triggers. On the other hand, low pH of intracellular vesicles and increased GSH intracellular concentration are reliable localized triggers for intracellular release and have been widely used in cancer vaccines formulation.

PH controlled antigen release. Upon endocytosis, exogenous antigens are engulfed in early endosomes (~100 nm diameter, pH 6.0-6.5) which can fuse with membrane-derived macropinosomes and form late endosomes (250-400 nm diameter, pH 5.0-5.5). Late endosomes are closer to the nucleus than early ones and have higher exchange with the trans-Golgi network, in what is called perinuclear cloud. Late endosomes then mature in more acidic lysosomes, where the pH reaches levels of 4.0-4.5. Both endosomes and lysosomes are characterized by low pH, creating the condition for locally activating proteases, uncoupling ligands from receptors for receptors recycling to the membrane and performing microbicidal activity, lipid homeostasis, cargo transportation, autophagy and antigen presentation.[186,187,188] Therefore, pH

responsive linkers and materials have been used to deliver drugs intracellularly or in regions characterized by low pH, such as the tumor microenvironment. PH sensitive groups (tertiary amines, carboxylic acids, sulphonamides), monomers (acrylic acid, metacrylic acid, maleic anhydride, N,N-dimethylaminoethyl methacrylate, histidine) or linkers (acyl hyrazone, acetals and 2,3-dimethylmaleic amide) have been employed for production and cross-linking of pH -responsive nanoparticles.[189] These groups are stable at neutral pH but are degraded in acidic environment. The molecules released disrupt the osmotic equilibrium in endosomes and cause membrane rupture and the cytosolic release of the cargo. For example, OVA was cross-linked to alginate via a pH sensitive Schiff base. The resulting ALG=OVA was mixed with mannose modified alginate (MAN-ALG) and cross-linked in presence of $CaCl_2$ to form MAN-ALG/ALG=OVA nanoparticles. Nanoparticles were better up taken *in vitro* by BMDC and controlled tumor growth in E.G7-OVA tumor bearing mice following subcutaneous therapeutic vaccination *in vivo* compared to soluble OVA.[110] Cholesterol modified with an acid-labile vinyl ether group was used to form acid-labile CHP (acL-CHP) with azido-modified pullulan via click reaction. Compared to stable CHP (acS-CHP) in acidic media (pH 4) and to acL-CHP in neutral media (pH 7.4), acL-CHP in acidic solution (pH 4) showed increased swelling.[190] Additionally, a pH sensitive hydrazone bond has been used to link galactosyl-dextran retinal (GDR) to all-trans retinal to deliver OVA to BMDC. The resulting nanogel proved to swell and release retinal upon decreasing pH from 7.4 to 5.0 and to increase antigen uptake and lysosome escape in BMDCs. This reflected in increased *in vitro* proliferation of $CD4^+$ and $CD8^+$ T cells as well as increased survival in melanoma bearing mice following vaccination with nanogels compared to soluble OVA.[191]

A different strategy exploits the material responsiveness to pH changes due to ionic charges in the structure, such as cationic PEI, poly-lysine (PLL) and anionic poly(propylacrylic acid) (pPAA). For example, PEI-OVA and PLL-OVA nanocomplexes formed through electrostatic interaction of OVA with cationic PEI or electronic interaction with PLL. After uptake by BMDC, PEI-OVA induced higher expression of MHC-I OVA surface expression compared to PLL-OVA as well as IL-2 secretion following co-culture of pulsed BMDC with hybridoma T-cells.[192] Poly(propylacrylic acid) (pPAA) is a linear amphiphilic polyanion that was used to assemble through electrostatic interaction with antigen OVA modified with a cationic

oligolysine tail (K_{10}OVA) to form nanoplexes (K_{10}OVA/pPAA). Using DC2.4 murine cell line, OVA uptake and expression of SIINFEKL/H-2K^b were increased after pulsing with K_{10}OVA/pPAA compared to K_{10}OVA. Addition of inhibitors of different antigen processing pathways revealed that the transfer of ER to membrane and ER-localized aminopeptidases are necessary for antigen presentation on MHC-I.[193] A third strategy would be to co-deliver OVA and an endosome-disrupting agent, such as NH_4HCO_3 in PLGA microparticles. Compared to non-responsive particles, responsive ones demonstrated lysosome escape of OVA after incubation with BMDCs by confocal microscopy. Additionally, responsive particles could increase both humoral and cytotoxic immune responses compared to soluble antigen or non-responsive particles following mice immunization.[194]

Redox-controlled antigen release. The intracellular environment is known to have a higher concentration of glutathione (GSH) (2-10 mM) compared to the extracellular one (2-20 μM).[195] Intracellular GSH serves as reducing agent for disulfide bonds forming thiol groups in normal cellular homeostasis to react with excessive reactive oxygen species (ROS). Biocompatible proline oligomers, disulfide groups and its derivatives (cysteine, cystamines, disulfide-containing azide compounds, DL-thiomalic acid, 2-iminothiolane, N-succinimidyl-3-(2-pyridyldithiol) propionate, disulfide-based dimethacrylate, poly(propylene sulfide)) are responsive to the change in redox state and can be exploited for controlled intracellular delivery of the cargo.[196,197,198,199,200] Moreover, disulfide bonds can be disrupted after reduction and regenerated after oxidation in a reversible way.[201] In cancer vaccine applications, hyperbranched polymer poly(amido amine) and polyethylene imide (PAA-PEI_{600}) linked by a redox responsive linker were used for microwave-assisted pyrolysis to form cationic fluorescent polymer dots to deliver and track OVA (PDs/OVA). Following vaccination in mice and serum collection, PAA-PEI_{600}/OVA nanoparticles induced higher humoral immunity compared to free OVA, due to redox-responsive accelerating degradation of PAA-PEI_{600}. Their aggregation in smaller cationic PDs/OVA nanoparticles induced a higher level of cellular immunity.[202] A similar recent work used hyperbranched PAA (HPAA) and fluorinated HPAA (HPAA-F7) for the same purpose, combining its proton sponge effect and redox responsiveness to improve OVA delivery to DC2.4 cell line.[203] Another facile approach employed electrostatic interaction between OVA and a cysteine-containing cell-penetrating peptide. The resulting

peptide/OVA condensates were stabilized by spontaneous formation of disulfide bridges and therefore offered a redox-responsive platform. After incubation in a 10 mM dithiothreitol (DTT) solution for one hour, degradation of condensates was confirmed by decreased relative turbidity (%) and reduced size. Upon subcutaneous vaccination of mice, peptide/OVA induced significantly more potent humoral and cellular immune responses compared to soluble OVA.[204] The responsive disulfide bridge can be also introduced within the linker connecting antigen (diverse synthetic long peptides (SLPs)) and adjuvants used for the formulation of redox-responsive polycondensate neoepitope (PNE). In presence of 2 mM solution of DTT, release of LEQ peptide from PNE(LEQ-Pam) over 24 hours was higher compared to non-responsive PNE(LEQ-Pam) and responsive PNE(LEQ-Pam) without DTT. Prophylactic vaccination of mice with responsive PNE(LEQ-Pam) induced delayed tumor growth and prolonged survival compared to soluble neoantigen LEQ.[205]

1.4.5. Nanoparticles release their cargo: co-delivery of antigen and adjuvants

Adjuvants are employed in vaccines formulation to improve the immune response and use a lower dose of vaccines to reduce systemic side-effects. Pattern Recognition Receptors (PRRs) are molecules on the surface of APCs that recognize typical bacterial and viral evolutionarily conserved molecular structures termed Pathogen Associated Molecular Patterns (PAMPs), such as unmethylated CpG motifs, double stranded RNA, and typical bacterial proteins (flagellin, lipopolysaccharide). Toll Like Receptors (TLRs) belong to PRRs and are expressed on the surface of the cells (TLR1, 2, 4, 5 and 6) or intracellularly on the membrane of endosomes (TLR3, 7, 8 and 9). Cancer vaccines aim at inducing a Th1 polarized response and for this, intracellular TLRs on endosomes are a favourable target.[206] TLR ligands represent a fundamental tool in cancer vaccination, although it is difficult to predict whether targeting TLRs could potentially promote tumor proliferation. In fact, recent research underlines that TLRs could act as a double-edged sword in immunotherapy.[207] TLR ligands currently tested or used in the clinic are double stranded RNA analogues (poly I:C) targeting TLR3, lipid A analogues (monophosphoril lipid A, MPLA) targeting TLR4, Entolimod, a flagellin derivative, targeting TLR5, imidazoquinolines (Imiquimod) targeting TLR7/8 and unmethylated CpG targeting TLR9 (however expressed only in human plasmacytoid DCs).[76,95,120,208,209] In cancer vaccination, poly I:C has been co-encapsulated with

another adjuvant, FDA approved TLR7 agonist Resiquimod (R848), and with chemokine Macrophage Inflammatory Protein-3 alpha (MIP3α; CCL20) in PEG-coated PLGA nanoparticles. Intratumoral injection in mice of nanoparticles with different combinations of adjuvants and SLP as antigen source could significantly eradicate TC-1 tumors in mice compared to vaccination with SLP alone, although the chemokine MIP3α needed combination with polyI:C and R848 to nearly double progression-free survival.[210] Another TLR7 agonist (Gardiquimod) was entrapped in the core of lipid coated PLGA particles, while the mRNA encoding for the antigen was loaded *via* electrostatic interaction in the lipid bilayer. Enhanced BMDCs maturation was demonstrated *in vitro* and a stronger antigen-specific immune response was obtained *in vivo* when co-delivering the mRNA and the adjuvant compared to sole mRNA. However, when used for therapeutic or prophylactic vaccination in B16 melanoma mouse model, the vaccines could control tumor growth but could not prolong significantly mice survival.[211] Alternatively, stimulator of interferon genes (STING) pathway is a recently discovered adjuvant target. Upon binding to 2′,5′-3′5′-cyclic guanosine monophosphate - adenosine monophosphate (cGAMP), STING induces a type-I interferon (IFN-I)-driven inflammatory response that promotes cross-presentation. OVA epitope SIINFEKL and cGAMP were co-encapsulated in pH responsive polymersomes to generate nanoSTING-vax. SIINFEKL specific response was generated when pulsing DC2.4 cell line or BMDCs with nanoSTING-vax compared to polymersomes loaded only with the epitope and to a similar extent to a mixture of NP-cGAMP and epitope. Following *in vivo* vaccination, nanoSTING-vax enhanced antigen and adjuvant delivery to APCs residing in draining lymph nodes and increased antigen-specific $CD8^+$ T cells number in blood. NanoSTING-vax could reduce tumor growth following *in vivo* prophylactic vaccination of mice challenged with B16.F10 melanoma. Interestingly, adapting nanoSTING-vax with the appropriate antigen, in both MC38 murine colorectal adenocarcinoma model and poorly immunogenic B16.F10 melanoma, nanoSTING-vax could only induce a therapeutic effect if combined with ICBIs (anti-CTLA-4 and anti-PD-1).[212,213] In fact, it has underlined the importance of a combination strategy with ICBIs for immune stimulation and immunogenic cell death (ICD) for antigen release from apoptotic cancer cells that could reiterate the immune response. [65] Emerging studies combine immune-stimulating biomaterials for delivery of antigens and immune-stimulating drugs. More and more evidence underlines the

importance of combination therapy to address multiple targets and especially impact the TME.[214] However, doses and timing of administration should be carefully studied to avoid toxicities. It has been suggested that a minimal approach should be preferred to avoid tolerogenicity. For example, a proposed treatment would be: first vaccination, followed by TME reshaping therapies (with direct or indirect antiangiogenic therapies) and chemo/radiotherapy for continuous antigen release following ICD.[26] Depending on the result, the therapy should be adapted with following TME reshaping and ICBIs therapies if needed.[65]

1.5. Conclusions

Immunotherapy has changed completely the way cancers are treated, first with the approval of checkpoint blockade inhibitors (Ipilimumab (Yervoy) in 2011, Nivolumab (Opdivo) in 2014, Pembrolizumab (Keytruda) in 2015, Atezolizumab (Tecentriq) in 2016, Avelumab (Bavencio) in 2015, Durvalumab (Imfinzi) in 2016, Cemiplimab (Libtayo) in 2018), more recently with CAR T-cell technology (Tisagenlecleucel (Kymriah) and Axicabtagene ciloleucel (Yescarta) in 2017, Brexucabtagene autoleucel (Tecartus) in 2020 and lastly Lisocabtagene maraleucel in 2021) but only one therapeutic cancer vaccine (DC cancer vaccine Sipuleucel-T (Provenge) in 2010).[215,216] Cancer vaccines success is currently limited by the ability of the antigen to induce a proper immune response. In this Chapter we have introduced nanoparticles as an antigen delivery platform that could increase vaccination efficiency. However, no formulation has shown clinical benefit until now. One reason might be the antigen source, since most vaccines rely on neoantigens, but tumors have developed mechanisms to evade the recognition of neoantigens by the immune system. A second cause is the heterogeneity of tumors and their microenvironment, which cannot be predicted *in vitro* and *in vivo*, since mouse models are limited by the use of well-known mice strains and tumor cell lines for experimental reproducibility and consistency. Finally, the changing shape of cancer and the results obtained by other groups suggest that cancer vaccination in a therapeutic setting requires combination treatment with immune checkpoint blockade inhibitors and drugs reshaping the TME to boost its efficacy.

Additionally, most of the research presented in this first chapter was conducted on murine cell lines or murine primary cells (BMDCs), but few works employ human monocyte-derived DCs. For example, most of the formulations cited in **Table 1** were tested in DC2.4 murine DC cell line, RAW murine macrophage cell line and BMDCs, with few PLGA NPs tested on human primary cells. Using human cells and planning experiments that reproduce the complex tumor microenvironment is an important requirement to predict anticancer effects of cancer vaccines in humans and better understand the poor translatability of nanoparticle-based cancer vaccines in the clinic.

1.6. References

1. Miller, K. D. *et al.* Cancer treatment and survivorship statistics, 2019. *CA. Cancer J. Clin.* **69**, 363–385 (2019).

2. Dagogo-Jack, I. & Shaw, A. T. Tumour heterogeneity and resistance to cancer therapies. *Nat. Rev. Clin. Oncol.* **15**, 81–94 (2018).

3. Oiseth, S. J. & Aziz, M. S. Cancer immunotherapy: a brief review of the history, possibilities, and challenges ahead. *J. Cancer Metastasis Treat.* **3**, 250 (2017).

4. Waldman, A. D., Fritz, J. M. & Lenardo, M. J. A guide to cancer immunotherapy: from T cell basic science to clinical practice. *Nat. Rev. Immunol.* **20**, 651–668 (2020).

5. Herr, H. W. & Morales, A. History of Bacillus Calmette-Guerin and Bladder Cancer: An Immunotherapy Success Story. *J. Urol.* **179**, 53–56 (2008).

6. Finn, O. J. Immuno-oncology: Understanding the function and dysfunction of the immune system in cancer. *Ann. Oncol.* **23**, viii6–viii9 (2012).

7. Hanahan, D. & Weinberg, R. A. The Hallmarks of Cancer. *Cell* **100**, 57–70 (2000).

8. Hanahan, D. & Weinberg, R. A. Hallmarks of cancer: The next generation. *Cell* **144**, 646–674 (2011).

9. Yi, Q. *et al.* Optimizing dendritic cell-based immunotherapy in multiple myeloma: intranodal injections of idiotype-pulsed CD40 ligand- matured vaccines led to induction of type-1 and cytotoxic T-cell immune responses in patients. *Br J Haematol.* **150**, 554–564 (2010).

10. Hubo, M. *et al.* Costimulatory molecules on immunogenic versus tolerogenic human dendritic cells. *Front. Immunol.* **4**, 1–14 (2013).

11. Katz, S. G. & Rabinovich, P. M. *T Cell Reprogramming Against Cancer*. *Methods Mol Biol* **2097**, (2020).

12. Voskoboinik, I., Whisstock, J. C. & Trapani, J. A. Perforin and granzymes:

Function, dysfunction and human pathology. *Nat. Rev. Immunol.* **15**, 388–400 (2015).

13. Waldman, A. D., Fritz, J. M. & Lenardo, M. J. A guide to cancer immunotherapy: from T cell basic science to clinical practice. *Nat. Rev. Immunol.* **20**, 651–668 (2020).

14. Zitvogel, L. & Faure, F. Cancer immunotherapy. *Sciences (New. York).* **342**, 1432–1433 (2013).

15. Sharpe, A. H. Introduction to checkpoint inhibitors and cancer immunotherapy. *Immunol. Rev.* **276**, 5–8 (2017).

16. Graciotti, M., Berti, C., Klok, H. A. & Kandalaft, L. The era of bioengineering : how will this affect the next generation of cancer immunotherapy ? *J. Transl. Med.* 1–16 (2017). doi:10.1186/s12967-017-1244-2

17. Fridman, W. H., Zitvogel, L., Sautès-Fridman, C. & Kroemer, G. The immune contexture in cancer prognosis and treatment. *Nat. Rev. Clin. Oncol.* **14**, 717–734 (2017).

18. Berraondo, P. *et al.* Cytokines in clinical cancer immunotherapy. *Br. J. Cancer* **120**, 6–15 (2019).

19. Boyman, O. & Sprent, J. The role of interleukin-2 during homeostasis and activation of the immune system. *Nat. Rev. Immunol.* **12**, 180–190 (2012).

20. Kennedy, L. B. & Salama, A. K. S. A review of cancer immunotherapy toxicity. *CA. Cancer J. Clin.* **70**, 86–104 (2020).

21. Berraondo, P. *et al.* Cytokines in clinical cancer immunotherapy. *Br. J. Cancer* **120**, 6–15 (2019).

22. Yan, Y. *et al.* Combining Immune Checkpoint Inhibitors With Conventional Cancer Therapy. *Front. Immunol.* **9**, 1739 (2018).

23. Salama, A. K. S. & Force, J. First-line treatment of metastatic melanoma: role of nivolumab. *ImmunoTargets Ther.* **6**, 1–10 (2017).

24. Finck, A., Gill, S. I. & June, C. H. Cancer immunotherapy comes of age and looks for maturity. *Nat. Commun.* **11**, 1–4 (2020).

25. Tsimberidou, A. M., Fountzilas, E., Nikanjam, M. & Kurzrock, R. Review of precision cancer medicine: Evolution of the treatment paradigm. *Cancer Treat. Rev.* **86**, 102019 (2020).

26. Harari, A., Graciotti, M., Bassani-Sternberg, M. & Kandalaft, L. E. Antitumour dendritic cell vaccination in a priming and boosting approach. *Nat. Rev. Drug Discov.* **19**, 635–652 (2020).

27. Isser, A., Livingston, N. K. & Schneck, J. P. Biomaterials to enhance antigen-specific T cell expansion for cancer immunotherapy. *Biomaterials* **268**, 120584 (2021).

28. Isser, A., Livingston, N. K. & Schneck, J. P. Biomaterials to enhance antigen-specific T cell expansion for cancer immunotherapy. *Biomaterials* **268**, 120584 (2021).

29. Lokhov, P. G. & Balashova, E. E. Antigenic Essence: Upgrade of Cellular Cancer Vaccines. *Cancers (Basel).* **13**, 774 (2021).

30. Finck, A., Gill, S. I. & June, C. H. Cancer immunotherapy comes of age and looks for maturity. *Nat. Commun.* **11**, 1–4 (2020).

31. Giordano-Attianese, G. *et al.* A computationally designed chimeric antigen receptor provides a small-molecule safety switch for T-cell therapy. *Nat. Biotechnol.* **38**, 426–432 (2020).

32. Jou, J., Harrington, K. J., Zocca, M. B., Ehrnrooth, E. & Cohen, E. E. W. The changing landscape of therapeutic cancer vaccines-novel platforms and neoantigen identification. *Clin. Cancer Res.* **27**, 689–703 (2021).

33. Hu, Z., Ott, P. A. & Wu, C. J. Towards personalized, tumour-specific, therapeutic vaccines for cancer. *Nat. Rev. Immunol.* **18**, 168–182 (2018).

34. Tan, S., Li, D. & Zhu, X. Cancer immunotherapy: Pros, cons and beyond. *Biomed. Pharmacother.* **124**, (2020).

35. Martin, J. D., Cabral, H., Stylianopoulos, T. & Jain, R. K. Improving cancer immunotherapy using nanomedicines: progress, opportunities and challenges. *Nat. Rev. Clin. Oncol.* **17**, 251–266 (2020).

36. Rappuoli, R., Pizza, M., Del Giudice, G. & De Gregorio, E. Vaccines, new opportunities for a new society. *Proc. Natl. Acad. Sci. U. S. A.* **111**, 12288–12293 (2014).

37. Plotkin, S. A. & Plotkin, S. L. The development of vaccines: How the past led to the future. *Nat. Rev. Microbiol.* **9**, 889–893 (2011).

38. Alard, E. *et al.* Advances in Anti-Cancer Immunotherapy: Car-T Cell, Checkpoint Inhibitors, Dendritic Cell Vaccines, and Oncolytic Viruses, and Emerging Cellular and Molecular Targets. *Cancers (Basel).* **12**, 1–38 (2020).

39. Anassi, E. & Ndefo, U. A. Sipuleucel-T (Provenge) injection the first immunotherapy agent (Vaccine) for hormone-refractory prostate cancer. *P T* **36**, 197–202 (2011).

40. Jou, J., Harrington, K. J., Zocca, M.-B., Ehrnrooth, E. & Cohen, E. E. W. The Changing Landscape of Therapeutic Cancer Vaccines—Novel Platforms and Neoantigen Identification. *Clin. Cancer Res.* **27**, 689–703 (2021).

41. Wimmers, F., Schreibelt, G., Sköld, A. E., Figdor, C. G. & De Vries, I. J. M. Paradigm shift in dendritic cell-based immunotherapy: From in vitro generated monocyte-derived DCs to naturally circulating DC subsets. *Front. Immunol.* **5**, 1–12 (2014).

42. Bol, K. F. *et al.* The clinical application of cancer immunotherapy based on naturally circulating dendritic cells. *J. Immunother. Cancer* **7**, 1–13 (2019).

43. Saxena, M., Balan, S., Roudko, V. & Bhardwaj, N. Towards superior dendritic-cell vaccines for cancer therapy. *Nat. Biomed. Eng.* **2**, 341–344 (2018).

44. Daniotti, J. L., Lardone, R. D. & Vilcaes, A. A. Dysregulated expression of glycolipids in tumor cells: From Negative Modulator of Anti-tumor Immunity to Promising Targets for Developing Therapeutic Agents. *Front. Oncol.* **5**, 1–11 (2016).

45. Smith, C. C. *et al.* Alternative tumour-specific antigens. *Nat. Rev. Cancer* **19**, 465–478 (2019).

46. Banchereau, J. & Palucka, K. Cancer vaccines on the move. *Nat. Rev. Clin.*

Oncol. **15**, 9–10 (2018).

47. Calvo Tardón, M., Allard, M., Dutoit, V., Dietrich, P. Y. & Walker, P. R. Peptides as cancer vaccines. *Curr. Opin. Pharmacol.* **47**, 20–26 (2019).

48. Maeng, H., Terabe, M. & Berzofsky, J. A. Cancer vaccines : translation from mice to human clinical trials. *Curr. Opin. Immunol.* **51**, 111–122 (2018).

49. Shetty, K. & Ott, P. A. Personal Neoantigen Vaccines for the Treatment of Cancer. *Annu. Rev. Cancer Biol.* **5**, 259–276 (2021).

50. Maeng, H., Terabe, M. & Berzofsky, J. A. Cancer vaccines : translation from mice to human clinical trials. *Curr. Opin. Immunol.* **51**, 111–122 (2018).

51. Cachot, A. *et al.* Tumor-specific cytolytic CD4 T cells mediate protective immunity against human cancer. *Sci. Adv.* **7**, eabe3348 (2021).

52. Grimm, J. *et al.* Are dendritic cells the most appropriate therapeutic vaccine for patients with ovarian cancer ? *Curr. Opin. Biotechnol.* **65**, 190–196 (2020).

53. Briquez, P. S. *et al.* Engineering Targeting Materials for Therapeutic Cancer Vaccines. *Front. Bioeng. Biotechnol.* **8**, 1–26 (2020).

54. Neller, M. A., López, J. A. & Schmidt, C. W. Antigens for cancer immunotherapy. *Semin. Immunol.* **20**, 286–295 (2008).

55. Chiang, C. L., Coukos, G. & Kandalaft, L. E. Whole Tumor Antigen Vaccines: Where Are We? *Vaccines* **3**, 344–372 (2015).

56. Chiang, C. L., Ledermann, J. A., Rad, A. N., Katz, D. R. & Chain, B. M. Hypochlorous acid enhances immunogenicity and uptake of allogeneic ovarian tumor cells by dendritic cells to cross-prime tumor-specific T cells. *Cancer Immunol. Immunother.* **55**, 1384–1395 (2006).

57. Prokopowicz, Z. M. *et al.* Hypochlorous Acid: A Natural Adjuvant That Facilitates Antigen Processing, Cross-Priming, and the Induction of Adaptive Immunity. *J. Immunol.* **184**, 824–835 (2010).

58. Graciotti, M. *et al.* Deciphering the Mechanisms of Improved Immunogenicity of Hypochlorous Acid-Treated Antigens in Anti-Cancer Dendritic Cell-Based Vaccines. *Vaccines* **8**, 1–24 (2020).

59. Chiang, C. L. *et al.* Cancer Therapy : Preclinical Oxidation of Ovarian Epithelial Cancer Cells by Hypochlorous Acid Enhances Immunogenicity and StimulatesT Cells that Recognize Autologous Primary T umor. *Clin. Cancer Res.* **14**, 4898–4908 (2008).

60. Tanyi, J. L. *et al.* Personalized cancer vaccine effectively mobilizes antitumor T cell immunity in ovarian cancer. *Sci.Transl.Med.* **10**, 1–15 (2018).

61. Tanyi, J. L. *et al.* Personalized cancer vaccine strategy elicits polyfunctional T cells and demonstrates clinical benefits in ovarian cancer. *npj Vaccines* **6**, 1–14 (2021).

62. Dafni, U. *et al.* Efficacy of cancer vaccines in selected gynaecological breast and ovarian cancers : A 20-year systematic review and meta-analysis. *Eur. J. Cancer* **142**, 63–82 (2021).

63. Saung, M. T., Ke, X., Howard, G. P., Zheng, L. & Mao, H. Particulate carrier systems as adjuvants for cancer vaccines. *Biomater. Sci.* **7**, 4873–4887 (2019).

64. Bisso, S. & Leroux, J. C. Nanopharmaceuticals: A focus on their clinical translatability. *Int. J. Pharm.* **578**, (2020).

65. Martin, J. D., Cabral, H., Stylianopoulos, T. & Jain, R. K. Improving cancer immunotherapy using nanomedicines: progress, opportunities and challenges. *Nat. Rev. Clin. Oncol.* **17**, 251–266 (2020).

66. Salatin, S. & Yari Khosroushahi, A. Overviews on the cellular uptake mechanism of polysaccharide colloidal nanoparticles. *J. Cell. Mol. Med.* **21**, 1668–1686 (2017).

67. Liu, K. & Nussenzweig, M. C. Origin and development of dendritic cells. *Immunol. Rev.* **234**, 45–54 (2010).

68. Banchereau, J. *et al.* Immunobiology of Dendritic Cells. *Annu. Rev. Immunol.* **18**, 767–811 (2000).

69. Manolova, V. *et al.* Nanoparticles target distinct dendritic cell populations according to their size. *Eur. J. Immunol.* **38**, 1404–1413 (2008).

70. Shima, F., Uto, T., Akagi, T., Baba, M. & Akashi, M. Size effect of amphiphilic

poly(γ-glutamic acid) nanoparticles on cellular uptake and maturation of dendritic cells in vivo. *Acta Biomater.* **9**, 8894–8901 (2013).

71. Jia, J. *et al.* Interactions Between Nanoparticles and Dendritic Cells: From the Perspective of Cancer Immunotherapy. *Front. Oncol.* **8**, 1–11 (2018).

72. Hilligan, K. L. & Ronchese, F. Antigen presentation by dendritic cells and their instruction of CD4+ T helper cell responses. *Cell. Mol. Immunol.* **17**, 587–599 (2020).

73. Foroozandeh, P. & Aziz, A. A. Insight into Cellular Uptake and Intracellular Trafficking of Nanoparticles. *Nanoscale Res. Lett.* **13**, (2018).

74. Mosquera, J., García, I. & Liz-Marzán, L. M. Cellular Uptake of Nanoparticles versus Small Molecules: A Matter of Size. *Acc. Chem. Res.* **51**, 2305–2313 (2018).

75. Almeida, M. S. De, Susnik, E., Drasler, B. & Rothen-rutishauser, B. Understanding nanoparticle endocytosis to improve targeting strategies in nanomedicine. *Chem Soc Rev* (2021). doi:10.1039/d0cs01127d

76. Reed, S. G., Orr, M. T. & Fox, C. B. Key roles of adjuvants in modern vaccines. *Nat. Med.* **19**, 1597–1608 (2013).

77. Chang, T. Z., Stadmiller, S. S., Staskevicius, E. & Champion, J. A. Effects of ovalbumin protein nanoparticle vaccine size and coating on dendritic cell processing. *Biomater. Sci.* **5**, 223–233 (2017).

78. Koppolu, B. & Zaharoff, D. A. The effect of antigen encapsulation in chitosan particles on uptake, activation and presentation by antigen presenting cells. *Biomaterials* **34**, 2359–2369 (2013).

79. Zhou, S. *et al.* Engineering ApoE3-incorporated biomimetic nanoparticle for efficient vaccine delivery to dendritic cells via macropinocytosis to enhance cancer immunotherapy. *Biomaterials* **235**, 119795 (2020).

80. Burgdorf, S. & Kurts, C. Endocytosis mechanisms and the cell biology of antigen presentation. *Curr. Opin. Immunol.* **20**, 89–95 (2008).

81. Verma, A. & Stellacci, F. Effect of Surface Properties on Nanoparticle – Cell

Interactions. *Small* 12–21 (2010). doi:10.1002/smll.200901158

82. El-Sayed, N., Korotchenko, E., Scheiblhofer, S., Weiss, R. & Schneider, M. Functionalized multifunctional nanovaccine for targeting dendritic cells and modulation of immune response. *Int. J. Pharm.* **593**, 120123 (2021).

83. Mou, Y. *et al.* The Effect of Superparamagnetic Iron Oxide Nanoparticle Surface Charge on Antigen Cross-Presentation. *Nanoscale Res. Lett.* **12**, (2017).

84. Chiu, Y. L. *et al.* The characteristics, cellular uptake and intracellular trafficking of nanoparticles made of hydrophobically-modified chitosan. *J. Control. Release* **146**, 152–159 (2010).

85. Shima, F., Akagi, T., Uto, T. & Akashi, M. Manipulating the antigen-specific immune response by the hydrophobicity of amphiphilic poly(γ-glutamic acid) nanoparticles. *Biomaterials* **34**, 9709–9716 (2013).

86. Dong, H. *et al.* Polyethyleneimine modification of aluminum hydroxide nanoparticle enhances antigen transportation and cross-presentation of dendritic cells. *Int. J. Nanomedicine* **13**, 3353–3365 (2018).

87. Bastings, M. M. C. *et al.* Modulation of the Cellular Uptake of DNA Origami through Control over Mass and Shape. *Nano Lett.* **18**, 3557–3564 (2018).

88. Sharma, G. *et al.* Polymer particle shape independently influences binding and internalization by macrophages. *J. Control. Release* **147**, 408–412 (2010).

89. Doshi, N. & Mitragotri, S. Macrophages recognize size and shape of their targets. *PLoS One* **5**, 1–6 (2010).

90. Paul, D. *et al.* Phagocytosis dynamics depends on target shape. *Biophys. J.* **105**, 1143–1150 (2013).

91. Yao, C. *et al.* Effect of elasticity on the phagocytosis of micro/nanoparticles. *J. Mater. Chem. B* **8**, 2381–2392 (2020).

92. Anselmo, A. C. *et al.* Elasticity of Nanoparticles Influences Their Blood Circulation, Phagocytosis, Endocytosis, and Targeting. *ACS Nano* **9**, 3169–3177 (2015).

93. Anselmo, A. C. & Mitragotri, S. Impact of particle elasticity on particle-based

drug delivery systems. *Adv. Drug Deliv. Rev.* **108**, 51–67 (2017).

94. Trombetta, E. S. & Mellman, I. Cell biology of antigen processing in vitro and in vivo. *Annu. Rev. Immunol.* **23**, 975–1028 (2005).

95. Kastenmüller, W., Kastenmüller, K., Kurts, C. & Seder, R. A. Dendritic cell-targeted vaccines-hope or hype? *Nat. Rev. Immunol.* **14**, 705–711 (2014).

96. Stead, S. O. *et al.* Murine and Non-Human Primate Dendritic Cell Targeting Nanoparticles for in Vivo Generation of Regulatory T-Cells. *ACS Nano* **12**, 6637–6647 (2018).

97. Wei, H. *et al.* Targeted delivery of tumor antigens to activated dendritic cells via CD11c molecules induces potent antitumor immunity in mice. *Clin. Cancer Res.* **15**, 4612–4621 (2009).

98. Bandyopadhyay, A., Fine, R. L., Demento, S., Bockenstedt, L. K. & Fahmy, T. M. The impact of nanoparticle ligand density on dendritic-cell targeted vaccines. *Biomaterials* **32**, 3094–3105 (2011).

99. Tacken, P. J., De Vries, I. J. M., Torensma, R. & Figdor, C. G. Dendritic-cell immunotherapy: From ex vivo loading to in vivo targeting. *Nat. Rev. Immunol.* **7**, 790–802 (2007).

100. De Coen, R. *et al.* PH-Degradable Mannosylated Nanogels for Dendritic Cell Targeting. *Biomacromolecules* **17**, 2479–2488 (2016).

101. Cruz, L. J. *et al.* Targeting nanoparticles to CD40 , DEC-205 or CD11c molecules on dendritic cells for ef fi cient CD8 + T cell response : A comparative study. *J. Control. Release* **192**, 209–218 (2014).

102. Liu, Y. *et al.* Dendritic Cell Targeting Peptide-Based Nanovaccines for Enhanced Cancer Immunotherapy. *ACS Appl. Bio Mater.* **2**, 1241–1254 (2019).

103. Castro, F. *et al.* Chitosan/γ-PGA nanoparticles-based immunotherapy as adjuvant to radiotherapy in breast cancer. *Biomaterials* **257**, (2020).

104. Shi, G. N. *et al.* Enhanced antitumor immunity by targeting dendritic cells with tumor cell lysate-loaded chitosan nanoparticles vaccine. *Biomaterials* **113**, 191–202 (2017).

105. Xu, C. *et al.* Immunostimulatory effect of N-2-hydroxypropyltrimethyl ammonium chloride chitosan-sulfate chitosan complex nanoparticles on dendritic cells. *Carbohydr. Polym.* **251**, 117098 (2021).

106. Bachelder, E. M., Pino, E. N. & Ainslie, K. M. Acetalated Dextran: A Tunable and Acid-Labile Biopolymer with Facile Synthesis and a Range of Applications. *Chem. Rev.* **117**, 1915–1926 (2017).

107. Chen, N. *et al.* Tunable degradation of acetalated dextran microparticles enables controlled vaccine adjuvant and antigen delivery to modulate adaptive immune responses. *J. Control. Release* **273**, 147–159 (2018).

108. Sinha, A. *et al.* Carbohydrate-Functionalized rGO as an Effective Cancer Vaccine for Stimulating Antigen-Specific Cytotoxic T Cells and Inhibiting Tumor Growth. *Chem. Mater.* **29**, 6883–6892 (2017).

109. Kordalivand, N. *et al.* Cationic synthetic long peptides-loaded nanogels : An e ffi cient therapeutic vaccine formulation for induction of T-cell responses. *J. Control. Release* **315**, 114–125 (2019).

110. Zhang, C. *et al.* Targeted antigen delivery to dendritic cell via functionalized alginate nanoparticles for cancer immunotherapy. *J. Control. Release* **256**, 170–181 (2017).

111. Yuan, J. *et al.* Preparation of self-assembled nanoparticles of ε-polylysine-sodium alginate: A sustained-release carrier for antigen delivery. *Colloids Surfaces B Biointerfaces* **171**, 406–412 (2018).

112. Miyazaki, M., Yuba, E., Hayashi, H., Harada, A. & Kono, K. Development of pH-Responsive Hyaluronic Acid-Based Antigen Carriers for Induction of Antigen-Specific Cellular Immune Responses. *ACS Biomater. Sci. Eng.* **5**, 5790–5797 (2019).

113. Liu, L. *et al.* Hyaluronic Acid-Modified Cationic Lipid-PLGA Hybrid Nanoparticles as a Nanovaccine Induce Robust Humoral and Cellular Immune Responses. *ACS Appl. Mater. Interfaces* **8**, 11969–11979 (2016).

114. Kageyama, S. *et al.* Dose-dependent effects of NY-ESO-1 protein vaccine complexed with cholesteryl pullulan (CHP-NY-ESO-1) on immune responses

and survival benefits of esophageal cancer patients. *J. Transl. Med.* **11**, 1–10 (2013).

115. Kageyama, S. *et al.* Randomized phase II clinical trial of NY-ESO-1 protein vaccine combined with cholesteryl pullulan (CHP-NY-ESO-1) in resected esophageal cancer patients. *Ann. Oncol.* **30**, v496 (2019).

116. El-Sayed, N., Korotchenko, E., Scheiblhofer, S., Weiss, R. & Schneider, M. Functionalized multifunctional nanovaccine for targeting dendritic cells and modulation of immune response. *Int. J. Pharm.* **593**, 120123 (2021).

117. Lin, S. F. *et al.* Surface assembly of poly(I:C) on polyethyleneimine-modified gelatin nanoparticles as immunostimulatory carriers for mucosal antigen delivery. *J. Biomed. Mater. Res. - Part B Appl. Biomater.* **107**, 1228–1237 (2019).

118. Zhu, G. *et al.* Albumin/vaccine nanocomplexes that assemble in vivo for combination cancer immunotherapy. *Nat. Commun.* **8**, (2017).

119. Dong, X. *et al.* A Visible Codelivery Nanovaccine of Antigen and Adjuvant with Self-Carrier for Cancer Immunotherapy. *ACS Appl. Mater. Interfaces* **11**, 4876–4888 (2019).

120. Temizoz, B., Kuroda, E. & Ishii, K. J. Vaccine adjuvants as potential cancer immunotherapeutics. *Int. Immunol.* **28**, 329–338 (2016).

121. Koudelka, K. J., Pitek, A. S., Manchester, M. & Steinmetz, N. F. Virus-Based Nanoparticles as Versatile Nanomachines. *Annu. Rev. Virol.* **2**, 379–401 (2015).

122. Chang, M. H. *et al.* Decreased incidence of hepatocellular carcinoma in hepatitis B vaccinees: A 20-year follow-up study. *J. Natl. Cancer Inst.* **101**, 1348–1355 (2009).

123. Heuts, J. *et al.* Cationic Liposomes: A Flexible Vaccine Delivery System for Physicochemically Diverse Antigenic Peptides. *Pharm. Res.* **35**, (2018).

124. Affandi, A. J. *et al.* Selective tumor antigen vaccine delivery to human CD169+ antigen-presenting cells using ganglioside-liposomes. *Proc. Natl. Acad. Sci. U. S. A.* **117**, 27528–27539 (2020).

125. Kranz, L. M. *et al.* Systemic RNA delivery to dendritic cells exploits antiviral defence for cancer immunotherapy. *Nature* **534**, 396–401 (2016).

126. Sayour, E. J. *et al.* Systemic activation of antigen-presenting cells via RNA-Loaded nanoparticles. *Oncoimmunology* **6**, 1–14 (2017).

127. Oberli, M. A. *et al.* Lipid Nanoparticle Assisted mRNA Delivery for Potent Cancer Immunotherapy. *Nano Lett.* **17**, 1326–1335 (2017).

128. Sayour, E. J., Mendez-Gomez, H. R. & Mitchell, D. A. Cancer vaccine immunotherapy with RNA-loaded liposomes. *Int. J. Mol. Sci.* **19**, (2018).

129. Jin, J. O. *et al.* Nucleic acid nanotechnology for cancer treatment. *Biochim. Biophys. Acta - Rev. Cancer* **1874**, 188377 (2020).

130. Comberlato, A., Paloja, K. & Bastings, M. M. C. Nucleic acids presenting polymer nanomaterials as vaccine adjuvants. *J. Mater. Chem. B* **7**, 6321–6346 (2019).

131. Qi, X. *et al.* RNA Origami Nanostructures for Potent and Safe Anticancer Immunotherapy. (2020). doi:10.1021/acsnano.0c00602

132. Liu, S. *et al.* A DNA nanodevice-based vaccine for cancer immunotherapy. *Nat. Mater.* **20**, (2020).

133. Khisamutdinov, E. F. *et al.* Enhancing immunomodulation on innate immunity by shape transition among RNA triangle, square and pentagon nanovehicles. *Nucleic Acids Res.* **42**, 9996–10004 (2014).

134. Iranpour, S., Nejati, V., Delirezh, N., Biparva, P. & Shirian, S. Enhanced stimulation of anti-breast cancer T cells responses by dendritic cells loaded with poly lactic-co-glycolic acid (PLGA) nanoparticle encapsulated tumor antigens. *J. Exp. Clin. cancer Res.* **35**, 1–11 (2016).

135. Shashi Prasad, Virginia Cody, Jennifer K. Saucier-Sawyer, Tarek R. Fadel, Richard L. Edelson, Martin A. Birchall, D. J. H. Optimization of Stability, Encapsulation, Release, and Cross- Priming of Tumor Antigen-Containing PLGA Nanoparticles. *Pharm. Res.* **29**, 2565–2577 (2012).

136. Hanlon, D. J. Enhanced stimulation of anti-ovarian cancer CD8+ T cells by

dendritic cells loaded with nanoparticle encapsulated tumor antigen. *Am J Reprod Immunol* **65**, 597–609 (2011).

137. Mueller, M., Reichardt, W., Koerner, J. & Groettrup, M. Coencapsulation of tumor lysate and CpG-ODN in PLGA-microspheres enables successful immunotherapy of prostate carcinoma in TRAMP mice. *J. Control. Release* **162**, 159–166 (2012).

138. Gross, B. P. *et al.* Biotinylated Streptavidin Surface Coating Improves the Efficacy of a PLGA Microparticle-Based Cancer Vaccine. *Bioconjug. Chem.* **31**, 2147–2157 (2020).

139. Rosalia, R. A. *et al.* CD40-targeted dendritic cell delivery of PLGA-nanoparticle vaccines induce potent anti-tumor responses. *Biomaterials* **40**, 88–97 (2015).

140. Jahan, S. T., Sadat, S. M. A., Yarahmadi, M. & Haddadi, A. Potentiating Antigen Specific Immune Response by Targeted Delivery of the PLGA-Based Model Cancer Vaccine. *Mol. Pharm.* **16**, 498–509 (2019).

141. Zhang, Q. *et al.* Employing ATP as a New Adjuvant Promotes the Induction of Robust Antitumor Cellular Immunity by a PLGA Nanoparticle Vaccine. *ACS Appl. Mater. Interfaces* **12**, 54399–54414 (2020).

142. Ma, J. *et al.* Copresentation of Tumor Antigens and Costimulatory Molecules via Biomimetic Nanoparticles for Effective Cancer Immunotherapy. *Nano Lett.* **20**, 4084–4094 (2020).

143. Li, H. *et al.* Rational design of polymeric hybrid micelles to overcome lymphatic and intracellular delivery barriers in cancer immunotherapy. *Theranostics* **7**, (2017).

144. Zhao, Y., Zhao, X., Cheng, Y., Guo, X. & Yuan, W. Iron Oxide Nanoparticles-Based Vaccine Delivery for Cancer Treatment. *Mol. Pharm.* **15**, 1791–1799 (2018).

145. Lee, J. Y., Kim, M. K., Nguyen, T. L. & Kim, J. Hollow Mesoporous Silica Nanoparticles with Extra-Large Mesopores for Enhanced Cancer Vaccine. *ACS Appl. Mater. Interfaces* **12**, 34658–34666 (2020).

146. Li, X., Wang, X., Ito, A. & Tsuji, N. M. A nanoscale metal organic frameworks-based vaccine synergises with PD-1 blockade to potentiate anti-tumour immunity. *Nat. Commun.* **11**, (2020).

147. Kang, S. *et al.* Effects of gold nanoparticle-based vaccine size on lymph node delivery and cytotoxic T-lymphocyte responses. *J. Control. Release* **256**, 56–67 (2017).

148. Lybaert, L. *et al.* Cancer Cell Lysate Entrapment in CaCO3 Engineered with Polymeric TLR-Agonists: Immune-Modulating Microparticles in View of Personalized Antitumor Vaccination. *Chem. Mater.* **29**, 4209–4217 (2017).

149. Moran, H. B. T., Turley, J. L., Andersson, M. & Lavelle, E. C. Immunomodulatory properties of chitosan polymers. *Biomaterials* **184**, 1–9 (2018).

150. Garg, U., Chauhan, S., Nagaich, U. & Jain, N. Current Advances in Chitosan Nanoparticles Based Drug Delivery and Targeting. *Adv. Pharm. Bull.* **9**, 195–204 (2019).

151. Wang, S., Fontana, F., Shahbazi, M.-A. & Santos, H. A. Acetalated dextran based nano- and microparticles: synthesis, fabrication, and therapeutic applications. *Chem. Commun.* (2021). doi:10.1039/d1cc00811k

152. Nesamony, J., Singh, P. R., Nada, S. E., Shah, Z. A. & Kolling, W. M. Calcium alginate nanoparticles synthesized through a novel interfacial cross-linking method as a potential protein drug delivery system. *J. Pharm. Sci.* **101**, 2177–2184 (2012).

153. Kim, J. H., Moon, M. J., Kim, D. Y., Heo, S. H. & Jeong, Y. Y. Hyaluronic acid-based nanomaterials for cancer therapy. *Polymers (Basel).* **10**, 1–15 (2018).

154. Ding, L., Jiang, Y., Zhang, J., Klok, H. A. & Zhong, Z. PH-Sensitive Coiled-Coil Peptide-Cross-Linked Hyaluronic Acid Nanogels: Synthesis and Targeted Intracellular Protein Delivery to CD44 Positive Cancer Cells. *Biomacromolecules* **19**, 555–562 (2018).

155. Li, S. *et al.* Redox-Sensitive and Intrinsically Fluorescent Photoclick Hyaluronic Acid Nanogels for Traceable and Targeted Delivery of Cytochrome c to Breast

Tumor in Mice. *ACS Appl. Mater. Interfaces* **8**, 21155–21162 (2016).

156. Yuan, H. *et al.* Preparation of cholesteryl-modified aminated pullulan nanoparticles to evaluate nanoparticle of hydrophobic degree on drug release and cytotoxicity. *J. Nanomater.* **2020**, (2020).

157. Zhang, T. *et al.* Research progress of self-assembled nanogel and hybrid hydrogel systems based on pullulan derivatives. *Drug Deliv.* **25**, 278–292 (2018).

158. Yasmin, R., Shah, M., Khan, S. A. & Ali, R. Gelatin nanoparticles: A potential candidate for medical applications. *Nanotechnol. Rev.* **6**, 191–207 (2017).

159. Hoogenboezem, E. N. & Duvall, C. L. Harnessing albumin as a carrier for cancer therapies. *Adv. Drug Deliv. Rev.* **130**, 73–89 (2018).

160. Sandra, F., Khaliq, N. U., Sunna, A. & Care, A. Developing protein-based nanoparticles as versatile delivery systems for cancer therapy and imaging. *Nanomaterials* **9**, (2019).

161. Neek, M., Kim, T. Il & Wang, S. W. Protein-based nanoparticles in cancer vaccine development. *Nanomedicine Nanotechnology, Biol. Med.* **15**, 164–174 (2019).

162. Diaz, D., Care, A. & Sunna, A. Bioengineering strategies for protein-based nanoparticles. *Genes (Basel).* **9**, (2018).

163. European Medicines Agency (EMA). COVID-19 Vaccine AstraZeneca. 1–34 (2021).

164. Wang, N., Chen, M. & Wang, T. Liposomes used as a vaccine adjuvant-delivery system: From basics to clinical immunization. *J. Control. Release* **303**, 130–150 (2019).

165. Buschmann, M. D. *et al.* Nanomaterial delivery systems for mRNA vaccines. *Vaccines* **9**, 1–30 (2021).

166. Steinle, H. *et al.* International Council for Harmonisation (ICH) Technical Requirements for Registration of Pharmaceuticals for Human Use, E6(R2) Good Clinical Practice (GCP) Guidance. *Viruses* **12**, 133–143 (2020).

167. Chandrasekaran, A. R. DNA origami and biotechnology applications: A perspective. *J. Chem. Technol. Biotechnol.* **91**, 843–846 (2016).

168. Bila, H., Kurisinkal, E. E. & Bastings, M. M. C. Engineering a stable future for DNA-origami as a biomaterial. *Biomater. Sci.* **7**, 532–541 (2019).

169. Jiang, Q., Liu, S., Liu, J., Wang, Z. & Ding, B. Rationally Designed DNA-Origami Nanomaterials for Drug Delivery In Vivo. **1804785**, 1–6 (2019).

170. Shen, T. *et al.* Nucleic Acid Immunotherapeutics for Cancer. (2020). doi:10.1021/acsabm.0c00101

171. Afonin, K. A., Dobrovolskaia, M. A., Church, G. & Bathe, M. Opportunities, Barriers, and a Strategy for Overcoming Translational Challenges to Therapeutic Nucleic Acid Nanotechnology. (2020). doi:10.1021/acsnano.0c04753

172. Dobrovolskaia, M. A. Nucleic acid nanoparticles at a crossroads of vaccines and immunotherapies. *Molecules* **24**, (2019).

173. Smith, J. D., Morton, L. D. & Ulery, B. D. Nanoparticles as synthetic vaccines. *Curr. Opin. Biotechnol.* **34**, 217–224 (2015).

174. Prasad, S. *et al.* Polymer nanoparticles containing tumor lysates as antigen delivery vehicles for dendritic cell-based antitumor immunotherapy. *Nanomedicine Nanotechnology, Biol. Med.* **7**, 1–10 (2011).

175. Han, J. *et al.* Polymer-based nanomaterials and applications for vaccines and drugs. *Polymers (Basel).* **10**, 1–14 (2018).

176. Yao, H. *et al.* Effective melanoma immunotherapy with interleukin-2 delivered by a novel polymeric nanoparticle. *Mol. Cancer Ther.* **10**, 1082–1092 (2011).

177. De Titta, A. *et al.* Nanoparticle conjugation of CpG enhances adjuvancy for cellular immunity and memory recall at low dose. *Proc. Natl. Acad. Sci. U. S. A.* **110**, 19902–19907 (2013).

178. Anderson, J. M. & Shive, M. S. Biodegradation and biocompatibility of PLA and PLGA microspheres. *Adv. Drug Deliv. Rev.* **64**, 72–82 (2012).

179. Danhier, F. *et al.* PLGA-based nanoparticles: An overview of biomedical

applications. *J. Control. Release* **161**, 505–522 (2012).

180. Li, Y. P. *et al.* PEGylated PLGA nanoparticles as protein carriers: Synthesis, preparation and biodistribution in rats. *J. Control. Release* **71**, 203–211 (2001).

181. Ajnai, G. *et al.* Trends of Gold Nanoparticle-based Drug Delivery System in Cancer Therapy. *J. Exp. Clin. Med.* **6**, 172–178 (2014).

182. Yang, W., Liang, H., Ma, S., Wang, D. & Huang, J. Gold nanoparticle based photothermal therapy: Development and application for effective cancer treatment. *Sustain. Mater. Technol.* **22**, e00109 (2019).

183. Zhao, Y., Guo, Y. & Tang, L. Engineering cancer vaccines using stimuli-responsive biomaterials. *Nano Res.* **11**, 5355–5371 (2018).

184. Pacifici, N., Bolandparvaz, A. & Lewis, J. S. Stimuli-Responsive Biomaterials for Vaccines and Immunotherapeutic Applications. *Adv. Ther.* **3**, 2000129 (2020).

185. Varypataki, E. M. *et al.* Combined photosensitization and vaccination enable CD8 T-cell immunity and tumor suppression independent of CD4 T-cell help. *Front. Immunol.* **10**, 1–12 (2019).

186. Wang, C. *et al.* Investigation of endosome and lysosome biology by ultra pH-sensitive nanoprobes. *Adv. Drug Deliv. Rev.* **113**, 87–96 (2017).

187. Cabukusta, B. & Neefjes, J. Mechanisms of lysosomal positioning and movement. *Traffic* **19**, 761–769 (2018).

188. Saffi, G. T. & Botelho, R. J. Lysosome Fission: Planning for an Exit. *Trends Cell Biol.* **29**, 635–646 (2019).

189. Wang, C. *et al.* Investigation of endosome and lysosome biology by ultra pH-sensitive nanoprobes. *Adv. Drug Deliv. Rev.* **113**, 87–96 (2017).

190. Morimoto, N. *et al.* Self-assembled pH-sensitive cholesteryl pullulan nanogel as a protein delivery vehicle. *Biomacromolecules* **14**, 56–63 (2013).

191. Wang, C. *et al.* Self-adjuvanted nanovaccine for cancer immunotherapy: Role of lysosomal rupture-induced ROS in MHC class I antigen presentation. *Biomaterials* **79**, 88–100 (2016).

192. Chen, J. *et al.* Improved antigen cross-presentation by polyethyleneimine-based nanoparticles. *Int. J. Nanomedicine* **6**, 77–84 (2011).

193. Qiu, F. *et al.* Poly(propylacrylic acid)-peptide nanoplexes as a platform for enhancing the immunogenicity of neoantigen cancer vaccines. *Biomaterials* **182**, 82–91 (2018).

194. Liu, Q. *et al.* pH-Responsive Poly (D , L - lactic- co -glycolic acid) Nanoparticles with Rapid Antigen Release Behavior Promote Immune. 4925–4938 (2015).

195. Raza, A., Hayat, U., Rasheed, T., Bilal, M. & Iqbal, H. M. N. Redox-responsive nano-carriers as tumor-targeted drug delivery systems. *Eur. J. Med. Chem.* **157**, 705–715 (2018).

196. Zhang, X. *et al.* Recent progress and advances in redox-responsive polymers as controlled delivery nanoplatforms. *Mater. Chem. Front.* **1**, 807–822 (2017).

197. Guo, X. *et al.* Advances in redox-responsive drug delivery systems of tumor microenvironment. *J. Nanobiotechnology* **16**, 1–10 (2018).

198. Yu, S. S. *et al.* Physiologically relevant oxidative degradation of oligo(proline) cross-linked polymeric scaffolds. *Biomacromolecules* **12**, 4357–4366 (2011).

199. Lee, S. H. *et al.* ROS-cleavable proline oligomer crosslinking of polycaprolactone for pro-angiogenic host response. *J. Mater. Chem. B* **2**, 7109–7113 (2014).

200. Napoli, A., Valentini, M., Tirelli, N., Müller, M. & Hubbell, J. A. Oxidation-responsive polymeric vesicles. *Nat. Mater.* **3**, 183–189 (2004).

201. Fukino, T., Yamagishi, H. & Aida, T. Redox-Responsive Molecular Systems and Materials. *Adv. Mater.* **29**, (2017).

202. Lv, M. *et al.* Redox-responsive hyperbranched poly(amido amine) and polymer dots as a vaccine delivery system for cancer immunotherapy. *J. Mater. Chem. B* **5**, 9532–9545 (2017).

203. Yuan, H., Yang, Y., Xue, W. & Liu, Z. Fluorinated Redox-Responsive Poly(amidoamine) as a Vaccine Delivery System for Antitumor

Immunotherapy. *ACS Biomater. Sci. Eng.* **5**, 644–653 (2019).

204. Wang, K., Yang, Y., Xue, W. & Liu, Z. Cell Penetrating Peptide-Based Redox-Sensitive Vaccine Delivery System for Subcutaneous Vaccination. *Mol. Pharm.* **15**, 975–984 (2018).

205. Wei, L., Zhao, Y., Hu, X. & Tang, L. Redox-Responsive Polycondensate Neoepitope for Enhanced Personalized Cancer Vaccine. *ACS Cent. Sci.* **6**, 404–412 (2020).

206. Jin, B., Sun, T., Yu, X. H., Yang, Y. X. & Yeo, A. E. T. The effects of TLR activation on T-cell development and differentiation. *Clin. Dev. Immunol.* **2012**, (2012).

207. Urban-Wojciuk, Z. *et al.* The role of TLRs in anti-cancer immunity and tumor rejection. *Front. Immunol.* **10**, 1–10 (2019).

208. Bode, C., Zhao, G., Steinhagen, F., Kinjo, T. & Klinman, D. M. CpG DNA as a vaccine adjuvant. *Expert Rev Vaccines* **10**, 499–511 (2011).

209. Braunstein, M. J., Kucharczyk, J. & Adams, S. Targeting Toll-Like Receptors for Cancer Therapy. *Target. Oncol.* **13**, 583–598 (2018).

210. Da Silva, C. G. *et al.* Co-delivery of immunomodulators in biodegradable nanoparticles improves therapeutic efficacy of cancer vaccines. *Biomaterials* **220**, (2019).

211. Yang, J. *et al.* Hybrid nanovaccine for the co-delivery of the mRNA antigen and adjuvant. *Nanoscale* **11**, 21782–21789 (2019).

212. Yu, J. W. *et al.* Tumor-immune profiling of murine syngeneic tumor models as a framework to guide mechanistic studies and predict therapy response in distinct tumor microenvironments. *PLoS One* **13**, 1–27 (2018).

213. Shae, D. *et al.* Co-delivery of Peptide Neoantigens and Stimulator of Interferon Genes Agonists Enhances Response to Cancer Vaccines. *ACS Nano* **14**, 9904–9916 (2020).

214. Shofolawe-Bakare, O. T., Stokes, L. D., Hossain, M., Smith, A. E. & Werfel, T. A. Immunostimulatory biomaterials to boost tumor immunogenicity. *Biomater.*

Sci. **8**, 5516–5537 (2020).

215. Vaddepally, R. K., Kharel, P., Pandey, R., Garje, R. & Chandra, A. B. Review of indications of FDA-approved immune checkpoint inhibitors per NCCN guidelines with the level of evidence. *Cancers (Basel).* **12**, 1–19 (2020).

216. FDA approves fourth CAR-T cell therapy. *Nat. News Anal.* **20**, 166 (2021).

2. Polymer Nanoparticle-Mediated Delivery of oxidized Tumor Lysate-based Cancer Vaccines

2.1. Introduction

Cancer vaccination has been acquiring growing interest in oncology, with the aim of stimulating the patient's immune system against tumor cells.[1,2,3,4,5] While the promises of cancer vaccines with very limited side effects have attracted great interest over the past ~ 20 years, results in clinical trials are still limited, or achieved mostly in therapies that combine vaccines with conventional cancer therapies.[6,7,8] One approach to cancer vaccination involves the use of tumor antigens to provoke an immune response. For this purpose, a variety of tumor antigens has been used, which includes both single, unique peptides or proteins, as well as mixtures of specific proteins or peptides, and whole tumor cell lysates. While soluble peptide-based tumor-associated antigens are relatively easy to produce and able to induce antigen-specific cytotoxic T lymphocytes on a large scale, clinical outcomes have been mostly disappointing.[9,10] The use of whole tumor lysate-based vaccines, on the other hand, has the advantage that it allows to challenge the immune system with a broad spectrum of tumor-related epitopes. Interestingly, metadata analysis showed superior clinical benefits with whole tumor lysate antigen-based approaches, compared to peptide-based ones.[11,12]

Effective antigen delivery is a key step towards cancer vaccination. The use of nanoparticle-based formulations has shown promise to improve antigen delivery.[13,14,15,16,17,18,19,20,21,22] On the one hand, the nanoparticle carrier helps to prevent premature degradation of the antigen. In addition, by tailoring size and surface chemistry, nanoparticle-based carriers can also allow targeted delivery to, and augment antigen uptake by dendritic cells. Nanoparticles can also possess inherent immunoregulatory properties that can be beneficial to promote antigen presentation, can stimulate immune responses, and can also promote antigen cross presentation. The use of nanoparticles to enhance cancer immunotherapy has also been explored for the delivery of whole tumor lysate.[23,24,25,26] These studies showed that nanoparticles loaded with tumor lysate were efficiently internalized by monocyte-derived dendritic cells, not toxic, and successfully stimulated T cell proliferation and IFN-γ production when co-cultured with autologous $CD8^+$ T cells.[27,28]

The immunogenicity of whole cell tumor lysate can be further enhanced by treatment with hypochlorous acid (HOCl).[29,30,31] HOCl mediated oxidation has been shown to improve the immunogenicity of proteins *in vivo* and *ex vivo*.[32,33] The stimulation of dendritic cells (DCs) with HOCl-oxidized tumor lysate has been proven safe and has been successfully used in preliminary phase I clinical trials in ovarian cancer.[34,35,36,37] So far, dendritic cell stimulation using oxidized tumor lysate has been performed mostly by challenging the cells directly with the free lysate.

This study investigates the use of poly(lactic-co-glycolic acid) (PLGA) nanoparticles to enhance the delivery of oxidized tumor lysate and compares the therapeutic efficacy of free oxidized tumor lysate vaccine with that of a nanoparticle-based vaccine formulation. In *in vitro* experiments, human donor-derived mo-DCs were used to study the effect of the nanoparticle formulation on antigen uptake and DC viability and activation, and to stimulate autologous peripheral blood mononuclear cells (PBMCs), which were subsequently assessed in a real time live cell co-culture experiment for their cytotoxicity towards A375 melanoma cells. Finally, the PLGA nanoparticle-based oxidized tumor lysate formulation was evaluated *in vivo*

in a therapeutic vaccination model study with B16F10 melanoma-bearing C57BL/6J mice.

2.2. Experimental Section

2.2.1. Materials

mPEG(5.1k)-b-PLGA(50/50)(48k) block copolymer was purchased from Advanced Polymer Materials Inc. (Montreal, Canada). Dichloromethane (DCM) was obtained from Sigma-Aldrich (The Netherlands) and polyvinyl alcohol (PVA, 86-89% hydrolyzed, low molecular weight) from Abcr (GmbH, Germany). The Pierce™ BCA Protein Assay Kit from Life Technologies (Thermo Fisher Scientific, MA USA) was used for protein quantification.

Reagents employed for confocal microscopy and tumor lysate labelling were: CellTrace™ Violet proliferation dye (Life Technologies, Thermo Fisher Scientific, MA USA), WGA-Texas Red (Life Technologies, Thermo Fisher Scientific, MA USA), DRAQ5™ Fluorescent Probe Solution (Life Technologies, Thermo Fisher Scientific, MA USA), Fluoromount-G (Bioconcept AG, Switzerland).

The following dyes and anti-human antibodies were used in flow cytometry experiments: Alexa Fluor® 700 anti-human CD11c (BioLegend) and mouse IgG1 isotype (BioLegend), PE/Cy7 anti-human CD14 (BioLegend), LIVE/DEAD™ Fixable Near-IR Dead Cell (Thermo Fisher Scientific, MA USA), Pacific Blue™ anti-human HLA-DR (BioLegend) and mouse IgG2b isotype (Biolegend), FITC anti-human CD40 (BD Pharming) and mouse IgG1 isotype (BD Pharming), APC/Cy7 anti-human CD83 (BioLegend) and mouse IgG1 isotype (BioLegend), APC anti-human CD86 (BioLegend) and mouse IgG2b isotype (Biolegend), Zombie Aqua™ Fixable Viability Kit (BioLegend), PE-Dazzle594 anti-human CD3 (BioLegend), PerCP/Cy5.5 anti-human CD4 (BioLegend), AlexaFluor® 700 anti-human CD8 (BioLegend), FITC anti-human CD45RA (BioLegend), BV421 anti-human CCR7 (BioLegend).

Adjuvants: CpG oligonucleotide - Murine TLR9 agonist and Poly(I:C) (HMW) for *in vivo* experiments were purchased from InvivoGen Europe (Toulouse, France).

2.2.2. Methods

Double emulsions for nanoparticle preparation were generated using a Branson 450 Digital Sonifier®. Particle sizes and zeta-potentials were analyzed by Dynamic Light Scattering (DLS) using a Zetasizer Nano ZS (Malvern Panalytical LTD, Spectris plc) instrument. Measurements were performed in Milli-Q water at a concentration of 0.02 mg/mL. Flow cytometry analyses were performed using a BD LSRFortessa™ (BD Biosciences, San Jose, CA) instrument. For confocal microscopy, a Zeiss LSM700 Upright confocal and wide field microscope (Carl Zeiss Microscopy GmbH, Jena, Germany) was used. Image collection for the apoptotic-mediated killing assay was conducted with the IncuCyte® S3 Live-Cell Analysis System. Atomic force microscopy (AFM) images were recorded using a Cypher Asylum Research AFM instrument (Oxford Instruments, UK). The measurements were performed in tapping mode using a HQ:NSC14/Al BS cantilever (Mikromasch, USA) with a typical spring constant of 5 N/m.

2.2.3. Procedures

Atomic force microscopy sample preparation. 4 µL of a 0.05 mg/mL nanoparticle solution in Milli-Q water was deposited on a cleaned and plasma-treated silicon wafer (10 mm × 8 mm size). The wafers were dried overnight at room temperature.

Nanoparticle synthesis. First, 50 mg PEG-PLGA block copolymer was dissolved in 2.5 mL dichloromethane (DCM). Then, 500 µL PBS or oxidized tumor lysate (oxTL) were added to the organic phase. The mixture was sonicated for 60 sec with 10 sec intervals at 30 % intensity, added to 5 mL of a 5 wt % solution of PVA in Milli-Q water and sonicated again for 60 sec with 10 sec intervals at 30% intensity to

form a double emulsion. The resulting emulsion was diluted with 5 mL of 0.5 wt % PVA solution in Milli-Q water. After that, the DCM was removed by rotary evaporation. Nanoparticles were isolated by centrifugation (16000 rpm, 10 minutes) and washed three times with pure water. Nanoparticles were collected, lyophilized in 30 mL of 5 wt % sucrose solution and stored at -20 °C for further use.

Protein release. Nanoparticles (0.9-1.3 mg/mL) were incubated in PBS at 37 °C with constant shaking at 200 rpm. At defined timepoints, the nanoparticle suspension was centrifuged to collect the supernatant. The centrifuged particles were resuspended in PBS and the protein content in the supernatant measured by BCA assay following the supplier's instructions.

Preparation of oxidized tumor lysate (oxTL). Oxidized tumor lysate (oxTL) was obtained from A375 cells following a previously reported protocol.[29] Briefly, cells were harvested, incubated for 1 hour at 37 °C with 60 µM HOCl in DPBS (6 µL of a 10 mM HOCl stock solution in PBS was added per mL of cell suspension (1 x 10^6 cells/mL)) and washed extensively with DPBS. For uptake experiments, cells were stained at this point with a 5 mM stock solution of CellTrace™ Violet proliferation dye in DMSO; 1 µL stock solution per million cells was added at this point following manufacturer instructions for a final working concentration of 5 µM. Cells were then subjected to 6 freeze-thaw cycles and subsequently stored at -80 °C until further use.

Generation of monocyte derived DCs. Monocyte-derived dendritic cells (mo-DCs) were generated from monocytes isolated from fresh peripheral blood mononuclear cells (PBMCs) of healthy human donors collected at the local Blood Transfusion Center in Lausanne, Switzerland, under Institutional Review Board approval (Ethics Committee, University Hospital of Lausanne-CHUV). Written informed consent was obtained from all healthy subjects, in accordance with the Declaration of Helsinki. First, PBMCs were isolated by Ficoll density gradient

centrifugation (1000 g, 10 minutes). The PBMC layer was collected, washed three times and resuspended in DPBS + 2% FBS + 2 mM EDTA at 5 x 10^7 cells/mL. Monocytes were isolated using the EasySep™ Human Monocyte Enrichment Kit without CD16 Depletion (STEMCELL Technologies GmbH, Germany). Part of the PBMCs were cryopreserved for subsequent T cell stimulation, while the rest was resuspended in 500 mL DC medium (CellGeniX GmbH, Germany) supplemented with 2% human serum albumin (HSA), 2 mM L-Glutamine, 100 units/mL penicillin and 100 µg/mL streptomycin in the presence of 500 IU/mL recombinant GM-CSF and 250 IU/mL IL-4. Cells were incubated at 37 °C, 5% CO_2 for two days and then replenished with fresh media and cytokines. After other two days, immature monocyte-derived DCs (mo-iDC) were collected for subsequent experiments.

Mo-iDC viability and oxTL/nanoparticle uptake. Mo-iDCs in DC media replenished with 500 IU/mL recombinant GM-CSF and 250 IU/mL IL-4 were plated in 48-well plates (1 x 10^6 cells/mL). Cells were incubated with 100 µL DC media, oxTL-loaded nanoparticles resuspended in 100 µL DC media or free oxTL resuspended in 100 µL DC media at the indicated concentrations (0.5 or 1 mg oxTL-loaded nanoparticles / 10^6 cells and comparable amount of oxTL based on protein content) for 24 hours at 4 and 37 °C. Control mo-iDCs were kept in DC media under the same conditions. Cells were then collected and stained with Alexa Fluor® 700 anti-human CD11c, PE/Cy7 anti-human CD14 and LIVE/DEAD™ Fixable Near-IR Dead Cell reagent (Invitrogen) for FACS analysis. Data acquisition was performed on LSR II Fortessa (BD Biosciences) and data analysis carried out with FlowJo. The gating strategy that was used for data analysis is presented in **Supporting Information Figure S1**.

Confocal microscopy. Cells were plated at 0.2 or 0.4 x 10^6 cells/mL on glass coverslips (0.17 µm thickness) in DC medium in the presence of 1 mg/million cells oxTL-loaded nanoparticles, free oxTL or DC media for 24 hours. The samples were then fixed in 4% paraformaldehyde in DPBS, and stained with WGA-Texas Red (100

µg/mL) to visualize the cell membrane and with DRAQ5™ to stain the nucleus. Excess dye was removed by DPBS washing. Coverslips were then mounted in mounting medium (Fluoromount-G). Image acquisition was performed with a Zeiss LSM 700 confocal microscope with a 63 × NA 1.0 oil objective. Images were processed with ImageJ (National Institutes of Health).

DC maturation. Mo-iDCs were incubated with oxTL-loaded nanoparticles at the indicated concentrations, or free oxTL (in comparable amounts based on protein content) resuspended in 100 µL DC media, or 100 µL DC media for 24 h at 37 °C. After incubation, cells were either kept in culture, or further matured by the addition of IFN-γ (2000 IU/mL) and LPS (60 EU/mL) for 16 h at 37 °C. Finally, cells were collected and cryopreserved for *in vitro* stimulation experiments, or stained with Alexa Fluor® 700 anti-human CD11c, Pacific Blue™ anti-human HLA-DR, FITC anti-human CD40, APC/Cy7 anti-human CD83, APC anti-human CD86 antibodies and Zombie Aqua™ Fixable Viability reagent, washed in PBS and analyzed with flow cytometry. The gating strategy that was used for data analysis is presented in **Supporting Information Figure S2**.

***In vitro*, A375 melanoma cell apoptosis assay.** First, DCs were incubated with 100 µL DC media, or the different antigen source resuspended in 100 µL DC media and further stimulated with LPS and IFN-γ.

The matured DCs were subsequently co-cultured with autologous PBMCs at a 1 : 10 ratio in RPMI cell media (Thermo Fisher Scientific) supplemented with 8% HSA, 2 mM l-glutamine, Na-pyruvate, non-essential amino acids, kanamycin sulfate, 50 mM β-mercaptoethanol, 100 units/mL penicillin and 100 µg/mL streptomycin in presence of interleukin-2 (IL-2) 100 IU/mL. Every two days, cell cultures were replenished with fresh media and IL-2. Stimulation was repeated three times at a one-week interval. After stimulation PBMCs were collected and used for further experiments.

Stimulated PBMCs (or unstimulated PBMCs, as baseline control) were co-cultured with A375 melanoma cells at a 5 : 1 cell ratio in RPMI media supplemented with 8% HSA, 2 mM l-glutamine, Na-pyruvate, non-essential amino acids, kanamycin sulfate, 50 mM β-mercaptoethanol, 100 units/mL penicillin and 100 µg/mL streptomycin in the presence of the apoptotic Caspase 3/7 sensitive dye (IncuCyte). Image collection was conducted every 2 h for up to 48 h with the IncuCyte® S3 Live-Cell Analysis System. Apoptosis quantification was carried out measuring the total green area (μm^2/well) using the IncuCyte S3 v2017A software, defined by setting the limit for the definition of the green areas to 200 μm^2.

***In vivo* therapeutic vaccination of C57BL/6J OlaHsd mice.** Female C57BL/6J OlaHsd mice of 6 weeks of age were purchased from Envigo. Upon arrival, mice were allowed to acclimate for two weeks in a pathogen-free facility prior to vaccination. In two separate experiments, 8-week old mice were subcutaneously challenged with B16F10 melanoma cells (1×10^5 cells). Two days post tumor inoculation, mice were randomly assigned to five treatment groups. Mice were subcutaneously vaccinated with 100 µL PBS, adjuvant (50 µg PolyI:C and 50 µg CpG per mice), oxTL and adjuvant, empty nanoparticles and adjuvants or oxTL-loaded nanoparticles (1.5 mg nanoparticle in 100 µL per animal) and adjuvants. The amount of oxTL was kept the same (122 µg in 100 µL injected volume) in both experiments, either in soluble form or loaded in nanoparticles. Vaccination was repeated three times with one-week interval. Tumour size was measured every other day and mice were sacrificed with CO_2 when the tumor volume reached 1000 mm^3 or when mice showed physical or behavioural distress. This study was approved by the Veterinary Authority of the Swiss Canton Vaud (authorization no. 3308) and performed in accordance with Swiss ethical guidelines.

Statistical analysis. Comparisons between groups were assessed using a two-tailed unpaired Student's t test. Comparison between groups in Incucyte time-

course experiment was assessed using Two-way ANOVA (Post-Hoc Tukey Test) Analysis by GraphPad Prism. Comparison between groups in *in vivo* experiments for survival were assessed using Log-rank (Mantel-Cox) test Analysis by GraphPad Prism. In all statistical analyses * = $p < 0.05$, ** = $p < 0.01$, *** = $p < 0.001$.

2.3. Results and Discussion

2.3.1. Nanoparticle preparation

For vaccine delivery, in order to enhance dendritic cell (DC) uptake and lymphoid trafficking, nanoparticles with sizes around 200 nm are beneficial.[38,39] Oxidized tumor lysate-loaded poly(ethylene glycol)-b-poly(lactic-co-glycolic acid) (PEG-PLGA) nanoparticles were prepared via a double emulsion solvent evaporation protocol as schematically outlined in **Figure 1A**.[40] This protocol, using 4 wt% oxidized tumor lysate (oxTL) with respect to the PEG-PLGA block copolymer, afforded nanoparticles with an average diameter of 161 ± 41 nm and a polydispersity (PDI) of 0.065 according to DLS. Using the same procedure, control, non-loaded PEG-PLGA particles with a diameter of 181 ± 65 nm and PDI of 0.133 were obtained. **Figure 1B** shows a representative atomic force microscopy (AFM) image of OxTL loaded nanoparticles. Analysis of these images affords a particle diameter of 168 ± 33 nm, which agrees well with the results obtained with DLS.

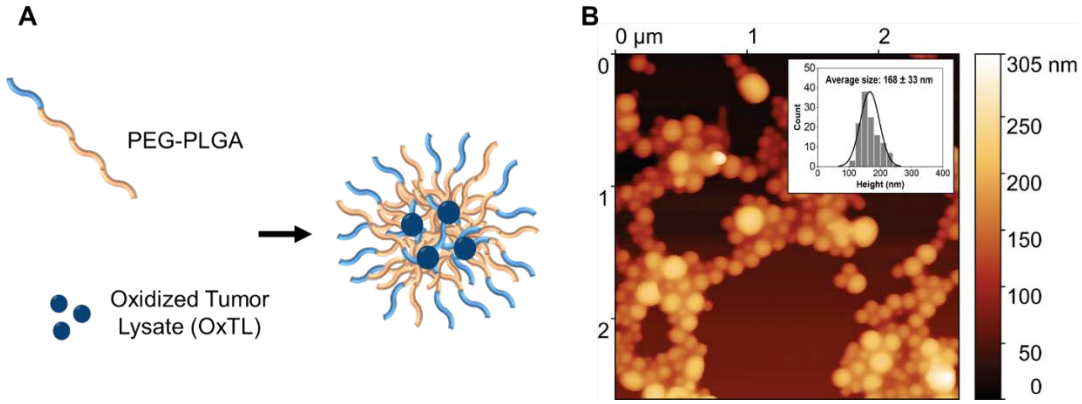

Figure 1. (A) Schematic representation of the preparation of oxidized tumor lysate-loaded PEG-PLGA nanoparticles via double emulsion solvent evaporation; (B) AFM image of oxidized tumor lysate loaded nanoparticles deposited on a silicon substrate. The histogram represents the nanoparticle size distribution obtained from the analysis of 125 nanoparticles.

The nanoparticles could be stably dispersed in Milli-Q water and DC culture medium, and retained their size and PDI for up to 24 h at 37 °C (**Supporting Information Figure S3**). Lyophilization is an attractive strategy for the long-term storage of nanoparticles. DLS analysis, however, revealed that re-dispersion of as-prepared, tumor lysate loaded nanoparticles in Milli-Q water resulted in a broad, multimodal particle size distribution (**Supporting Information Figure S4**). This problem could be overcome by the addition of sucrose as a cryoprotectant. The addition of 5 wt% sucrose allowed to resuspend the nanoparticles after lyophilization without significant changes in the particle size and size distribution (**Supporting Information Figure S4**). Release of oxidized tumor lysate from the nanoparticles was assessed at 37 °C in PBS with the bicinchoninic acid (BCA) assay (**Supporting Information Figure S5**). The particles were found to release 12 wt % of the total oxidized tumor lysate payload in 24 h, and 37 wt % within one week.

2.3.2. Mo-iDC viability and nanoparticle uptake

The viability of human donor-derived mo-DCs towards oxTL-loaded PLGA nanoparticles, and the uptake of the nanoparticles by these cells was investigated by flow cytometry. Cell viability and uptake of oxTL-loaded nanoparticles, both at 4 °C as well as at 37 °C, was compared with that of free oxTL as well as with control cells that were kept in culture medium. In order to monitor cellular uptake of oxTL and oxTL-loaded nanoparticles with flow cytometry, for these experiments, oxTL was stained with CellTrace™ Violet. These experiments were performed using nanoparticle concentrations of 0.5 mg/mL (dose 1) and 1.0 mg/mL (dose 2). Experiments with free oxTL were performed at the equivalent oxTL concentration. The results in **Figure 2A** show that delivery of oxTL as a nanoparticle formulation can lead to an up to 10-fold increase in the number of cells that internalize oxTL as compared to the use of an equivalent concentration of free oxTL. Specifically, for the experiment with free oxTL at 37 °C and at dose 1, 4.33 ± 2.13 % of the cell population stained positive for oxTL, while 43.6 ± 12.9% of the cells had internalized oxTL when the nanoparticle formulation was used. Increasing the nanoparticle concentration from 0.5 mg/mL to 1.0 mg/mL (dose 2) resulted in a significant increase in oxTL uptake. At dose 2, 73.3 ± 15.3 % of the mo-iDCs internalize the oxTL-loaded nanoparticles, as compared to 9.96 ± 3.14 % mo-iDCs when free oxTL was delivered. The very low internalization at 4 °C indicates that the nanoparticles are internalized via an active mechanism. As shown in **Figure 2B**, cell viability was not compromised under these conditions. The use of higher nanoparticle concentrations (> 1.0 mg/mL), however, was found to result in a decrease in cell viability (**Supporting Information Figure S6**).

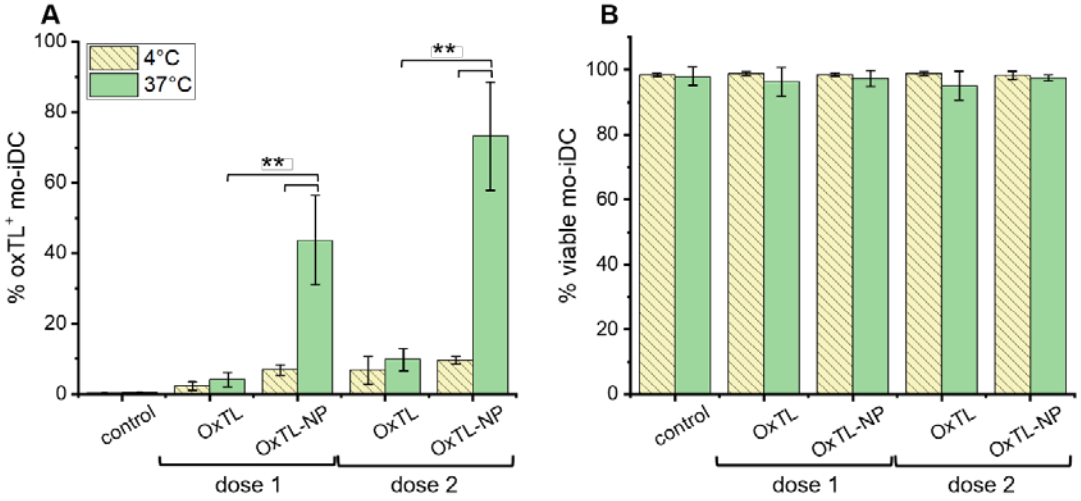

Figure 2. (A) mo-iDC uptake of oxTL or oxTL-loaded nanoparticles at 4 °C (in yellow oblique lines) or 37 °C (in green) for 24 hours. The data present the percentage of oxTL-positive cells as determined by flow cytometry. Dose 1 corresponds to 0.5 mg/mL oxidized tumor lysate loaded nanoparticles and the corresponding amount of oxTL. Dose 2 corresponds to 1 mg/mL NP-oxTL and the corresponding amount of oxTL. (B) Percentage of viable mo-iDC upon incubation with oxTL or oxTL-loaded PLGA nanoparticles at dose 1 or dose 2 after 24 h. For all experiments, the cell concentration was 1 million cells/mL. Experiments represent the average of three independent experiments with three different donors (n = 3). Statistical analysis was performed with Student's t-test, **: $p < 0.01$.

The internalization of oxTL mediated by the PLGA nanoparticles was also studied by confocal microscopy. For these experiments, Cell Trace Violet labelled oxTL was used. Mo-iDCs were incubated with oxTL-loaded PLGA nanoparticles (at dose 2, 1 mg/mL) for 24 h at 37 °C. After that, cells were fixed, their membrane stained with WGA-Texas Red, and placed on a cover slip to be analyzed by confocal microscopy. **Figure 3** presents confocal microscopy images of mo-iDCs that were presented with oxTL-loaded nanoparticles, free oxTL together with that of control mo-iDCs that were not challenged with oxTL. The confocal images show the

evolution in cell morphology upon presentation to the antigen. While the control mo-iDCs have a round shape, cells that were exposed to free oxTL or oxTL-loaded PLGA nanoparticles develop dendrites.[41,42,43] The confocal micrographs also validate the uptake of oxTL by the cells. While some blue fluorescence is visible in cells that have been exposed to free oxTL, the Cell Trace Violet stain is prominently visible intracellularly in mo-iDCs that were presented oxTL-loaded nanoparticles, which confirms the increased cellular internalization that was also observed by flow cytometry (**Figure 2**).

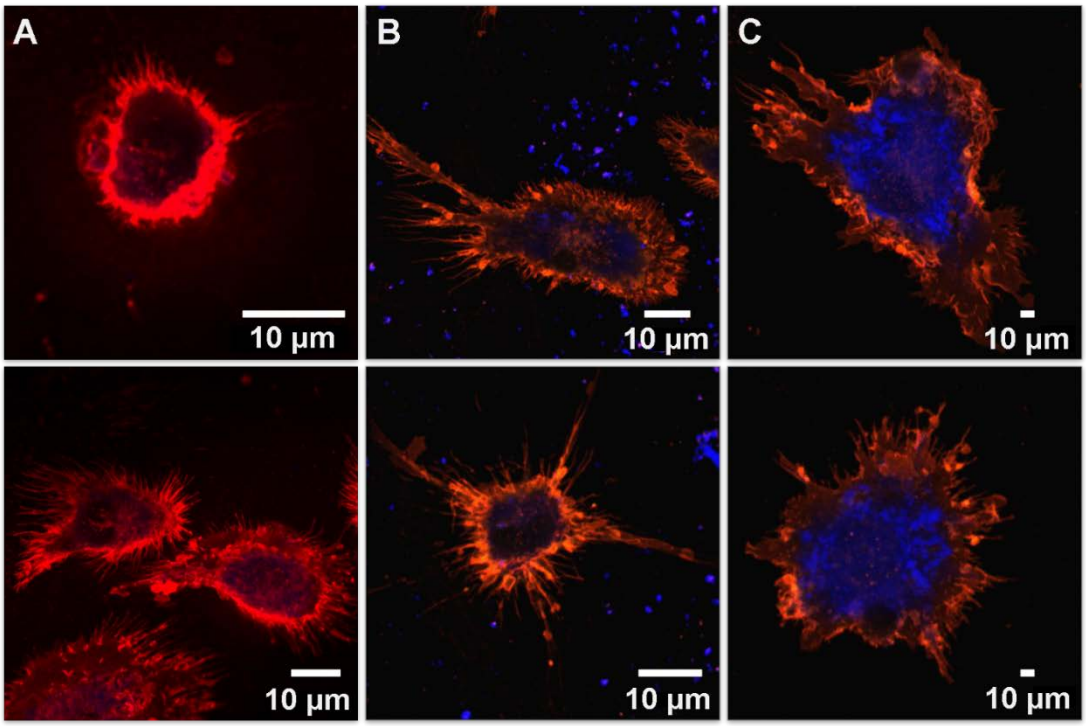

Figure 3. Fluorescent confocal microscopy images of mo-iDCs that have been exposed to DC media (A), oxTL (B) and oxTL-loaded nanoparticles (C) for 24 h at 37 °C. For each condition, two representative images are shown on top of each other. OxTL was fluorescently labelled with Cell Trace Violet (shown in blue). Cells were fixed and stained with WGA-Texas Red (shown in red) to visualize the cell membrane.

2.3.3. Effect of nanoparticle uptake on mo-iDC maturation

Maturation of dendritic cells commences upon antigen internalization and results in the presentation of antigen-derived epitopes as MHC complexes on the surface of the matured cell. During maturation, also cell surface expression of costimulatory receptors such as CD86, CD80, CD83, CD40 and HLA-DR is augmented. In a first experiment to monitor maturation, mo-iDCs from three human donors were challenged with free oxTL, as well as oxTL-loaded and empty PLGA nanoparticles and cell surface expression of CD40, CD83, CD86 and HLA-DR assessed after 24 h with flow cytometry. As a control, mo-iDCs were analyzed that were kept in culture medium to which DC media (100 µL/million cells) was added. **Figure 4** compares the percentages of CD40, CD83, CD86 and HLA-DR positive cells determined by flow cytometry. **Supporting Information Figure S7** presents the change in costimulatory receptor associated mean fluorescence intensity (MFI) relative to the non-treated control cells for each of the different conditions, which provides a measure for the cell surface concentrations of the respective receptor molecules. The data in **Figure 4A** indicate for all 3 donors an increase in the percentage of CD40 positive cells when mo-iDCs are exposed to oxTL-loaded PLGA nanoparticles as compared to the use of free oxTL or empty PLGA nanoparticles (both at dose 1 and dose 2). The MFI data presented in **Supporting Information Figure S7A** show the same trend and also point to an increase in the CD40 cell surface concentration when mo-iDCs from all 3 donors are challenged with ox-TL loaded PLGA nanoparticles. Experiments conducted with mo-iDCs from Donor 1 and Donor 2 also indicated increases in the percentage of CD83 positive cells, and CD83 cell surface concentration when oxTL-loaded nanoparticles are used as compared to empty nanoparticles and free oxidized tumor lysate (**Figure 4B** and **Supporting Information Figure S7B**). Experiments with mo-iDCs from Donor 1 and Donor 3 point towards an increase in the percentage of CD86 positive cells upon delivery of oxTL-loaded or empty PLGA nanoparticles, albeit less pronounced as it was observed for the CD40 and CD83 surface presentation (**Figure 4C**). The other experiments, in particular to evaluate HLA-DR expression, did not reveal clear trends but showed

substantial variations between the different conditions, which illustrates a significant donor-to-donor variability. On the one hand, the results of these experiments underline the ability of the PLGA nanoparticle formulation to enhance DC maturation as compared to the use of the free oxTL antigen. On the other hand, the data in **Figure 4** also illustrate the variabilities in human donor-derived cells and the challenges that come with this to investigate and further refine cancer nanovaccines.

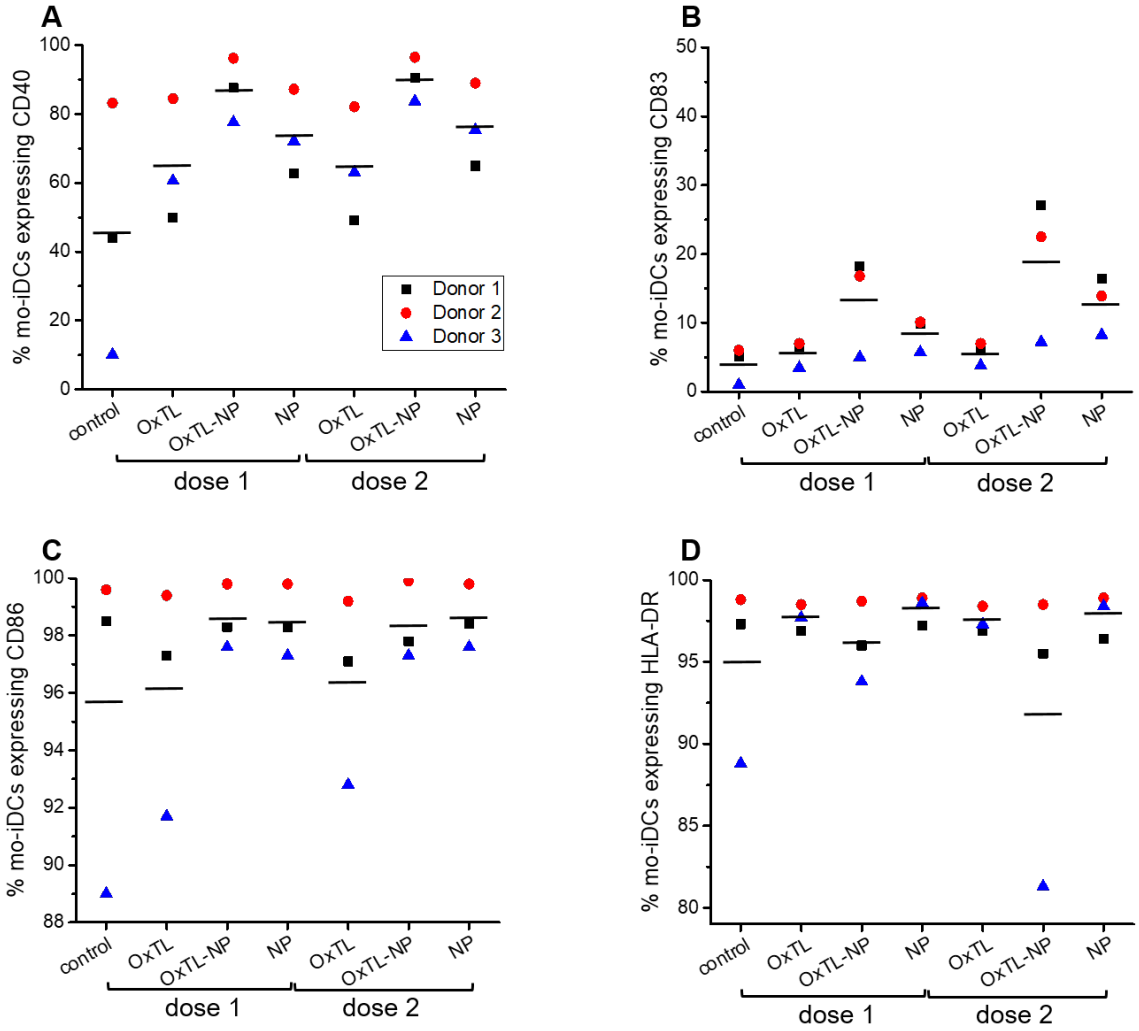

Figure 4: Percentage of CD40 (A), CD83 (B), CD86 (C) and HLA-DR (D) positive mo-iDCs as determined by flow cytometry upon exposure of these cells to oxTL, oxTL loaded or empty PLGA nanoparticles for 40 h. Mo-iDCs were analyzed that

were obtained from three different human donors. As a control mo-iDCs were analyzed that were kept in DC culture medium.

In clinical applications, in order to enhance maturation and mitigate tolerance effects, cancer vaccines are often produced using DCs that have been treated with maturation cocktails that include inflammatory cytokines, such as interferon-γ (IFN-γ), eventually in combination with Toll-like receptor (TLR) 4 agonist lipopolysaccharides (LPS) that help to further enhance the release of inflammatory cytokines.[44] In a second set of experiments therefore, maturation of DCs, which were additionally challenged with IFN-γ and LPS after being exposed to free or nanoparticle-formulated oxidized tumor lysate, was investigated. The results of these experiments for mo-iDCs obtained from three human donors are summarized in **Supporting Information Figures S8** and **S9**. Comparison of **Supporting Information Figure S8** and **Figure 4** indicates that the additional treatment with the IFN-γ/LPS maturation cocktail further increases the percentage of CD40, CD83 and CD86 positive cells and reveals more consistent data across the 3 donors. Due to the relatively large variability in the data from the different donors, however, it is not possible to unambiguously conclude whether this increase in CD40, CD83 and CD86 positive cells is also accompanied by a concurrent increase in the cell surface concentration of these maturation markers (**Supporting Information Figure S9**).

2.3.4. *In vitro* A375 melanoma cell apoptosis

Next, mo-iDCs that were challenged with free oxTL or oxTL-loaded PLGA nanoparticles were co-cultured with autologous PBMCs. The cytotoxic properties of the stimulated PBMCs were subsequently evaluated *in vitro* via real time live cell analysis in an experiment in which PBMCs were co-cultured with A375 melanoma cells. For these experiments, PBMCs from three different human donors were used that had been stimulated with autologous mo-mDCs activated with free oxTL, oxTL-

loaded PLGA nanoparticles or empty PLGA nanoparticles, and subsequently further matured with IFN-γ/LPS. To allow for the detection and quantification of A375 cell apoptosis, the Incucyte® Caspase-3/7 Dye was added to the co-culture. **Figure 5** illustrates the analysis of the results of this live cell analysis experiment. **Figure 5A** and **Figure 5B** present images of A375 melanoma cells and PBMCs alone, respectively. **Figure 5C** is an image from an A375 / PBMC co-culture experiment taken after 24 h. The PBMCs in this image were stimulated with DCs that had been presented with oxTL-loaded PLGA nanoparticles. In this figure, apoptotic cells are stained green. The image in **Figure 5C** was quantified with a computer-assisted algorithm, where the areas in magenta represent the apoptotic A375 cells as shown in **Figure 5D**. Taking advantage of the difference in size between the A375 cells and the PBMCs and by setting the limit for the definition of the magenta areas to 200 μm^2 this allows to exclude apoptotic PBMCs and monitor A375 cell death. This image analysis protocol provides a measure of the total green area per well (in μm^2 per well), which, by comparing images recorded at different conditions and time points, allows to quantitatively monitor A375 melanoma cell apoptosis.

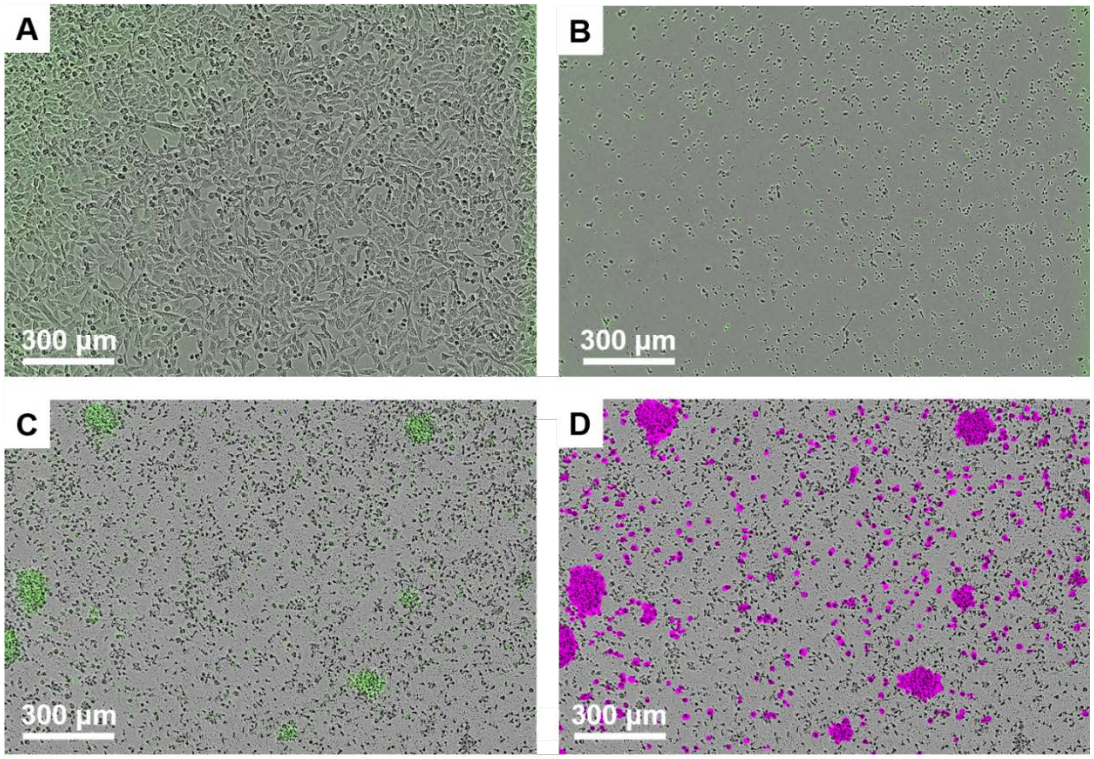

Figure 5. Real time live cell images of (A) A375 melanoma cells alone (B) and PBMCs alone, both after 24 h culture. Panel C is an image taken after 24 h from a co-culture of A375 melanoma cells and PBMCs stimulated with mo-mDCs that were activated with 0.5 mg oxTL-NP per million cells. Highlighted in green in Panel C are apoptotic A375 cells. Panel D is a computer-generated representation of the image in panel C where the areas in magenta represent the apoptotic A375 cells, and which was used to quantify the extent of A375 cell apoptosis in μm^2/well. PBMCs and DCs for the experiments shown in this image are from Donor 9.

Figure 6 summarizes the results of experiments in which A375 melanoma cells were co-cultured with human donor-derived PBMCs that had been activated with autologous mo-mDCs. For these experiments, cells from three different human donors were used. For each donor, A375 cell apoptosis was monitored as a function of time over a period of 48 h and PBMCs stimulated with mo-mDCs, which had been matured by being challenged with first free oxTL, or with 0.5 mg oxTL-loaded or empty PLGA

nanoparticles per million cells, and that were subsequently additionally challenged with IFN-γ and LPS. As a control, apoptosis of A375 cells that were not co-cultured with PBMCs as well as of A375 cells co-cultured with PBMCs, which had been stimulated with mo-mDCs that had been matured exclusively with IFN-γ and LPS was monitored over the same period of time. Images were then collected at different time points and subsequently analyzed to quantify levels of induced apoptosis. **Figure 6** compares A375 apoptosis, presented as total green area (in μm^2) per well, as a function of time for the three different donors and these different conditions.

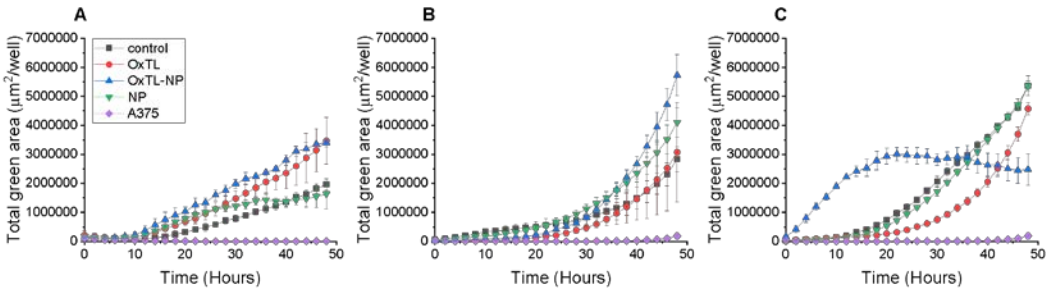

Figure 6. A375 melanoma apoptosis, expressed as total green area per well, as a function of time in a co-culture experiment with PBMCs that were stimulated with differently activated mo-mDCs. Mo-mDCs were activated with DC media (control, black square), oxidized tumor lysate (OxTL, red circle), OxTL-loaded nanoparticles (OxTL-NP, blue triangle) and empty nanoparticles (NP, green reverse triangle) and subsequently additionally challenged with IFN-γ and LPS. Spontaneous cell death of A375 cells was followed in parallel (A375, lilac turbot). Panel A, B and C represent data from experiments conducted with PMBCs and autologous DCs from 3 different human donors (donor 7 (A), donor 8 (B) and donor 9 (C)). Statistical analysis was performed with two-way ANOVA with post hoc Tukey test, *: $p < 0.05$, **: $p < 0.01$, ***: $p < 0.001$.

The results in **Figure 6** are interesting as they both highlight the potential of nanoparticle-mediated antigen delivery to DCs and also provide another illustration of the donor-to-donor variability that can be inherent to the use of human-derived cells and the challenges this presents to study and refine vaccines and other medicines. As

can be seen from **Figure 6B**, the experiments that used PBMCs and mo-mDCs from Donor 8 did not reveal any significant differences in A375 cell apoptosis between the different conditions that were evaluated. **Figure 6A** summarizes the results of the experiments that were conducted with PBMCs and mo-mDCs from Donor 7. In this case, A375 cell apoptosis was enhanced in co-cultures that use PBMCs that had been stimulated with mo-mDCs activated with free oxTL or oxTL-loaded PLGA nanoparticles. Finally, in the experiment in which PBMCs and mo-mDCs from Donor 9 were used (**Figure 6C**) very efficient and strongly enhanced A375 cell apoptosis was observed in the co-culture in which PBMCs were used that had been activated with oxTL loaded PLGA nanoparticles, as compared to all other experimental conditions. In this experiment, no further increase in the total green area per well was observed after 20 h, due to the complete elimination of cancer cells on the well by activated PBMCs.

2.3.5. *In vivo* therapeutic vaccination with OxTL-NP

Finally, the efficacy of the oxTL-loaded PLGA nanoparticle formulation was evaluated *in vivo* in a therapeutic vaccination study using B16F10 tumor-bearing C57BL/6J mice. For these experiments, oxidized tumor lysate was used that was produced from the same B16F10 cells that were used to challenge the mice. Survival of B16F10 tumor bearing mice upon subcutaneous administration of 1.5 mg per mice of oxTL-loaded PLGA nanoparticles was compared with that of mice that were treated in the same way with free oxTL and empty PLGA nanoparticles. Together with the free oxTL or the empty or oxTL-loaded nanoparticles, mice were administered poly(I:C) and CpG as adjuvants. Control animals were vaccinated with PBS or with the adjuvants alone. All animals were treated 3 times, at 2 days, 9 days and 16 days after tumor cell inoculation (**Figure 7A**). **Figure 7B** compares the survival of animals treated with the different formulations. Survival plots with a statistical analysis of different treatments are presented in **Supporting Information Figure S10**. Animals

that were challenged with the nanoparticle-based oxidized tumor lysate formulation survived for up to 50 days, in contrast to a maximum of 41 days for the group that received the corresponding free oxidized tumor-lysate based vaccine. Survival is significantly increased for animals that were administered oxTL loaded nanoparticles in combination with poly(I:C) and CpG as compared to animals that only obtained PBS ($p < 0.001$, **Supporting Information Figure S10A**) or the adjuvants ($p < 0.05$, **Supporting Information Figure S10B**). For animals treated with oxTL-loaded nanoparticles, a prolonged survival was observed as compared to the use of free oxTL and (in particular) empty PLGA nanoparticles. As shown in **Supporting Information Figures S10C** and **S10D**, these improvements, however, are not statistically significant.

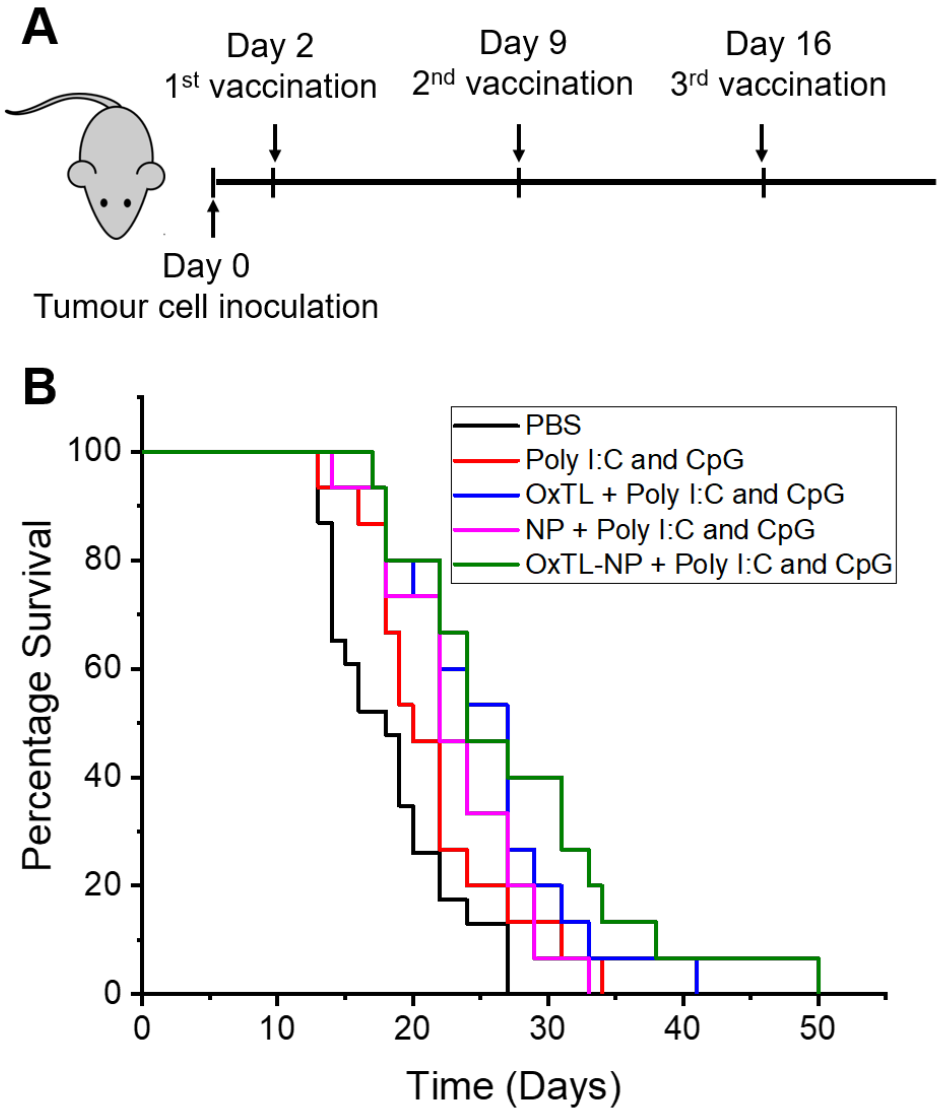

Figure 7. (A) Experimental design for the therapeutic vaccination of B16F10 melanoma bearing C57BL/6J mice; (B) Percentage survival for mice vaccinated with PBS (black line), adjuvants (Poly I:C and CpG, red line), oxTL (oxTL + Poly I:C and CpG, blue line), empty nanoparticles (NP + Poly I:C and CpG, magenta line) and oxTL loaded nanoparticles (NP-oxTL + Poly I:C and CpG, green line) (n = 23 for PBS, n = 15 for all other conditions).

2.4. Conclusions

Oxidized tumor lysate represents a powerful source of antigens for cancer vaccination. This study has explored the use of PLGA-based nanoparticle formulations to enhance the dendritic cell uptake and immunostimulatory activity of oxidized tumor lysate, *in vitro* using human donor-derived dendritic cells and PBMCs as well *in vivo* in a therapeutic vaccination study using B16F10 tumor-bearing C57BL/6J mice. Challenging dendritic cells with oxidized tumor lysate loaded nanoparticles was found to enhance antigen uptake and dendritic cell maturation as compared to the use of the free oxidized tumor lysate. The ability of these activated dendritic cells to stimulate autologous PMBCs was studied by real time live cell analysis of co-cultures of PBMCs with A375 melanoma cells. While these experiments revealed donor-to-donor variations, they also highlight the potential of nanoparticle-mediated dendritic cell-based vaccination approaches to augment the stimulation and cytotoxicity of PBMCs. Finally, the oxidized tumor lysate-loaded PLGA nanoparticle formulation was evaluated *in vivo* in a therapeutic vaccination study using B16F10 tumor-bearing C57BL/6J mice. Animals that were challenged with the nanoparticle-based oxidized tumor lysate formulation survived for up to 50 days, in contrast to a maximum of 41 days for the group that received the corresponding free oxidized tumor-lysate based vaccine.

2.5. References

1. Wculek, S. K. *et al.* Dendritic cells in cancer immunology and immunotherapy. *Nat. Rev. Immunol.* **20**, 7–24 (2020).
2. Harari, A., Graciotti, M., Bassani-Sternberg, M. & Kandalaft, L. E. Antitumor dendritic cell vaccination in a priming and boosting approach. *Nat. Rev. Drug Discov.* **19**, 635–652 (2020).
3. Abbott, M., Aocnp, Ò. & Ustoyev, Y. Nursing Cancer and the Immune System : The History and Background of Immunotherapy. *Semin. Oncol. Nurs.* **35**, 1–5 (2019).
4. Burg, S. H. Van Der, Arens, R., Ossendorp, F., Hall, T. Van & Melief, C. J. M. Vaccines for established cancer : overcoming the challenges posed by immune evasion. *Nat. Publ. Gr.* **16**, 219–233 (2016).
5. Lybaert, L., Vermaelen, K., Geest, B. G. De & Nuhn, L. Immunoengineering through cancer vaccines – A personalized and multi- step vaccine approach towards precise cancer immunity. *J. Control. Release* **289**, 125–145 (2018).
6. van der Burg, S. H. Correlates of immune and clinical activity of novel cancer vaccines. *Semin. Immunol.* **39**, 119–136 (2018).
7. Garg, A. D., Coulie, P. G., Eynde, B. J. Van Den & Agostinis, P. Integrating Next-Generation Dendritic Cell Vaccines into the Current Cancer Immunotherapy Landscape. *Trends Immunol.* **38**, 577–593 (2017).
8. Lluesma, S. M., Graciotti, M., Chiang, C. L. & Kandalaft, L. E. Does the Immunocompetent Status of Cancer Patients Have an Impact on Therapeutic DC Vaccination Strategies ? *Vaccines* **6**, 1–28 (2018).
9. Rosenberg, S. A. *et al.* Immunologic and therapeutic evaluation of a synthetic peptide vaccine for the treatment of patients with metastatic melanoma. *Nat. Med.* 321–327 (1998).
10. Rosenberg, S. A. *et al.* Tumor progression can occur despite the induction of very high levels of self/tumor antigen-specific CD8+ T Cells in patients with melanoma. *J. Immunol.* **175**, 6169–6176 (2005).

11. Neller, M. A., López, J. A. & Schmidt, C. W. Antigens for cancer immunotherapy. *Semin. Immunol.* **20**, 286–295 (2008).
12. Chiang, C. L. *et al.* Potential approaches for more successful dendritic cell-based immunotherapy. *Expert Opin. Biol. Ther.* **15**, 569–582 (2015).
13. Wang, S., Sun, Z. & Hou, Y. Engineering Nanoparticles toward the Modulation of Emerging Cancer Immunotherapy. *Adv. Healthc. Mater.* **10**, 1–33 (2021).
14. Lee, E. S. *et al.* Recent Advances in Polymeric Nanomedicines for Cancer Immunotherapy. *Adv. Healthc. Mater.* **8**, 1–44 (2019).
15. Shields, C. W. I., Wang, L. L., Evans, M. A. & Mitragotri, S. Materials for Immunotherapy. *Adv. Mater.* **32**, 1–56 (2020).
16. Dai, X., Yu, L., Zhao, X. & Ostrikov, K. K. Nanomaterials for oncotherapies targeting the hallmarks of cancer. *Nanotechnology* **31**, 1–18 (2020).
17. Dai, C., Hiep, T., Minh, L., Thuy, H. & Jeong, J. Current developments in nanotechnology for improved cancer treatment , focusing on tumor hypoxia. *J. Control. Release* **324**, 413–429 (2020).
18. Goldberg, M. S. Improving cancer immunotherapy through nanotechnology. *Nat. Rev. Cancer* **19**, 587–602 (2019).
19. Riley, R. S., June, C. H., Langer, R. & Mitchell, M. J. Delivery technologies for cancer immunotherapy. *Nat. Rev. Drug Discov.* **18**, 175–196 (2019).
20. Saung, M. T., Ke, X., Howard, G. P., Zheng, L. & Mao, H. Particulate carrier systems as adjuvants for cancer vaccines. *Biomater. Sci.* **7**, 4873–4887 (2019).
21. Leach, D. G., Young, S. & Hartgerink, J. D. Advances in immunotherapy delivery from implantable and injectable biomaterials. *Acta Biomater.* **88**, 15–31 (2019).
22. Zhang, R., Billingsley, M. M. & Mitchell, M. J. Biomaterials for vaccine-based cancer immunotherapy. *J. Control. Release* **292**, 256–276 (2018).
23. Prasad, S. *et al.* Optimization of stability, encapsulation, release, and cross-priming of tumor antigen-containing PLGA nanoparticles. *Pharm. Res.* **29**,

2565–2577 (2012).

24. Hanlon, D. J. *et al.* Enhanced Stimulation of Anti-Ovarian Cancer CD8+ T Cells by Dendritic Cells Loaded with Nanoparticle Encapsulated Tumor Antigen. *Am. J. Reprod. Immunol.* **65**, 597–609 (2011).
25. Mueller, M., Reichardt, W., Koerner, J. & Groettrup, M. Coencapsulation of tumor lysate and CpG-ODN in PLGA-microspheres enables successful immunotherapy of prostate carcinoma in TRAMP mice. *J. Control. Release* **162**, 159–166 (2012).
26. Gross, B. P., Wongrakpanich, A., Francis, M. B., Salem, A. K. & Norian, L. A. A therapeutic microparticle-based tumor lysate vaccine reduces spontaneous metastases in murine breast cancer. *AAPS J.* **16**, 1194–203 (2014).
27. Iranpour, S., Nejati, V., Delirezh, N., Biparva, P. & Shirian, S. Enhanced stimulation of anti-breast cancer T cells responses by dendritic cells loaded with poly lactic-co-glycolic acid (PLGA) nanoparticle encapsulated tumor antigens. *J. Exp. Clin. cancer Res.* **35**, 1–11 (2016).
28. Prasad, S. *et al.* Polymer nanoparticles containing tumor lysates as antigen delivery vehicles for dendritic cell-based antitumor immunotherapy. *Nanomedicine Nanotechnology, Biol. Med.* **7**, 1–10 (2011).
29. Chiang, C. L., Ledermann, J. A., Rad, A. N., Katz, D. R. & Chain, B. M. Hypochlorous acid enhances immunogenicity and uptake of allogeneic ovarian tumor cells by dendritic cells to cross-prime tumor-specific T cells. *Cancer Immunol. Immunother.* **55**, 1384–1395 (2006).
30. Chiang, C. L. *et al.* A Dendritic Cell Vaccines Pulsed with Autologous Hypochlorous Acid-Oxidized Ovarian Cancer Lysate Primes Effective Broad Antitumor Immunity : From Bench to Bedside. *Clin Cancer Res.* **19**, 4801–4815 (2013).
31. Chiang, C. L. L. *et al.* Oxidation of ovarian epithelial cancer cells by hypochlorous acid enhances immunogenicity and stimulates T cells that recognize autologous primary tumor. *Clin. Cancer Res.* **14**, 4898–4907

(2008).

32. Marcinkiewicz, J., Cha, B. M. N., Olszowska, E. W. A. & Wski, S. O. L. S. Enhancment of Immunogenic Properties of Ovalbumin as a Result of its Chlorination. **23**, 1393–1395 (1991).
33. Marcinkiewicz, J., Olszowska, E., Olszowski, S. & Zgliczynski, J. M. Enhancement of trinitrophenyl-specific humoral response to TNP proteins as the result of carrier chlorination. **76**, 385–388 (1992).
34. Allison, M. E. D. & Fearon, D. T. Enhanced immunogenicity of aldehyde-bearing antigens : a possible link between innate and adaptive immunity. *Eur. J. Immunol.* **30**, 2881–2887 (2000).
35. Kandalaft, L. E. *et al.* A Phase I vaccine trial using dendritic cells pulsed with autologous oxidized lysate for recurrent ovarian cancer. *J. Transl. Med.* **11**, 1–14 (2013).
36. Tanyi, J. L. *et al.* Personalized cancer vaccine effectively mobilizes antitumor T cell immunity in ovarian cancer. *Sci.Transl.Med.* **10**, 1–15 (2018).
37. Prokopowicz, Z. M. *et al.* Hypochlorous Acid: A Natural Adjuvant That Facilitates Antigen Processing, Cross-Priming, and the Induction of Adaptive Immunity. *J. Immunol.* **184**, 824–835 (2010).
38. Danhier, F. *et al.* PLGA-based nanoparticles: An overview of biomedical applications. *J. Control. Release* **161**, 505–522 (2012).
39. Fan, Y. & Moon, J. J. Nanoparticle Drug Delivery Systems Designed to Improve Cancer Vaccines and Immunotherapy. *Vaccines* **3**, 662–85 (2015).
40. Rietscher, R. *et al.* Impact of PEG and PEG-b-PAGE modified PLGA on nanoparticle formation, protein loading and release. *Int. J. Pharm.* **500**, 187–195 (2016).
41. Verdijk, P. *et al.* Morphological changes during dendritic cell maturation correlate with cofilin activation and translocation to the cell membrane. *Eur. J. Immunol.* **34**, 156–164 (2004).
42. Akkaya, B. *et al.* Regulatory T cells mediate specific suppression by depleting peptide – MHC class II from dendritic cells. *Nat. Immunol.* **20**,

218–231 (2019).

43. Kyung, M. & Kim, J. Properties of immature and mature dendritic cells : phenotype, phagocytosis, and migration. *RSC Adv.* **9**, 11230–11238 (2019).

44. Perez, C. R. & De Palma, M. Engineering dendritic cell vaccines to improve cancer immunotherapy. *Nat. Commun.* **10**, 1–10 (2019).

2.6. Supporting Information

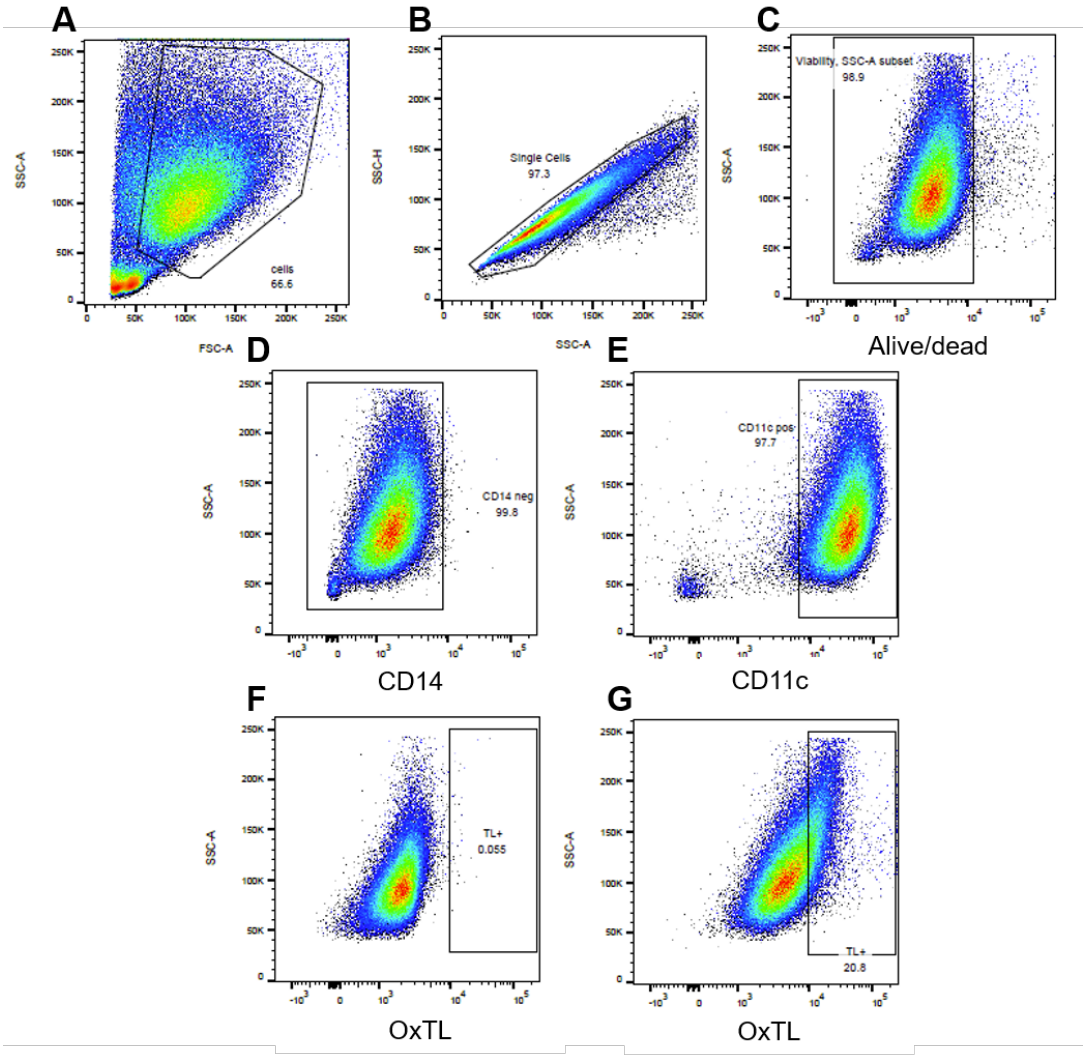

Figure S1. Gating strategy for the flow cytometry analysis of oxidized tumor lysate / nanoparticle uptake and mo-iDC viability (see **Figure 2**). Cells were gated from the top left considering forward and side scatter (FSC and SSC) to define cells from debris (A). Among the cells, single ones were selected (B) and from the single cells the live ones (negative for LIVE/DEAD™ Fixable Near-IR Dead Cell reagent) (C). In the second line, among the live single cells, the DCs were then selected by first gating the $CD14^-$ (D) and from there the $CD11c^+$ subpopulation (E). In panel F, the oxTL-associated (CellTrace Violet) autofluorescence of mo-DCs that have not been treated

with oxTL is used to define the gating setting for oxTL positive mo-DCs. Panel G, as an example shows a flow cytometry scatter plot of mo-DCs that have been exposed to 90 µg oxTL in 0.5 mg nanoparticles per million cells for 24 h.

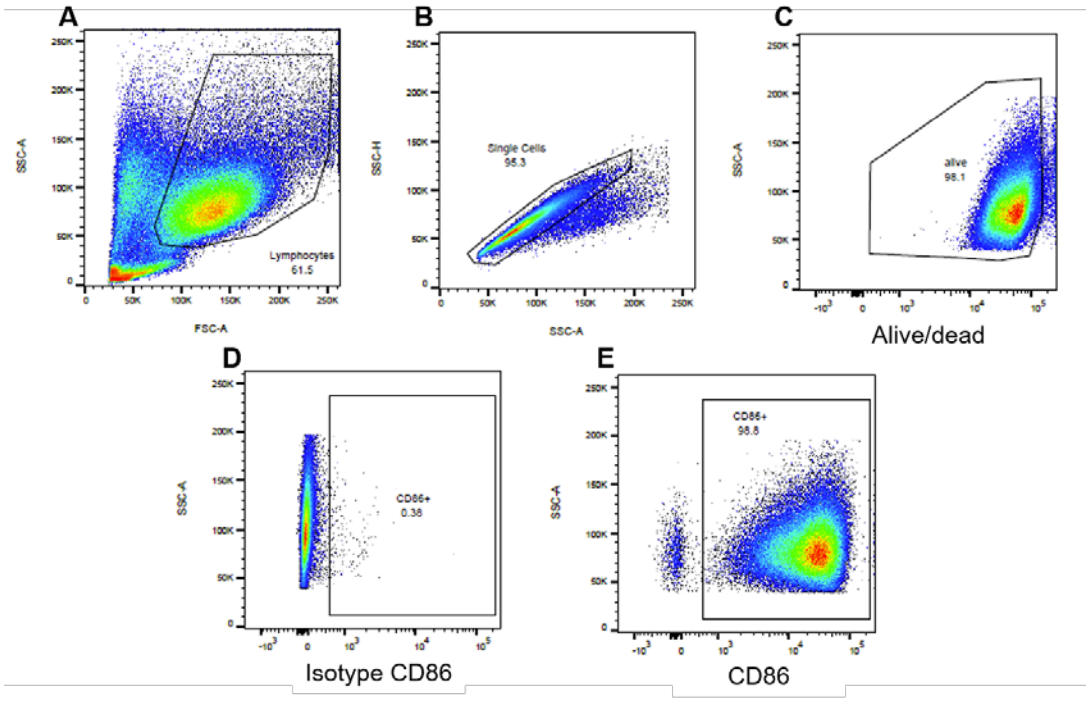

Figure S2. Gating strategy used to monitor mo-DC maturation with flow cytometry (**Figure 4**). Cells were gated from the top left line considering forward and side scatter (FSC and SSC) to define cells from debris (A). Among the cells, single ones were selected (B) and from the single cells the live ones (negative for LIVE/DEAD™ Fixable Near-IR Dead Cell reagent) (C). Subsequently, within the selected population of live cells isotype antibody staining was used to define the gating strategy for maturation markers. Labelling with isotype anti-CD86 (D) or antibody anti-CD86 (E) are shown as example.

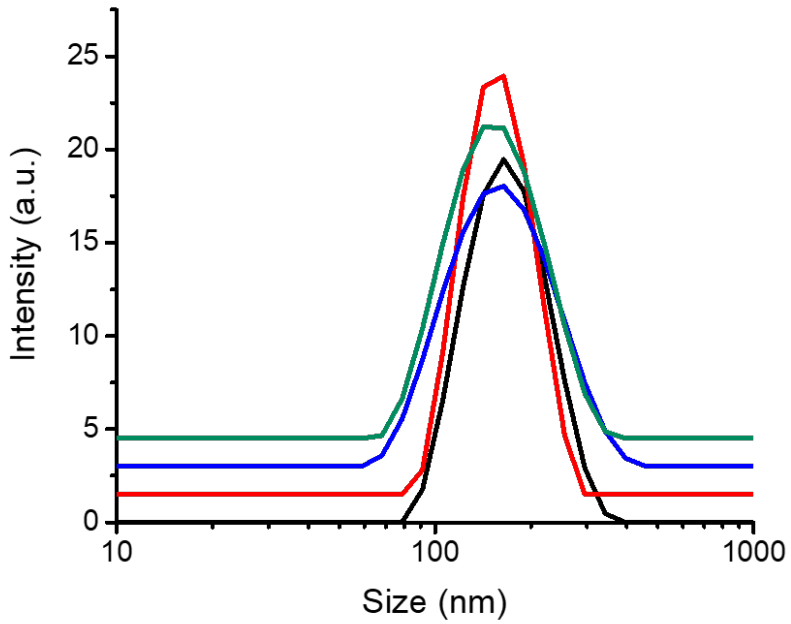

Figure S3. Intensity average size distribution of oxidized tumor lysate loaded nanoparticles measured at a particle concentration of 0.02 mg/mL: in Milli-Q water at t = 0 (black line; d = 161 ± 41 nm, PDI = 0.065), in Milli-Q water after 24 h (red line; d = 158.7 ± 28 nm, PDI = 0.033), in DC media at t = 0 (blue line; d = 144 ± 58 nm, PDI = 0.16) and in DC media after 24 h (green line; d = 142 ± 49 nm, PDI = 0.121).

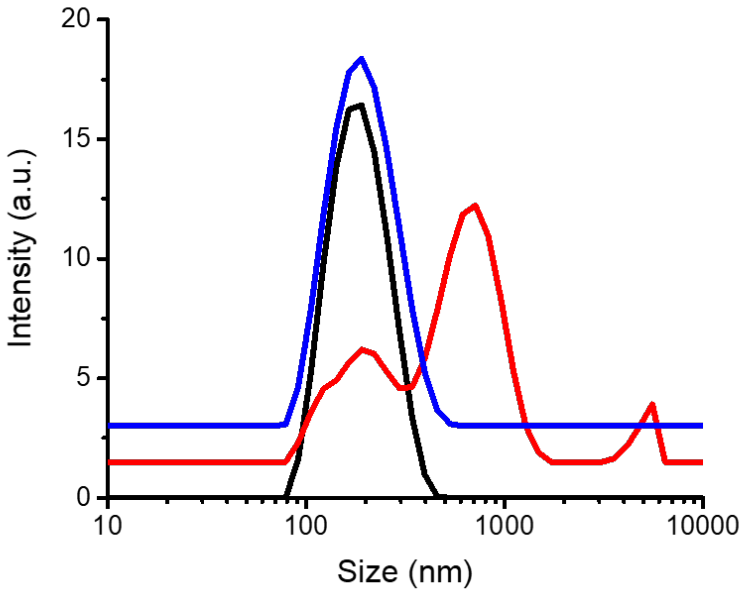

Figure S4. Size distributions of oxidized tumor lysate loaded nanoparticles (0.02 mg/mL): as prepared in Milli-Q water before lyophilization (black line), upon resuspension in Milli-Q water after lyophilization without cryoprotectant (red line), and in Milli-Q water after lyophilization using 5 wt% sucrose as a cryprotectant (blue line).

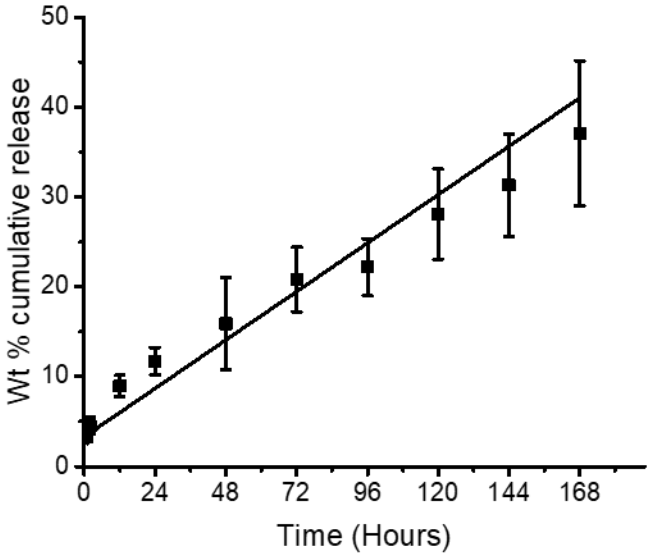

Figure S5. Cumulative release of oxidized tumor lysate from PLGA particles in PBS at 37 °C (data presented are the average of 2 independent experiments, n = 2).

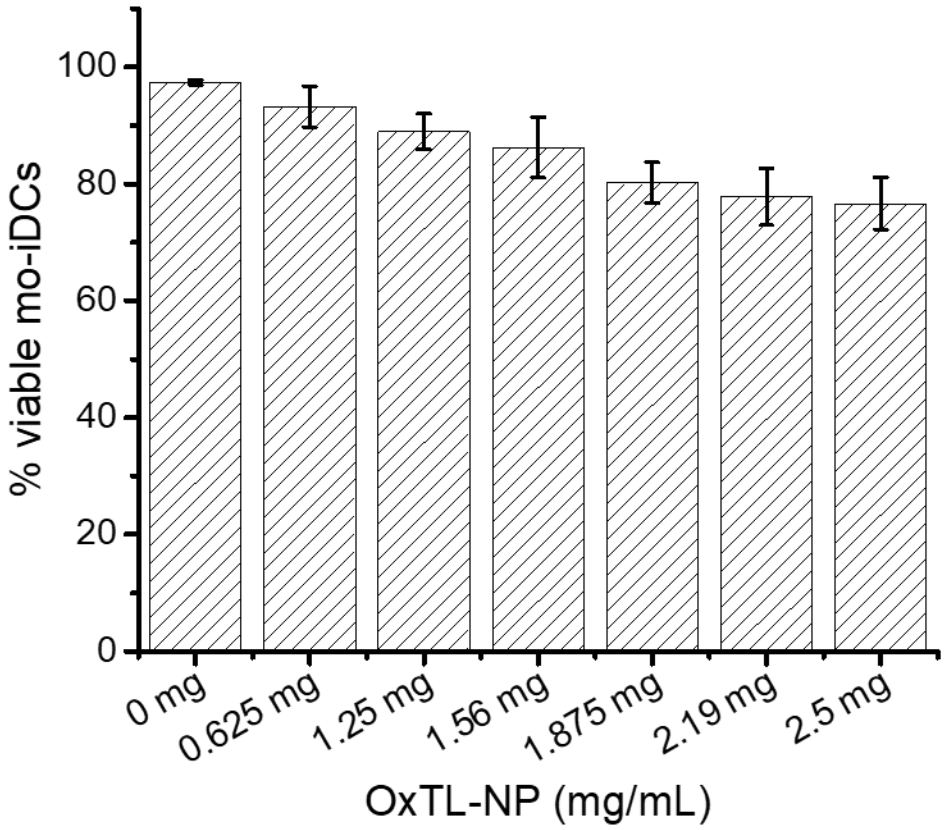

Figure S6. Viability of mo-iDCs upon exposure to different concentrations of oxTL-loaded PLGA nanoparticles after a period of 24 h at 37 °C as determined by flow cytometry. Experiments represent the average of 3 independent experiments with 3 different donors (n = 3).

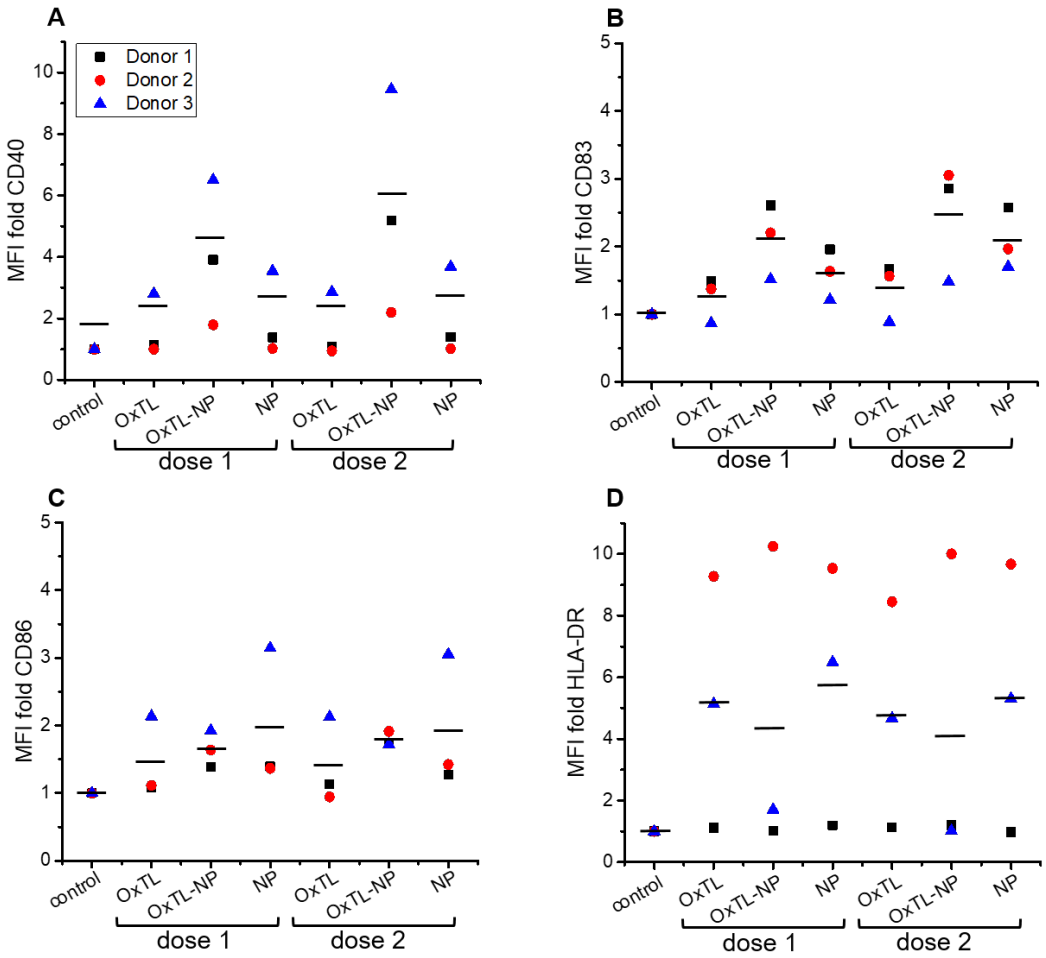

Figure S7. Mean fluorescence intensity (MFI) of (A) CD40, (B) CD83, (C) CD86 and (D) HLA-DR associated fluorescence as determined by flow cytometry of human mo-iDCs obtained from three donors after exposure of these cells to oxTL, oxTL loaded or empty PLGA nanoparticles for 40 h. As a control mo-iDCs were analysed that were kept in DC culture media.

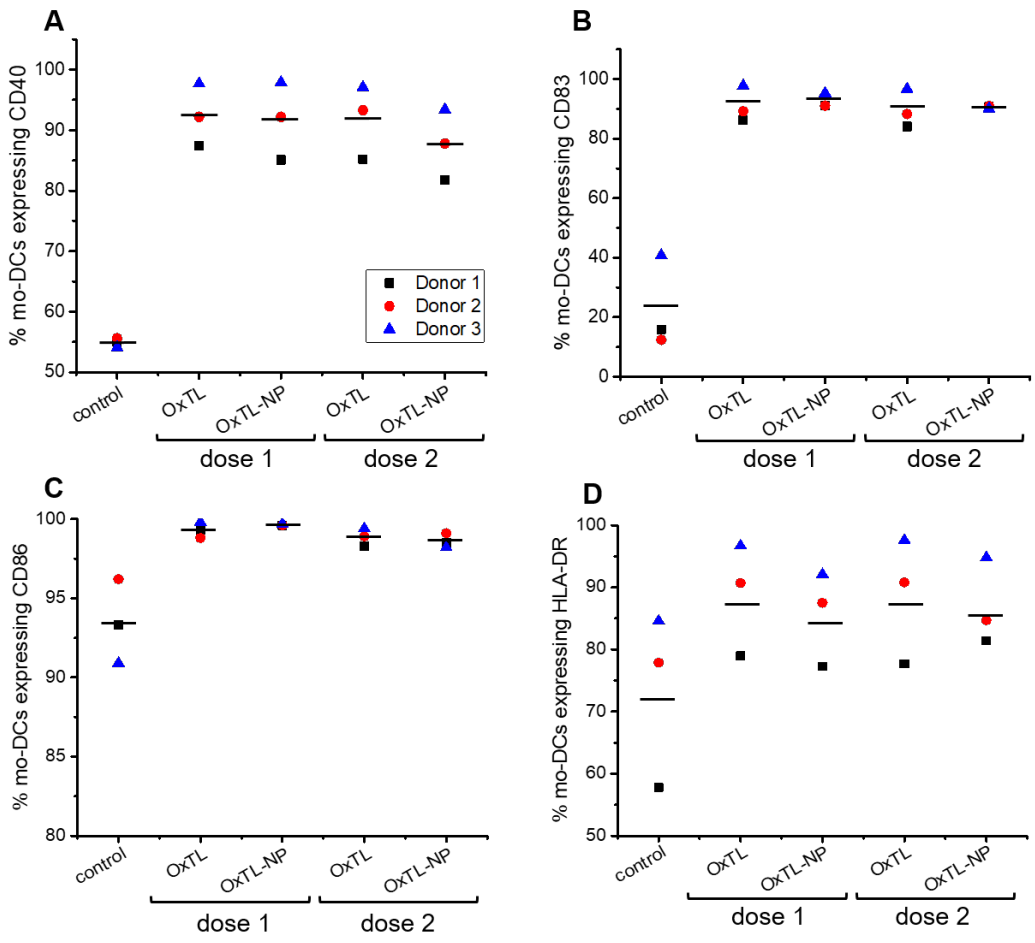

Figure S8. Percentage of CD40 (A), CD83 (B), CD86 (C) and HLA-DR (D) positive mo-iDCs as determined by flow cytometry upon exposure of these cells to oxTL, oxTL loaded or empty PLGA nanoparticles for 24 h and subsequent treatment with IFN and LPS for further 16 h. mo-iDCs were analysed that were obtained from three different human donors. As a control mo-iDCs were analysed that were kept in DC culture medium.

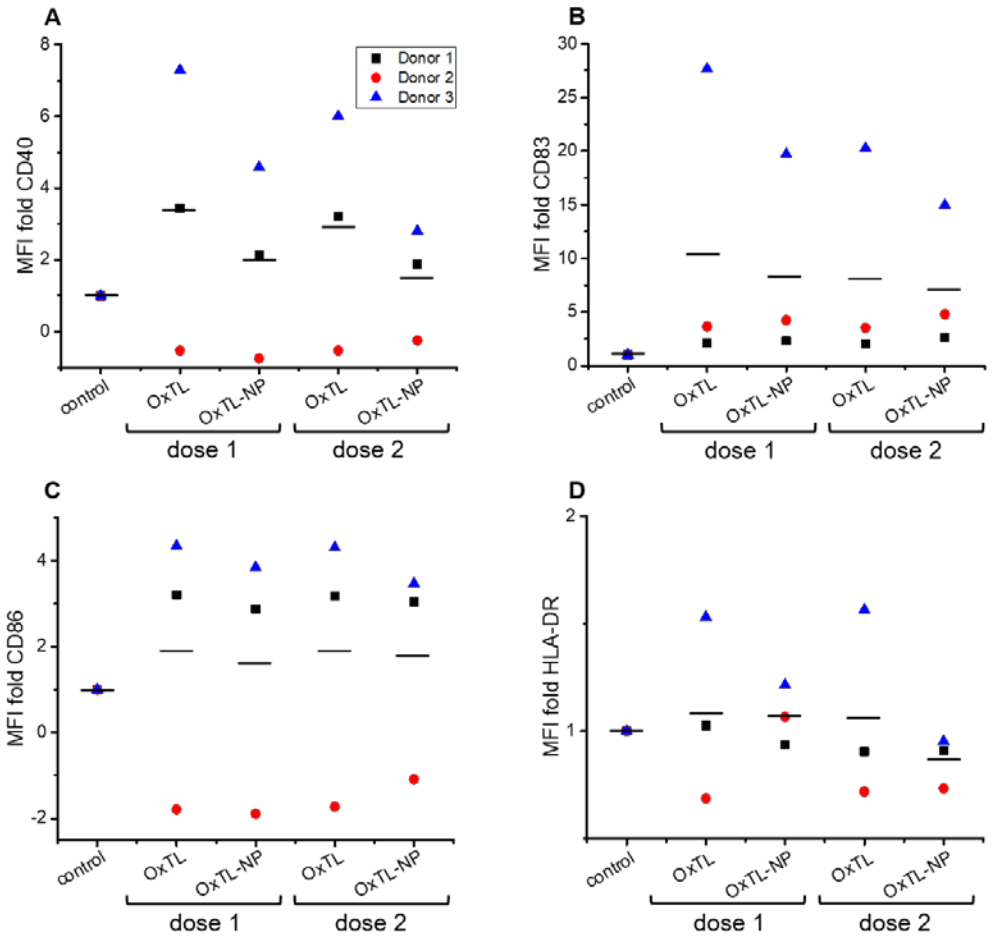

Figure S9. Mean fluorescence intensity (MFI) of (A) CD40, (B) CD83, (C) CD86 and (D) HLA-DR associated fluorescence as determined by flow cytometry of human mo-iDCs obtained from three donors after exposure of these cells to oxTL, oxTL loaded or empty PLGA nanoparticles for 24 h and subsequent treatment with IFN-γ and LPS for further 16 h. As a control mo-iDCs were analysed that were kept in DC culture medium.

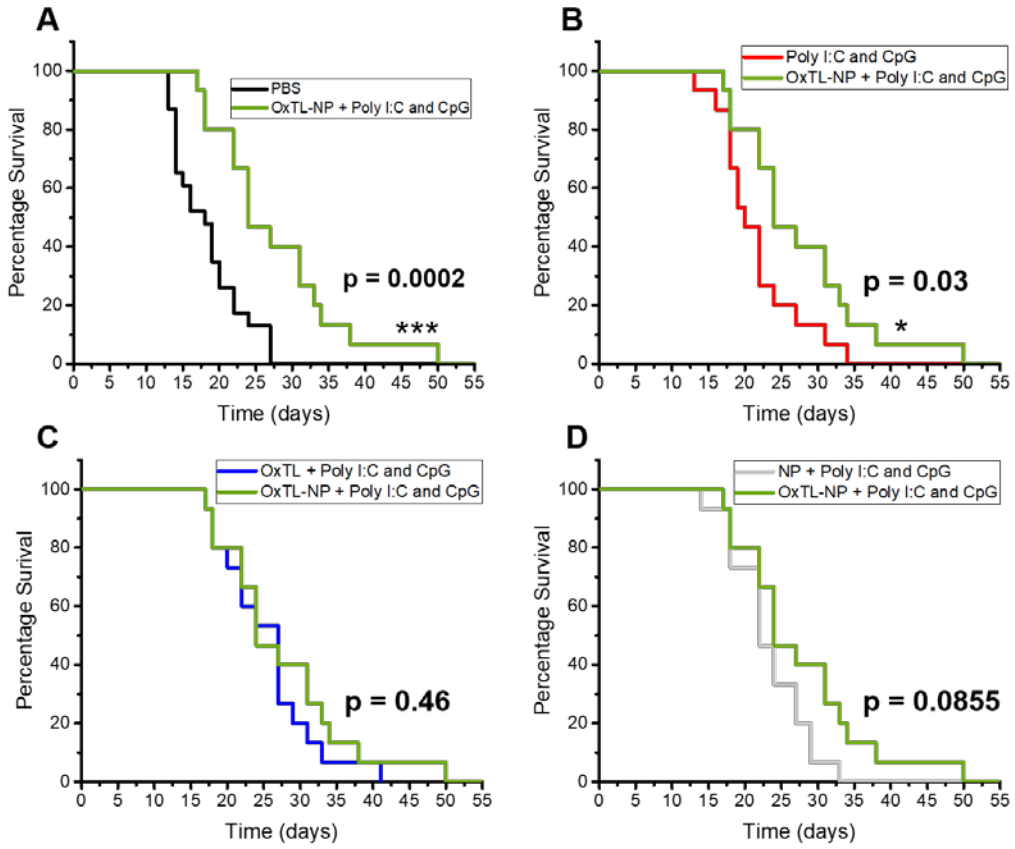

Figure S10. Percentage survival for mice vaccinated with oxTL loaded nanoparticles (NP-oxTL + Poly I:C and CpG, green line) compared to those vaccinated with (A) PBS (black line), (B) adjuvant (Poly I:C and CpG, red line), (C) oxTL (oxTL + Poly I:C and CpG, blue line) and (D) empty nanoparticles (NP + Poly I:C and CpG, lilac line). (n = 23 for PBS, n = 15 for all other conditions). Statistical analysis was performed with Log-rank test, * : $p < 0.05$, ** : $p < 0.01$, *** : $p < 0.001$.

3. Reduction-Sensitive Protein Nanogels Enhance Uptake of Model and Tumor Lysate Antigens *in vitro* by Mouse and Human-Derived Dendritic Cells

3.1. Introduction

Peptides and proteins have emerged as a powerful class of therapeutics.[1,2] The use of these biologics, however, presents several additional challenges as compared to many conventional drugs. One challenge is the susceptibility of these drugs towards degradation, and their limited stability.[3,4] Many peptide and protein-based drugs act on targets that are located intracellularly.[5,6] Efficient cellular uptake of protein and peptide-based drugs is another challenge. The use of nanosized formulations has been proven a promising strategy to alleviate some of these problems. Peptide and protein nanogels are particularly attractive as they allow to generate nanosized formulations of these biologics with essentially quantitative encapsulation efficiency.[7,8,9,10,11,12,13,14,15,16,17]

Peptide/protein nanogels have also been explored as vehicles for the transport of antigens and adjuvants in cancer immunotherapy.[15] Studies that have been reported have used both ovalbumin (as a model antigen) as well as specific peptide epitopes. These peptide/protein nanogels have been prepared both via non-covalent strategies that use electrostatic interactions[18,19,20] as well as via covalent approaches that use bifunctional active-ester crosslinkers.[21] An alternative strategy to the formation of covalently crosslinked peptide/protein nanogels is based on the formation of

intermolecular disulfide bonds.[22,23] These nanogels are attractive as the disulfide crosslinks are reduction sensitive and undergo cleavage, triggering nanogel disassembly, upon exposure to the intracellular milieu.

The *in vitro* work that has been reported so far has used mouse-derived dendritic cells to demonstrate the potential of peptide/protein nanogels for the transport of antigens and adjuvants. This study explores the use of reduction-sensitive protein nanogels for the delivery of ovalbumin and oxidized tumor lysate-based antigens to mouse and human donor-derived dendritic cells. The use of tumor lysate for cancer therapy and vaccination is attractive as it allows to challenge the immune system with a broad spectrum of epitopes.[24,25] Oxidation with hypochlorous acid further enhances the immunostimulatory activity of tumor lysate.[26,27,28,29,30] While tumor lysate has been delivered to dendritic cells using poly(lactic-co-glycolic acid) nanoparticles,[31,32,33,34,35,36,37,38,39] the use of nanogel formulations to challenge dendritic cells with this class of antigens has not yet been studied.

This report investigates the potential of reduction-sensitive protein nanogels for the delivery of ovalbumin and oxidized tumor lysate-based antigens *in vitro* in experiments that use mouse and human-donor derived dendritic cells. The use of the nanogel delivery platform was found to enhance uptake of ovalbumin, and subsequently augment dendritic cell activation, as compared to the use of the free protein antigen, both in mouse-derived as well as in human cells. The nanogels were also found to be efficient vectors for the delivery of oxidized tumor lysate and allowed to significantly enhance internalization of this antigen in dendritic cells that were harvested from three human donors as compared to challenging of these cells with the corresponding free oxidized tumor lysate.

3.2. Experimental Section

3.2.1. Materials

Zeba™ Spin Desalting Columns, 7K MWCO (Thermo Fisher Scientific, MA USA), ovalbumin, Alexa Fluor™ 488 Conjugate (Life Technologies, Thermo Fisher Scientific, MA USA), ovalbumin (Sigma-Aldrich, Merck kGaA, Darmstadt, Germany) and glutathione (Tokyo Chemical Industry Co., Ltd.) were used for nanogel synthesis. The Pierce™ BCA Protein Assay Kit from Life Technologies (Thermo Fisher Scientific, MA USA) was used for protein quantification. Reagents employed for confocal and oxidized tumor lysate labelling experiments were: Rabbit polyclonal to EEA1 - Early Endosome Marker (Abcam plc, Cambridge, UK), Rabbit polyclonal to LAMP1 - Lysosome Marker (Abcam plc, Cambridge, UK), Donkey anti-Mouse IgG (H+L) Highly Cross-Adsorbed Secondary Antibody, Alexa Fluor 647 (Thermo Fisher Scientific, MA USA), WGA-Texas Red (Life Technologies, Thermo Fisher Scientific, MA USA), Fluoromount-G (Bioconcept AG, Switzerland), CellTrace™ Violet proliferation dye (Life Technologies, Thermo Fisher Scientific, MA USA). The following antibodies were used in flow cytometry experiments: Alexa Fluor® 700 anti-human CD11c (BioLegend, San Diego, CA USA), PE/Cy7 anti-human CD14 (BioLegend, San Diego, CA USA), LIVE/DEAD™ Fixable Near-IR Dead Cell (Thermo Fisher Scientific, MA USA), FITC anti-human CD40 (Thermo Fisher Scientific, MA USA), Zombie Aqua™ Fixable Viability Kit (BioLegend, San Diego, CA USA), Alexa Fluor® 700 anti-mouse CD11c (BD Bioscience, San Jose, CA USA), BV785 anti-mouse MHC II (BioLegend, San Diego, CA USA), APC anti-mouse CD86 (BioLegend, San Diego, CA USA), BV421 anti-human CD83 (BD Bioscience, San Jose, CA USA), PE anti-mouse SIINFEKL-H-2kb (BioLegend, San Diego, CA USA). The following anti-mouse antibodies isotypes were used in flow cytometry experiments: Alexa Fluor® 700 Hamster IgG1, λ1 Isotype Control (BD Bioscience, San Jose, CA USA), BV421 Rat IgG1, κ Isotype Control Clone R3-34 (BD Bioscience, San Jose, CA USA), APC Rat IgG2a, λ Isotype (BioLegend, San Diego, CA USA), PE Mouse IgG1, κ Isotype (BioLegend, San Diego, CA USA).

3.2.2. Methods

Particle sizes and zeta-potentials were analysed by dynamic light scattering (DLS) using a Zetasizer Nano ZS (Malvern Panalytical LTD) instrument. Measurements were performed in Milli-Q water at a concentration of 0.04 mg/mL. Atomic force microscopy (AFM) images were recorded using a Cypher Asylum Research AFM instrument (Oxford Instruments, UK). The measurements were performed in tapping mode using a HQ:NSC14/Al BS cantilever (Mikromasch, USA) with a spring constant of 5 N/m to image dry samples and with a MLCT cantilever (Bruker, USA) with a spring constant of 0.07 N/m to measure nanogels in water. Cells were analysed by flow cytometry on a BD LSRFortessa™ (BD Biosciences, San Jose, CA) instrument. For confocal microscopy imaging an inverted Leica SP8 (Leica Microsystems, Wetzlar, Germany) microscope was used.

3.2.3. Procedures

Nanogel synthesis. The appropriate antigen (ovalbumin (10 mg/mL), a mixture of ovalbumin and OVA-AF488 (10 mg/mL, 0.5 wt % OVA-AF488), or oxidized tumor lysate (10 mg/mL)) was dissolved in 1 mL of a 50 mM GSH solution in Milli-Q water. The solution was stirred at 37 °C for 1 h. Then, GSH was removed by passing the protein solution over a Zebaspin™ desalting column (MWCO 7 kDa). After that, 4 mL ethanol was added dropwise under stirring to the protein solution (1 mL). The mixture was stirred for 45 min at 37 °C. Nanogels were isolated by centrifugation (16000 rpm, 10 min) and washed three times with Milli-Q water. Finally, the nanogels were collected, lyophilized in 1 mL of 2 wt % sucrose solution in Milli-Q water and stored at - 20 °C for further use.

Atomic force microscopy sample preparation. 4 µL of a 0.05 mg/mL nanogel solution in Milli-Q water was deposited on a cleaned and plasma-treated silicon wafer (10 mm × 8 mm size). To image dry samples, the wafers were dried overnight at room temperature before acquiring the images. Liquid AFM images were acquired after depositing of 4 µL Milli-Q water on the dry wafers.

Nanogel degradation experiments. Nanogels (0.04 mg/mL) were suspended in Milli-Q water or in 10 mM GSH solution. The particle size distribution was measured by DLS, both immediately after resuspension, or after incubation for 24 h at 37 °C with 200 rpm shaking.

Preparation of oxidized tumor lysate (oxTL). OxTL was prepared from A375 cells as previously described.[26] Briefly, cells were harvested, incubated for 1 h at 37 °C with 60 µM HOCl and washed extensively with PBS. For uptake experiments, at this point cells (1 x 10^6 cells/mL) were stained by adding 1 µL of a 5 mM solution of CellTrace™ Violet in DMSO. Finally, cells were subjected to six freeze-thaw cycles (dry ice / 37 °) and subsequently stored at - 80 °C until further use.

Generation of mouse bone marrow derived dendritic cells. Female C57BL/J mice were euthanized to collect femoral and tibial bones. This procedure was approved by the Veterinary Authority of the Swiss Canton Vaud (authorization no.3308) and performed in accordance with Swiss ethical guidelines. Bone marrow was collected by flushing femoral and tibial bones with BMDC media (500 mL IMDM media enriched with 10% FBS, 100 units/mL penicillin and 100 µg/mL streptomycin, 550 µL 2-β-mercaptoethanol) with a 25G syringe. Cells were centrifuged at 1400 rpm for 10 minutes and counted for plating in Petri dishes at concentration of 1 - 2 x 10^6 cells/mL in BMDC media enriched with GM-CSF (1000 U/mL). Cells were incubated at 37 °C, 5% CO_2 for two days and then replenished with fresh media and cytokines. On day 4, cells were stimulated with IL-4 (100 U/mL). On day 5, cells were counted and plated for antigen uptake or activation experiments.

Generation of human monocyte derived DC. Monocyte-derived dendritic cells (mo-iDCs) were generated from monocytes isolated from fresh peripheral blood mononuclear cells (PBMCs) of healthy human donors collected at the local Blood Transfusion Center (Lausanne, Switzerland), under Institutional Review Board approval (Ethics Committee, University Hospital of Lausanne-CHUV). Written informed consent was obtained from all healthy subjects, in accordance with the Declaration of Helsinki. PBMCs were isolated by Ficoll density gradient centrifugation (1000 g for 10 minutes).

The PBMC layer was collected, washed three times, and resuspended in DPBS + 2% FBS + 2 mM EDTA at 5 x 10^7 cells/mL. Monocytes were isolated using the EasySep™ Human Monocyte Enrichment Kit without CD16 Depletion (STEMCELL Technologies GmbH, Germany). Part of the PBMCs was cryopreserved, while the rest was resuspended in DC media (CellGeniX GmbH, Germany) supplemented with 2% human serum albumin (HSA), 2 mM *L*-glutamine, 100 units/mL penicillin and 100 µL streptomycin in the presence of 500 IU/mL recombinant GM-CSF and 250 IU/mL IL-4. Cells were incubated at 37 °C, 5% CO_2 for two days and then replenished with fresh media and cytokines. After other two days, immature monocyte-derived DCs (mo-iDCs) were collected for subsequent experiments.

Cell uptake experiments. BMDCs or mo-iDCs (1 x 10^6 cells/mL) were plated in a 48-well plate and incubated with 60 µg OVA/OVA-488 mixture or labelled OVA nanogels per 10^6 cells. For experiments with BMDCs, at defined time points (1 h, 4 h and 24 h), cells were harvested and stained with AF700 anti-mouse CD11c, BV786 anti-mouse MHC-II and IR Dead/Alive reagent, washed in PBS + 2 mM EDTA and analysed with flow cytometry. The gating strategy is shown in **Supporting Information S1**. For experiments with mo-iDCs, at defined timepoints (1 h, 4 h and 24 h), cells were stained with AF700 anti-human CD11c, PE/Cy7 anti-human CD14 and IR Dead/Alive reagent, washed in PBS + 2 mM EDTA and analysed with flow cytometry. The gating strategy is shown in **Supporting Information Figure S2**.

Confocal microscopy. Mo-iDCs were plated at 0.2 or 0.4 x 10^6 cells/mL on glass coverslips (0.17 µm thickness) in DC medium in the presence of labelled OVA nanogels, soluble OVA/OVA-488 mixture or DC medium for 1, 4 and 24 h. The samples were then fixed in 4% paraformaldehyde in PBS and stained with WGA-Texas Red (100 µg/mL). Excess dye was removed by PBS washing. Cells were then permeabilized with 0.2% Triton X-100 PBS solution for 10 min and incubated with blocking solution (1% BSA and 0.1% Tween 20 PBS solution) for 30 min. Primary rabbit polyclonal antibody to EEA1 and rabbit polyclonal antibody to LAMP1 (1 : 1000 dilution in blocking solution) were incubated overnight at 4 °C or for one hour at room temperature. Excess antibody was removed by PBS washing. Then, AF647 donkey anti-mouse IgG (1 : 1000

dilution in blocking solution) secondary antibody was added and the slides incubated for 1 h at room temperature. Excess antibody was removed by PBS washing. Coverslips were then mounted in mounting medium (Fluoromount-G). Image acquisition was performed with a Leica SP8 confocal microscope with a 63 × NA 1.0 oil objective. Images were processed with ImageJ (National Institutes of Health).

BMDC activation experiments. BMDCs (1 x 10^6 cells/mL) were plated in a 6-well plate and incubated with 60 µg OVA or OVA nanogels per 1 x 10^6 cells. After 24 h, one part of the BMDCs was left in culture. The other part of the cells was treated with murine LPS (120 U/mL) and IFN-γ (4000 U/mL). After 24 h, both the untreated cells, as well as the LPS/IFN-γ treated BMDCs were harvested and incubated with Fc blocker (Ludwig Institute for Cancer Research, Lausanne) for 15 min at 4 °C prior staining with AF700 anti-mouse CD11c, APC anti-mouse CD86, BV421 anti-mouse CD83, PE anti-mouse MHC I-SIINFEKL complex monoclonal antibodies and Zombie Aqua™ Fixable Viability reagent. Cells were washed in PBS + 2 mM EDTA and analysed with flow cytometry. The gating strategy is shown in **Supporting Information Figure S3.**

Cell uptake experiments with mo-iDCs. Mo-iDCs (1 x 10^6 cells/mL) were plated in a 48-well plate and incubated with soluble OxTL or OxTL-nanogels (20 µg/10^6 cells). At defined time points (1 h, 4 h and 24 h), cells were harvested and stained with AF700 anti-human CD11c, PE/Cy7 anti-human CD14 and IR Dead/Alive reagent, washed in PBS + 2 mM EDTA and analysed with flow cytometry. The gating strategy is shown in **Supporting Information Figure S4.**

Statistical analysis. Comparisons between groups were assessed using a two-tailed unpaired Student's t test. In all tests: * = $p < 0.05$, ** = $p < 0.01$, *** = $p < 0.001$.

3.3. Results and Discussion

3.3.1 Nanogel preparation

The nanogels used in this study were prepared from ovalbumin, which was selected as a well-studied model antigen, as well as from oxidized tumor lysate that was obtained from A375 melanoma cells. Tumor lysate has been successfully used clinically to stimulate dendritic cells and enhance T cell response. Oxidized tumor lysate was obtained by treating A375 cells with hypochlorous acid followed by a series of freeze-thaw cycles. Ovalbumin and oxidized tumor lysate (oxTL) nanogels were obtained following the disulfide reduction and desolvation protocol that is illustrated in **Figure 1** and which has been previously developed for the preparation of human serum albumin nanoparticles.[40] This process starts with dissolution of the appropriate protein in 50 mM GSH, followed by desolvation in ethanol. This results in the formation of disulfide cross-linked nanogels. The disulfide crosslinks are degraded intracellularly because of the increased intracellular GSH concentration, thereby facilitating release of ovalbumin or tumor lysate.

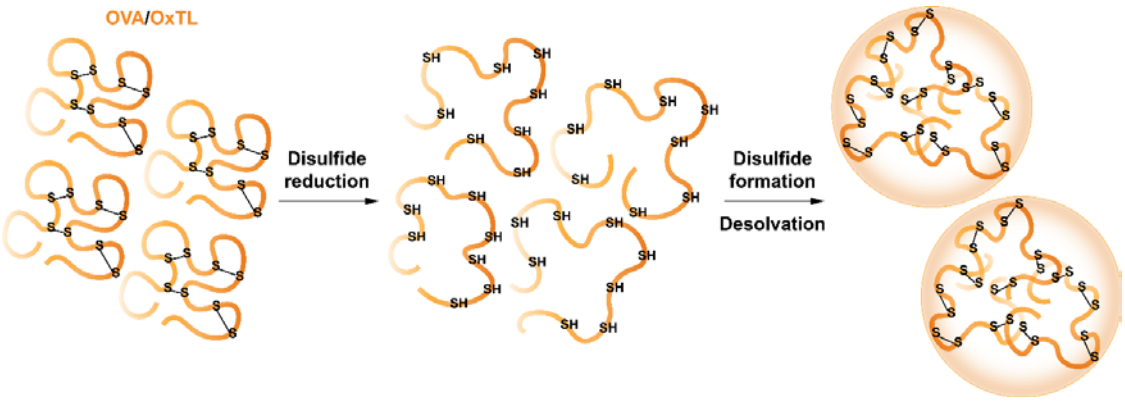

Figure 1. Synthesis of protein nanogels via intramolecular disulfide reduction and desolvation.

With ovalbumin, the procedure outlined in **Figure 1** affords nanogels with a diameter of 213 ± 30 nm and PDI of 0.13. By adding 2 wt% sucrose as a cryoprotectant before lyophilization, nanogels were obtained that can be stored at – 20 °C and subsequently

redispersed without change in particle size. Without the addition of sucrose, redispersion of the ovalbumin nanogels after storage resulted in larger particles with a size of 670 ± 441 nm and a PDI of 0.43 (**Figure 2A)**. For flow cytometry and confocal microscopy experiments, fluorescent-labelled ovalbumin nanogels were prepared by addition of 0.5 wt% ovalbumin, Alexa Fluor™ 488 (AF488) conjugate. The addition of the AF488 labelled ovalbumin did not lead to significant changes in particle size and afforded nanogels with a diameter of 173 ± 48 nm and a PDI of 0.08 (**Supporting Information Figure S5**). Using oxidized tumor lysate, the protocol illustrated in **Figure 1** afforded nanogel particles with a diameter of 242 ± 113 nm and a PDI of 0.22 (**Supporting Information Figure S6**). Fluorescent-labelled oxidized tumor lysate nanogels were prepared by staining HOCl treated A375 cells with CellTrace™ Violet.

To assess the effect of elevated concentrations of GSH and exposure to a reductive intracellular environment on particle size and stability, ovalbumin and oxidized tumor lysate nanogels were dispersed in Milli-Q water or in a 10 mM GSH solution for a period of 24 h and particle size was monitored with DLS. As illustrated in **Figure 2B**, incubation in a GSH solution resulted in complete degradation of the ovalbumin nanogel particles. Results of DLS analyses to monitor the reductive cleavage and disassembly of the oxidized tumor lysate nanogels are included in **Supporting Information Figure S8**. This analysis also revealed a compete disassembly of the oxidized tumor lysate nanogels within 24 h in 10 mM GSH.

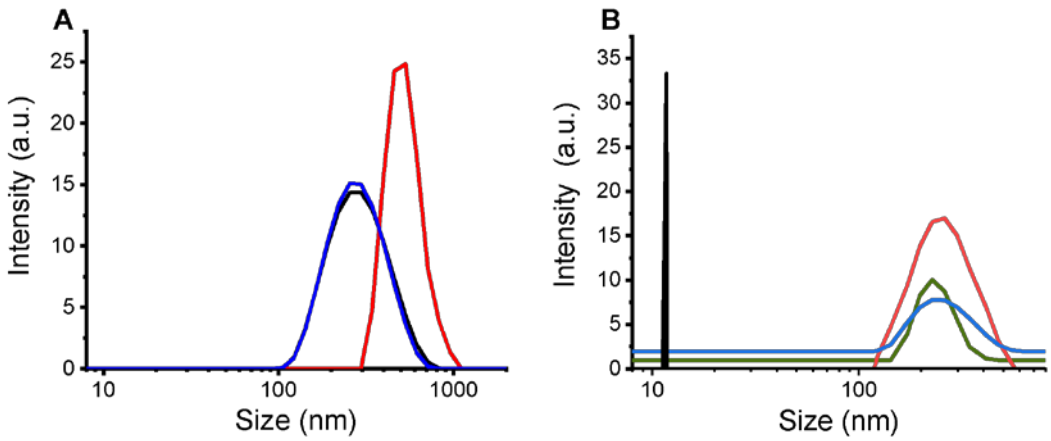

Figure 2. (A) Size distribution of ovalbumin nanogels directly after synthesis and before lyophilisation (black), after lyophilisation and resuspension in Milli-Q water without cryoprotectant (red), and upon redispersion in Milli-Q water after lyophilisation in the

presence of 2 wt% sucrose (blue); (B) Size distribution of ovalbumin nanogels (0.04 mg/mL) direct after dispersion in Milli-Q water (t = 0; green), after 24 h in Milli-Q water (blue), or in 10 mM GSH solution at t = 0 (red) and after 24 h (black).

Figure 3 summarizes the results of atomic force analyses that were conducted to further characterize the size and size distribution of the nanogels. The images presented in **Figure 3** were recorded on aqueous nanogel dispersions. Images of the same nanogels in the dry state are included in **Supporting Information Figure S7**. Analysis of the height of the particles in **Figure 3** reveals particle sizes of 165 ± 38 nm and 179 ± 18 nm for the ovalbumin and oxidized tumor lysate-based nanogels, which is in reasonable agreement with the information obtained from the dynamic light scattering analysis. Upon drying (see **Supporting Information Figure S7**), the particle size significantly decreases, which reflects the loss of water upon drying.

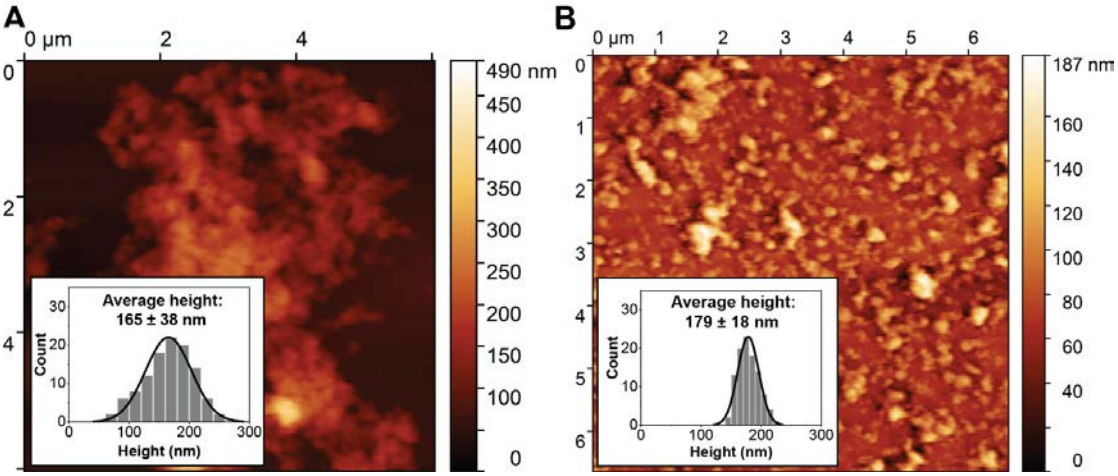

Figure 3. Atomic force microscopy images recorded on aqueous dispersions of (A) ovalbumin nanogels and (B) oxidized tumor lysate nanogels. The histograms represent the nanogel size distribution obtained from the analysis of 100 particles.

3.3.2. Ovalbumin nanogel uptake and activation of murine BMDCs

In a first series of experiments, the toxicity of the ovalbumin nanogels and their internalization by mouse bone marrow derived dendritic cells (BMDCs) was investigated. Cell viabilities were determined by incubating BMDCs with ovalbumin

nanogels. Control cells were presented with "free" ovalbumin or just with cell culture medium. After 1, 4 or 24 h, cells were collected and analysed with flow cytometry. To monitor internalization of the nanoparticles with flow cytometry, AF488-labelled nanogels were used. As shown in **Figure 4A**, cell viabilities were > 90 % for up to 24 h. As illustrated in **Figure 4B**, the use of the nanogel formulation significantly enhanced uptake of ovalbumin by the BMDCs. At all three time points, ovalbumin uptake, expressed as the percentage of ovalbumin-positive BMDCs, was 1.5 - 2.6 times larger when ovalbumin nanogels were used instead of "free" ovalbumin. **Figure 4C** presents the mean AF488-associated fluorescent intensity (MFI) of the fraction of cells that are ovalbumin-positive, i.e. which contain ovalbumin. The AF488-associated MFI is a measure of the average amount of ovalbumin internalized per cell. The data in **Figure 4C** show that after a period of 24 h, the use of the nanogel formulation not only results in a larger percentage of cells that contain ovalbumin, but also in a significant increase in the intracellular protein concentration as compared to the use of the "free" protein.

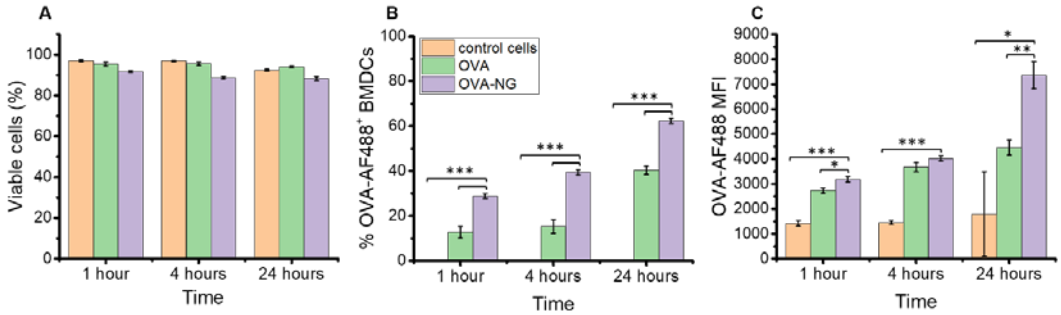

Figure 4. (A) Cell viability upon exposure to ovalbumin nanogels (OVA-NG), as well as free ovalbumin (OVA) compared to that of control cells for a period of 24 h. Ovalbumin internalization by BMDCs presented as (B) percentage of ovalbumin-containing cells and (C) the ovalbumin associated mean fluorescence intensity upon exposure of AF488 labelled ovalbumin for up to 24 h. Experiments were performed in triplicate. Statistical analysis was performed with Student's t-test, *: $p < 0.05$, **: $p < 0.01$, ***: $p < 0.001$.

Following internalization, the BMDCs digest the free or nanogel formulated ovalbumin. The resulting peptide fragments are then presented on the cell surface coupled to major histocompatibility complex (MHC) molecules. In case of ovalbumin this results in surface presentation of MHC-SIINFEKL molecules.[41] Simultaneously,

exposure to the antigen (ovalbumin in this case) triggers DC maturation, which results in the expression of increased levels of cell surface markers such as CD83 and CD86.[42,43,44] In clinical applications, in order to enhance maturation and to mitigate tolerance effects, cancer vaccines are often produced using DCs that have been treated with maturation cocktails that include inflammatory cytokines, such as interferon-γ (IFN), eventually in combination with Toll-like receptor (TLR) 4 agonist lipopolysaccharides (LPS) that help to further enhance the release of inflammatory cytokines.[45] To assess presentation of the SIINFEKL epitope and DC maturation, BMDCs were exposed to free ovalbumin or ovalbumin nanogels (60 µg/mL, 60 µg/10^6 cells) for 48 h and subsequently analysed by flow cytometry using allophycocyanin (APC) anti-mouse CD86, BV421 anti-mouse CD83 and PE anti-mouse MHC I-SIINFEKL antibodies. As a control, BDMCs were used that were not presented with the ovalbumin antigen. To assess the level of maturation upon exposure of the BMDCs to the ovalbumin antigen, two different experiments were performed. In a first experiment, epitope and CD83/CD86 presentation were measured on BMDCs that were presented with the ovalbumin nanogels and free ovalbumin. In a second experiment, BMDCs were analysed that had first been exposed to ovalbumin nanogels or free ovalbumin, and subsequently been stimulated with a maturation cocktail containing LPS and INF, as it has been done in clinical cancer vaccine development.[46]

Figure 5 compares SIINFEKL presentation and CD83/CD86 cell surface expression on BMDCs exposed to ovalbumin, and ovalbumin nanogels (**Figure 5A**) with that on BMDCs that were presented ovalbumin and ovalbumin nanogels and subsequently stimulated with INF-γ and LPS (**Figure 5B**). In **Figure 5**, CD83/CD86 and SIINFEKL presentation are shown as percentage of CD83/CD86, respectively, SIINFEKL positive BMDCs as determined by flow cytometry using CD83/CD86 and MHC I-SIINFEKL specific antibody markers. The data in **Figure 5A** evidence the presentation of the SIINFEKL epitope and demonstrate that surface presentation of the epitope is elevated when ovalbumin is delivered in form of a nanogel as compared to the free form of this antigen. **Supporting Information Figure S9** summarizes the results of dose-dependent BMDC maturation experiments which indicated a significant increase in SIINFEKL presentation upon increasing the OVA nanogel dose from 30 µg to 60 µg per 1 x 10^6 cells. Exposure to ovalbumin also results in an increase of the

fraction of cells that present CD83 and CD86 surface markers as compared to non-challenged DCs. In this case, the use of ovalbumin nanogels resulted in a significant increase in the percentage of CD83/CD86 positive cells as compared to the use of free ovalbumin. Stimulating cells with INF-γ and LPS after being exposed to free ovalbumin or ovalbumin nanogels results in a large increase in the percentage of CD83/CD86 positive cells (**Figure 5B**). For BDMCs that have been presented ovalbumin nanogels, for example, the percentage of CD83/CD86 positive cells increases from 47.4 ± 3.5 % to 67 ± 1 % upon stimulation with INF-γ and LPS. Stimulation with IFN-γ and LPS, however, has no effect of SIINFEKL presentation. Also for these experiments a significant increase in SIINFEKL presentation was observed when BDMCs were compared that were exposed to 30 µg, respectively 60 µg nanogel per 1 x 10^6 cells (**Supporting Information Figure S9B**).

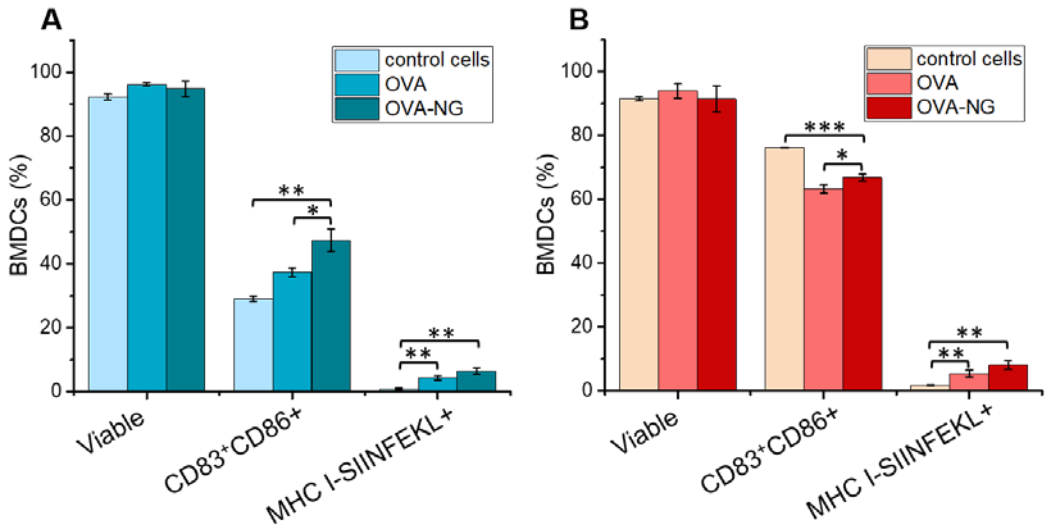

Figure 5. (A) Viability, percentage CD86/CD83 positive cells, and percentage cells that present MHC I-SIINFEKL for BDMCs challenged with media (control cells, light blue), OVA (60 µg/10^6 cells OVA, blue) or OVA nanogels (60 µg/10^6 cells OVA-NG, dark blue) for 48 h; (B) Viability, percentage CB86/CD83 positive cells, and percentage cells that present MHC I-SIINFEKL for BDMCs challenged with media (control cells, yellow), OVA (60 µg/10^6 cells OVA, pink) or OVA nanogels (60 µg/10^6 cells OVA-NG, red) for 48 h and that were additionally stimulated by adding LPS and IFN-γ after 24h. Statistical analysis was performed with Student's t-test, *: $p < 0.05$, **: $p < 0.01$, ***: $p < 0.001$.

3.3.3. *In vitro* uptake experiments of OVA nanogels in human primary cells

The results presented above illustrate the efficacy of the ovalbumin nanogels to enhance epitope presentation and maturation of mouse-derived DCs. An important step towards clinical application of these nanosized formulations is to assess their toxicity and validate their ability to facilitate antigen-uptake in human derived cells. To this end, a series of experiments was performed with monocyte-derived DCs (mo-DCs) that were obtained from three healthy human donors. The viability of the mo-DCs upon exposure to the ovalbumin nanogels as well as the internalization of the nanogels by these cells was investigated using flow cytometry as discussed earlier for the experiments with the mouse-derived BMDCs. In these experiments, the cell viability and internalization of ovalbumin by mo-DCs that were exposed to AF488 labelled ovalbumin nanogels was compared with that of cells that were presented with free ovalbumin as well as with that of control cells that were incubated in cell medium and not challenged with ovalbumin. The results of these experiments are summarized in **Figure 6**.

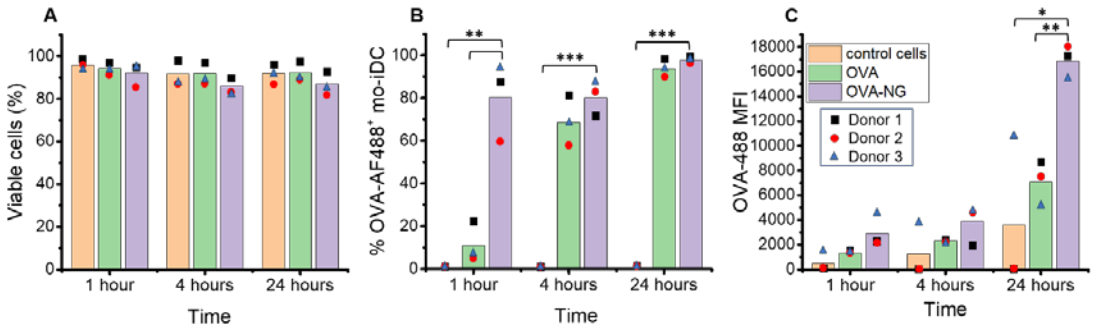

Figure 6. (A) Cell viability upon exposure to free ovalbumin (OVA), ovalbumin nanogels (OVA-NG) or cell culture medium (control cells) for 1, 4 or 24 h; (B) percentage of ovalbumin-containing cells after exposure to free ovalbumin (OVA), ovalbumin nanogels (OVA-NG) for 1, 4 or 24 h. Control cells were kept in cell culture medium for 1, 4 or 24 h; (C) OVA-AF488 associated mean fluorescence intensity (MFI) of cells after exposure to free ovalbumin (OVA), ovalbumin nanogels (OVA-NG) for 1, 4 or 24 h. Control cells were kept in cell culture medium for 1, 4 or 24 h. Experiments were repeated for 3 donors (Donor 1, black square, Donor 2, red circle and Donor 3, blue triangle). Statistical analysis was performed with Student's t-test, *: $p < 0.05$, **: $p < 0.01$, ***: $p < 0.001$.

A first observation from **Figure 6** is that the results that were obtained with these human-derived DCs were relatively consistent across the three donors. First, as indicated in **Figure 6A**, exposure of mo-iDCs to both ovalbumin nanogels as well as free ovalbumin has no significant impact on cell viability for a period of up to 24 h. **Figure 6B** presents the percentage of mo-iDCs that were gated as ovalbumin-positive, i.e. which contain ovalbumin, by flow cytometry. The results in **Figure 6B** illustrate that ovalbumin uptake by mo-iDCs is fast when nanogels are used. After 1 h, 80 ± 15% of the mo-iDCs contain ovalbumin. When mo-iDCs are presented with the same dose of free ovalbumin, it takes up to 24 h until a similar percentage of cells (93 ± 3%), have internalized ovalbumin. **Figure 6C** presents the AF488-associated MFIs of ovalbumin containing mo-iDCs, which are a measure of the average amount of antigen internalized, by the donor cells under the different conditions. In agreement with what was observed on the mouse-derived DCs, the use of ovalbumin nanogels also resulted in elevated intracellular levels of the antigen as compared to the use of free ovalbumin. The differences are moderate at t = 1 h and 4 h but substantial and statistically significant after 24 h.

Uptake of free ovalbumin and ovalbumin nanogels by mo-iDCs and the intracellular trafficking of the antigen was further studied by confocal microscopy. For these experiments, mo-iDCs were incubated with AF488-labelled ovalbumin or ovalbumin nanogels for 1, 4 and 24 h. After that, the cells were fixed, and stained with WGA Texas red to visualize the cell membrane, and with Anti-EEA1 antibody and Anti-LAMP1 antibody to highlight early endosomes, respectively, lysosomal compartments. **Figure 7** presents confocal images that were obtained in experiments using free ovalbumin (**Figure 7A** and **Figure 7B**) and ovalbumin nanogels (**Figure 7C** and **Figure 7D**). Confocal microscopy images of control cells that were incubated in cell culture media but not presented with ovalbumin or ovalbumin nanogels are included in **Supporting Information Figure S10**. In agreement with the flow cytometry results discussed earlier, while in the experiment with free ovalbumin it takes up to 24 h for the antigen to be discerned intracellularly (**Figure 7A** and **Figure 7B**), uptake of the nanogel formulation is much faster and the images already reveal the presence of intracellular ovalbumin after 1 hour incubation (**Figure 7C** and **Figure 7D**). The images in **Figure**

7C and **Figure 7D** also provide evidence for the reduction-sensitive nature of the nanogels and their intracellular degradation. This is illustrated by the intense, punctual AF488-associated fluorescence at the early times in the experiments, which becomes weaker and more diffuse across the cell body in the images recorded after 4 h and 24 h.

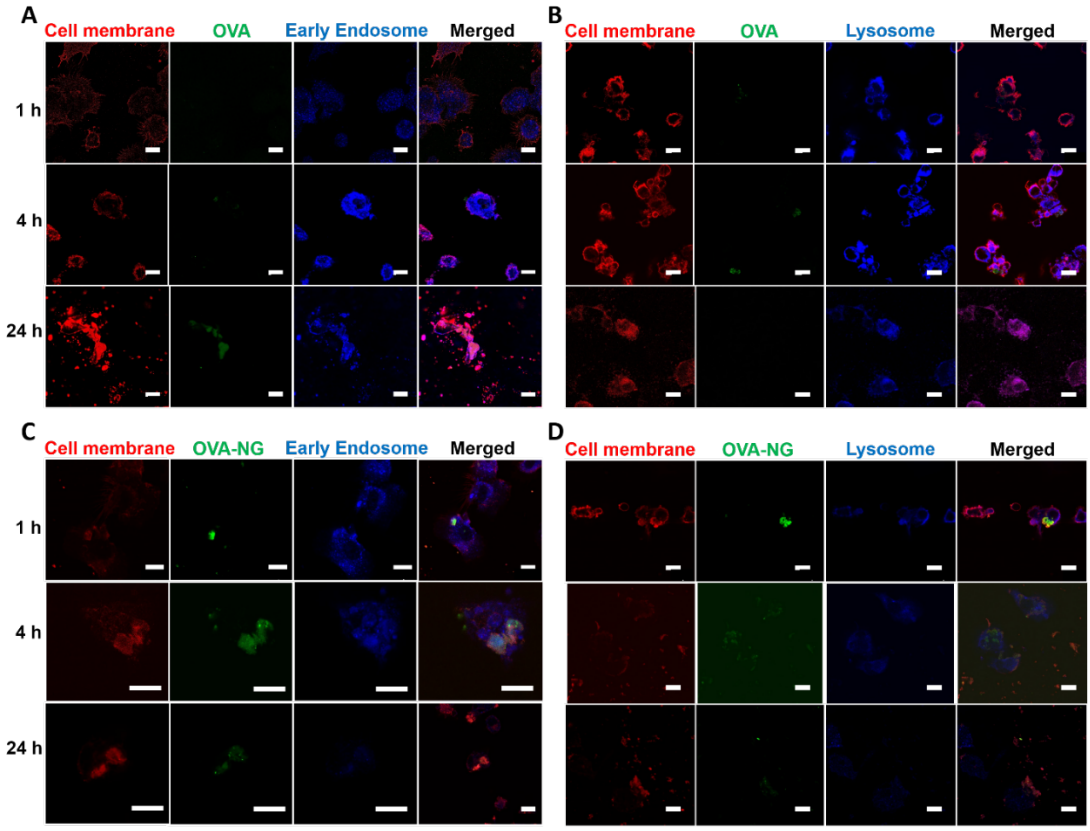

Figure 7. Confocal microscopy images of mo-iDCs that have been presented with AF488-labelled ovalbumin (A and B: OVA, 60 µg/10^6 cells) or AF488-labelled ovalbumin nanogels (C and D: OVA-NG, 60 µg/10^6 cells) at 37 °C for 1, 4 and 24 h. Panels A and C highlight the early endosomes and Panels B and D the lysosomes. The merged images represent the overlap of the cell membrane, OVA/OVA-NG and early endosome or lysosome channel. The scale bar represents 10 µm.

3.3.4. Uptake of oxidized tumor lysate-based nanogels in human donor-derived dendritic cells

In a final set of experiments to underline the potential of the nanogel formulations to enhance antigen update by dendritic cells, the use of this approach to deliver oxidized tumor lysate to human-derived mo-iDCs was studied. For these

experiments, nanogels with an average diameter of 224 ± 116 nm **were** used, which were generated from CellTrace Violet™ labelled oxidized tumor lysate (**Supporting Information Figure S8)**. The viability of and antigen uptake by mo-iDCs that were presented with oxidized tumor lysate nanogels was compared with that of mo-iDCs that were challenged with the corresponding free tumor lysate as well as with that of untreated control cells that were kept in culture medium. The viability of the mo-iDCs and oxidized tumor lysate uptake was assessed after 24 h using flow cytometry following the same approach as described above for the experiments with the ovalbumin nanogels. The results of these analyses, which provided relatively consistent outcomes across mo-iDCs from the 3 donors are summarized in **Figure 8**. Presentation of the mo-iDCs with oxidized tumor lysate, either in the free form or as nanogel, did not affect cell viability for a period up to 24 h (**Figure 8A**). As illustrated in **Figure 8B**, administration of oxidized tumor lysate in form of nanogels resulted in a significant increase in the percentage of cells that internalize the antigen. After 24 h, an average of 38 ± 16 % of mo-iDCs had taken up oxidized tumor lysate when it was delivered as nanogel as compared to 0.9 ± 0.5 % when free oxidized tumor lysate was used (**Figure 8B**). **Figure 8C** compares the CellTrace™ Violet associated mean fluorescence intensity (MFI) of the mo-iDC population that had internalized oxidized tumor lysate, which can be taken as a measure of the intracellular concentration of the antigen. The oxidized tumor lysate associated MFI observed for the control experiment reflects the autofluorescence of the cells. The oxidized tumor lysate associated MFI for mo-iDCs that were presented free and nanogel oxidized tumor lysate was significantly increased as compared to the control cells, but the experiment did not reveal a significant difference between cells that had been challenged with free versus nanogel oxidized tumor lysate.

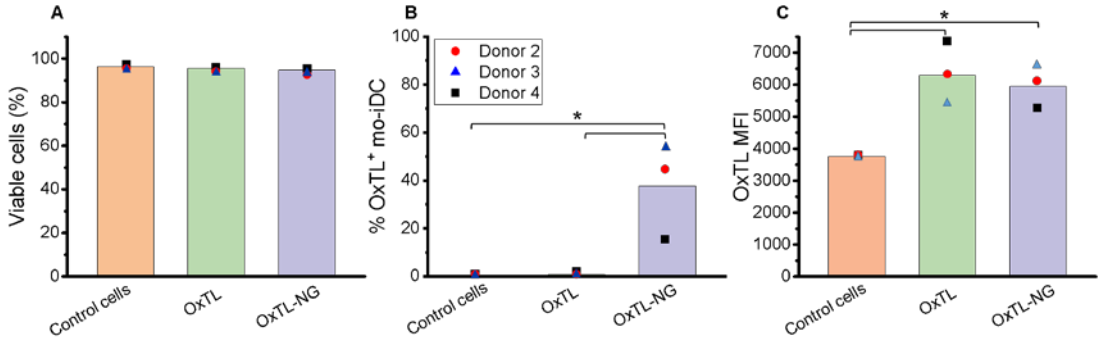

Figure 8. Viability (A), percentage of oxidized tumor lysate positive cells (B) and mean oxidized tumor lysate associated fluorescence intensity (MFI) (C) of mo-iDCs from three human donors (Donor 1, black square; Donor 2, red circle; Donor 3, blue triangle) that were challenged with DC media (control cells, orange), free oxidized tumor lysate (oxTL, green) or oxidized tumor lysate-based nanogels (OxTL-NG, in lilac). Statistical analysis was performed with Student's t-test, *: $p < 0.05$, **: $p < 0.01$

3.4. Conclusions

This study has demonstrated the use of reduction-sensitive protein nanogels for the delivery of antigens to mouse and human donor-derived dendritic cells. Work in this report has focused on ovalbumin as a model antigen, and on oxidized tumor lysate, which is a potent antigen that is of interest for cancer immunotherapy. Reduction-sensitive nanogels with diameters of ~200 nm could be prepared via a simple disulfide reduction – desolvation protocol from both these antigen sources. Both in experiments with mouse-derived dendritic cells as well as in experiments with dendritic cells that were harvested from human donors the use of the nanogel delivery platform was found to enhance uptake of ovalbumin, and subsequently augment dendritic cell activation, as compared to the use of the free protein antigen. The nanogels were also demonstrated to facilitate the delivery of oxidized tumor lysate as compared to the use of the corresponding free antigen, and allowed to significantly enhance internalization of this antigen in dendritic cells that were harvested from 3 human donors.

3.5. References

1. Cao, S. *et al.* Nanoparticles: Oral Delivery for Protein and Peptide Drugs. *AAPS PharmSciTech* **20**, 1–11 (2019).

2. Slastnikova, T. A., Ulasov, A. V., Rosenkranz, A. A. & Sobolev, A. S. Targeted intracellular delivery of antibodies: The state of the art. *Front. Pharmacol.* **9**, 1–21 (2018).

3. Posey, N. D., Hango, C. R., Minter, L. M. & Tew, G. N. The Role of Cargo Binding Strength in Polymer-Mediated Intracellular Protein Delivery. *Bioconjug. Chem.* **29**, 2679–2690 (2018).

4. Kimchi-Sarfaty, C. *et al.* Building better drugs: Developing and regulating engineered therapeutic proteins. *Trends Pharmacol. Sci.* **34**, 534–548 (2013).

5. Lv, J., Fan, Q., Wang, H. & Cheng, Y. Polymers for cytosolic protein delivery. *Biomaterials* **218**, 1–12 (2019).

6. Fu, A., Tang, R., Hardie, J., Farkas, M. E. & Rotello, V. M. Promises and Pitfalls of Intracellular Delivery of Proteins. *Bioconjug. Chem.* **25**, 1602–1608 (2014).

7. Raemdonck, K., Demeester, J. & De Smedt, S. Advanced nanogel engineering for drug delivery. *Soft Matter* **5**, 707–715 (2009).

8. Kabanov, A. V. & Vinogradov, S. V. Nanogels as pharmaceutical carriers: Finite networks of infinite capabilities. *Angew. Chemie - Int. Ed.* **48**, 5418–5429 (2009).

9. Li, Y., Maciel, D., Rodrigues, J., Shi, X. & Tomás, H. Biodegradable polymer nanogels for drug/nucleic acid delivery. *Chem. Rev.* **115**, 8564–8608 (2015).

10. Zhang, X., Malhotra, S., Molina, M. & Haag, R. Micro- and nanogels with labile crosslinks-from synthesis to biomedical applications. *Chem. Soc. Rev.* **44**, 1948–1973 (2015).

11. Lee, E. J., Lee, N. K. & Kim, I. S. Bioengineered protein-based nanocage for

drug delivery. *Adv. Drug Deliv. Rev.* **106**, 157–171 (2016).

12. Yin, L., Yuvienco, C. & Montclare, J. K. Protein based therapeutic delivery agents: Contemporary developments and challenges. *Biomaterials* **134**, 91–116 (2017).

13. Cheng, L., Yang, L., Meng, F. & Zhong, Z. Protein Nanotherapeutics as an Emerging Modality for Cancer Therapy. *Adv. Healthc. Mater.* **7**, 1–9 (2018).

14. Sikder, S., Gote, V., Alshamrani, M., Sicotte, J. & Pal, D. Long-term delivery of protein and peptide therapeutics for cancer therapies. *Expert Opin. Drug Deliv.* **16**, 1113–1131 (2019).

15. Froimchuk, E., Carey, S. T., Edwards, C. & Jewell, C. M. Self-Assembly as a Molecular Strategy to Improve Immunotherapy. *Acc Chem Res* **53**, 2534–2545 (2020).

16. Deng, C., Zhang, Q., Guo, J., Zhao, X. & Zhong, Z. Robust and smart polypeptide-based nanomedicines for targeted tumor therapy. *Adv. Drug Deliv. Rev.* **160**, 199–211 (2020).

17. Le Saux, S. *et al.* Nanotechnologies for Intracellular Protein Delivery : Recent Progress in Inorganic and Organic Nanocarriers. *Adv. Ther.* **4**, 1–23 (2021).

18. Tsai, S. J., Amerman, A. & Jewell, C. M. Altering Antigen Charge to Control Self-Assembly and Processing of Immune Signals During Cancer Vaccination. *Front. Immunol.* **11**, 1–14 (2021).

19. Pei, M. *et al.* Mannose-functionalized antigen nanoparticles for targeted dendritic cells, accelerated endosomal escape and enhanced MHC-I antigen presentation. *Colloids Surfaces B Biointerfaces* **197**, 1–9 (2021).

20. Xi, X. *et al.* Lymph node-targeting nanovaccine through antigen-CpG self-assembly potentiates cytotoxic T Cell activation. *J. Immunol. Res.* 1–10 (2018). doi:10.1155/2018/3714960

21. Wei, L., Zhao, Y., Hu, X. & Tang, L. Redox-Responsive Polycondensate Neoepitope for Enhanced Personalized Cancer Vaccine. *ACS Cent. Sci.* **6**, 404–

412 (2020).

22. Wang, K., Yang, Y., Xue, W. & Liu, Z. Cell Penetrating Peptide-Based Redox-Sensitive Vaccine Delivery System for Subcutaneous Vaccination. *Mol. Pharm.* **15**, 975–984 (2018).

23. Wang, K. *et al.* 'Minimalist' Nanovaccine Constituted from Near Whole Antigen for Cancer Immunotherapy. *ACS Nano* **12**, 6398–6409 (2018).

24. Chiang, C. L., Coukos, G. & Kandalaft, L. E. Whole Tumor Antigen Vaccines: Where Are We? *Vaccines* **3**, 344–372 (2015).

25. Won, J. E. *et al.* Enhanced Antitumor Immunity Using a Tumor Cell Lysate-Encapsulated CO2 - Generating Liposomal Carrier System and Photothermal Irradiation. *ACS Appl. Bio Mater.* **2**, 2481–2489 (2019).

26. Chiang, C. L., Ledermann, J. A., Rad, A. N., Katz, D. R. & Chain, B. M. Hypochlorous acid enhances immunogenicity and uptake of allogeneic ovarian tumor cells by dendritic cells to cross-prime tumor-specific T cells. *Cancer Immunol. Immunother.* **55**, 1384–1395 (2006).

27. Chiang, C. L. L. *et al.* Oxidation of ovarian epithelial cancer cells by hypochlorous acid enhances immunogenicity and stimulates T cells that recognize autologous primary tumor. *Clin. Cancer Res.* **14**, 4898–4907 (2008).

28. Chiang, C. L. *et al.* Adjuvants for Enhancing the Immunogenicity of Whole Tumor Cell Vaccines. *Int. Rev. Immunol.* **30**, 150–182 (2011).

29. Chiang, C. L. *et al.* A Dendritic Cell Vaccines Pulsed with Autologous Hypochlorous Acid-Oxidized Ovarian Cancer Lysate Primes Effective Broad Antitumor Immunity : From Bench to Bedside. *Clin Cancer Res.* **19**, 4801–4815 (2013).

30. Graciotti, M. *et al.* Deciphering the Mechanisms of Improved Immunogenicity of Hypochlorous Acid-Treated Antigens in Anti-Cancer Dendritic Cell-Based Vaccines. *Vaccines* **8**, 1–24 (2020).

31. Solbrig, C. M., Cody, V. & Saltzman, W. M. Polymer Nanoparticles for

Immunotherapy from Encapsulated Tumor-Associated Antigens and Whole Tumor Cells. **4**, 47–57 (2006).

32. Goforth, R. *et al.* Immune stimulatory antigen loaded particles combined with depletion of regulatory T-cells induce potent tumor speci W c immunity in a mouse model of melanoma. *Cancer Immunol. Immunother.* **58**, 517–530 (2009).

33. Prasad, S. *et al.* Polymer nanoparticles containing tumor lysates as antigen delivery vehicles for dendritic cell-based antitumor immunotherapy. *Nanomedicine Nanotechnology, Biol. Med.* **7**, 1–10 (2011).

34. Hanlon, D. J. *et al.* Enhanced Stimulation of Anti-Ovarian Cancer CD8+ T Cells by Dendritic Cells Loaded with Nanoparticle Encapsulated Tumor Antigen. *Am. J. Reprod. Immunol.* **65**, 597–609 (2011).

35. Mueller, M., Reichardt, W., Koerner, J. & Groettrup, M. Coencapsulation of tumor lysate and CpG-ODN in PLGA-microspheres enables successful immunotherapy of prostate carcinoma in TRAMP mice. *J. Control. Release* **162**, 159–166 (2012).

36. Gross, B. P., Wongrakpanich, A., Francis, M. B., Salem, A. K. & Norian, L. A. A therapeutic microparticle-based tumor lysate vaccine reduces spontaneous metastases in murine breast cancer. *AAPS J.* **16**, 1194–203 (2014).

37. Iranpour, S., Nejati, V., Delirezh, N., Biparva, P. & Shirian, S. Enhanced stimulation of anti-breast cancer T cells responses by dendritic cells loaded with poly lactic-co-glycolic acid (PLGA) nanoparticle encapsulated tumor antigens. *J. Exp. Clin. cancer Res.* **35**, 1–11 (2016).

38. Kohnepoushi, C., Nejati, V., Delirezh, N. & Biparva, P. Poly Lactic-co-Glycolic Acid Nanoparticles Containing Human Gastric Tumor Lysates as Antigen Delivery Vehicles for Dendritic Cell-Based Antitumor Immunotherapy. *Immunol. Invest.* **48**, 794–808 (2019).

39. Gross, B. P. *et al.* Biotinylated Streptavidin Surface Coating Improves the E ffi cacy of a PLGA Microparticle-Based Cancer Vaccine. *Bioconjug. Chem.* **31**, 2147–2157 (2020).

40. Rötzschke, O., Falk, K., Stevanovic, S., Jung, G. & Walden, Peter Rammensee, H.-G. Exact prediction of a natural T cell epitope. *Eur. J. Immunol.* **21**, 2891–2894 (1991).

41. Banchereau, J. & Steinman, R. M. Dendritic cells and the control of immunity. *Nature* **392**, 245–252 (1998).

42. Pardoll, D. M. Spinning molecular immunology into successful immunotherapy. *Nat. Rev. Drug Discov.* **2**, 227–238 (2002).

43. Timmerman, J. M. & Levy, R. Dendritic Cell Vaccines for Cancer Immunotherapy. *Annu. Rev. Med.* **50**, 507–529 (1999).

44. Perez, C. R. & Palma, M. De. Engineering dendritic cell vaccines to improve cancer immunotherapy. *Nat. Commun.* **10**, 1–10 (2019).

45. Tanyi, J. L. *et al.* Personalized cancer vaccine strategy elicits polyfunctional T cells and demonstrates clinical benefits in ovarian cancer. *npj Vaccines* **6**, 1–14 (2021).

3.6. Supporting Information

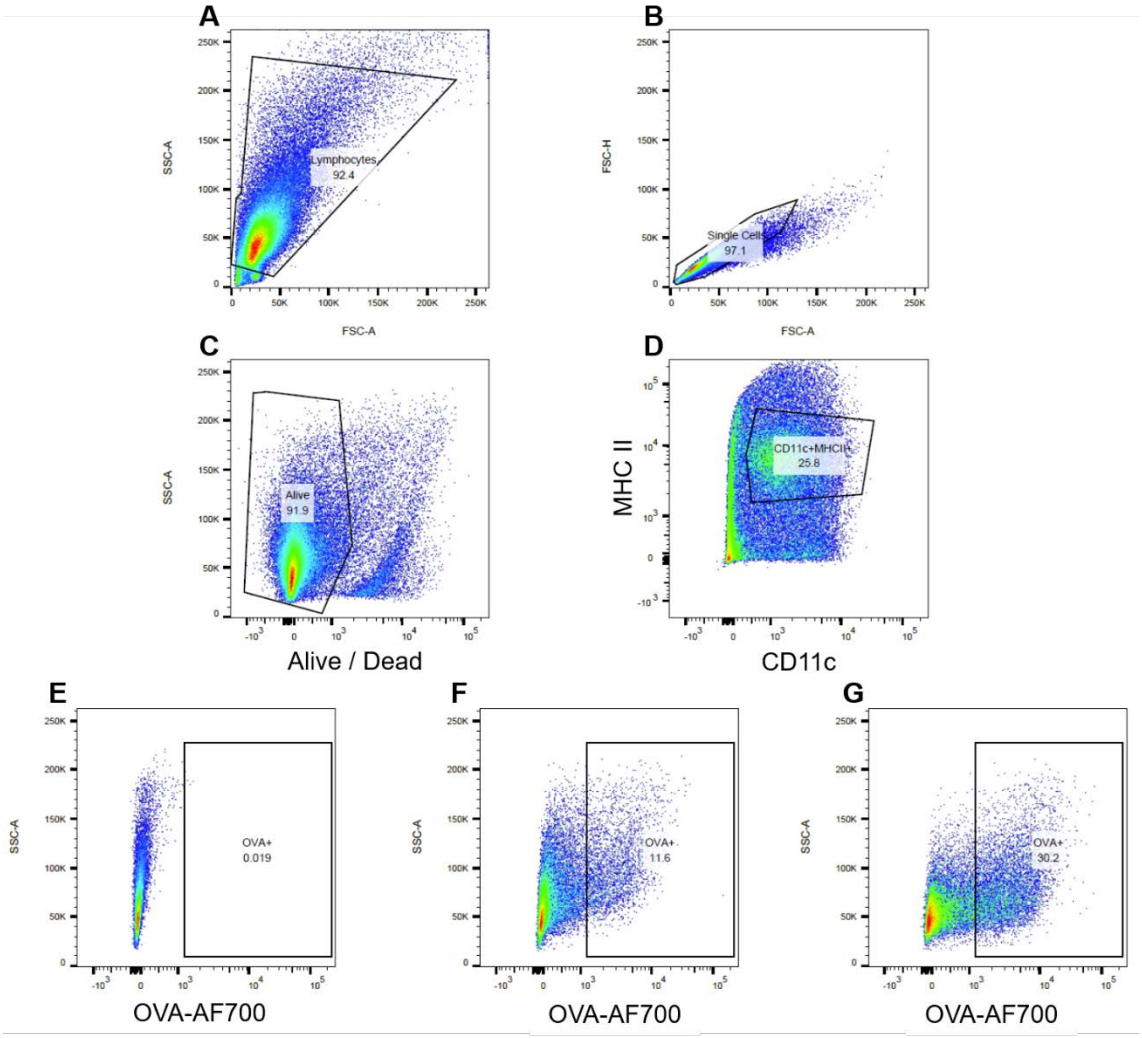

Figure S1. Gating strategy for the flow cytometry analysis of BMDCs incubated with OVA or OVA nanogels (see **Figure 4**). Cells were gated from the top left line considering forward and side scatter (FSC and SSC) to define cells from debris (A). Among the cells, single ones were selected (B) and from the single cells the live ones (negative for LIVE/DEAD™ Fixable Near-IR Dead Cell reagent) (C). Among the live single cells, the DCs were then selected by gating CD11c^{+} and MHC II^{+} cells (D). In panel E, the OVA-associated autofluorescence of BMDCs that have not been treated with OVA is used to define the gating setting for OVA positive BMDCs. Panel F and G, as an example show a flow cytometry scatter plot of BMDCs that have been exposed to 60 µg of OVA or OVA-NG per 1 x 10^{6} cells respectively.

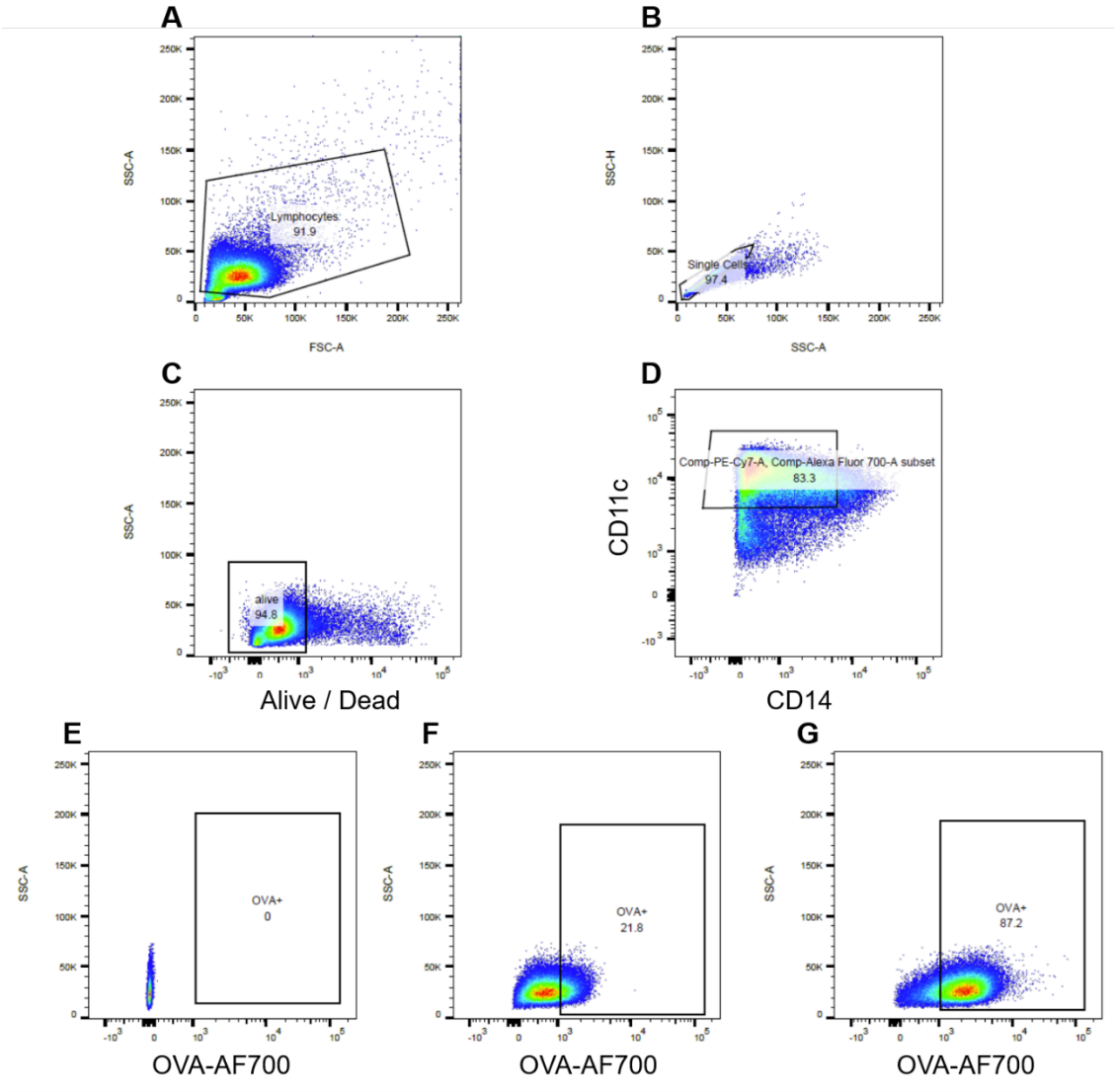

Figure S2. Gating strategy for the flow cytometry analysis of mo-iDCs incubated with OVA or OVA nanogels (see **Figure 6**). Cells were gated from the top left line considering forward and side scatter (FSC and SSC) to define cells from debris (A). Among the cells, single ones were selected (B) and from the single cells the live ones (negative for LIVE/DEAD™ Fixable Near-IR Dead Cell reagent) (C). Among the live single cells, the DCs were then selected by gating $CD11c^{+}$ and $CD14^{-}$ cells (D). In panel E, the OVA-associated autofluorescence of mo-iDCs that have not been treated with OVA is used to define the gating setting for OVA positive mo-iDCs. Panel F and G, as an example show a flow cytometry scatter plot of mo-iDCs that have been exposed to 60 µg of OVA or OVA-NG per 1 x 10^{6} cells respectively.

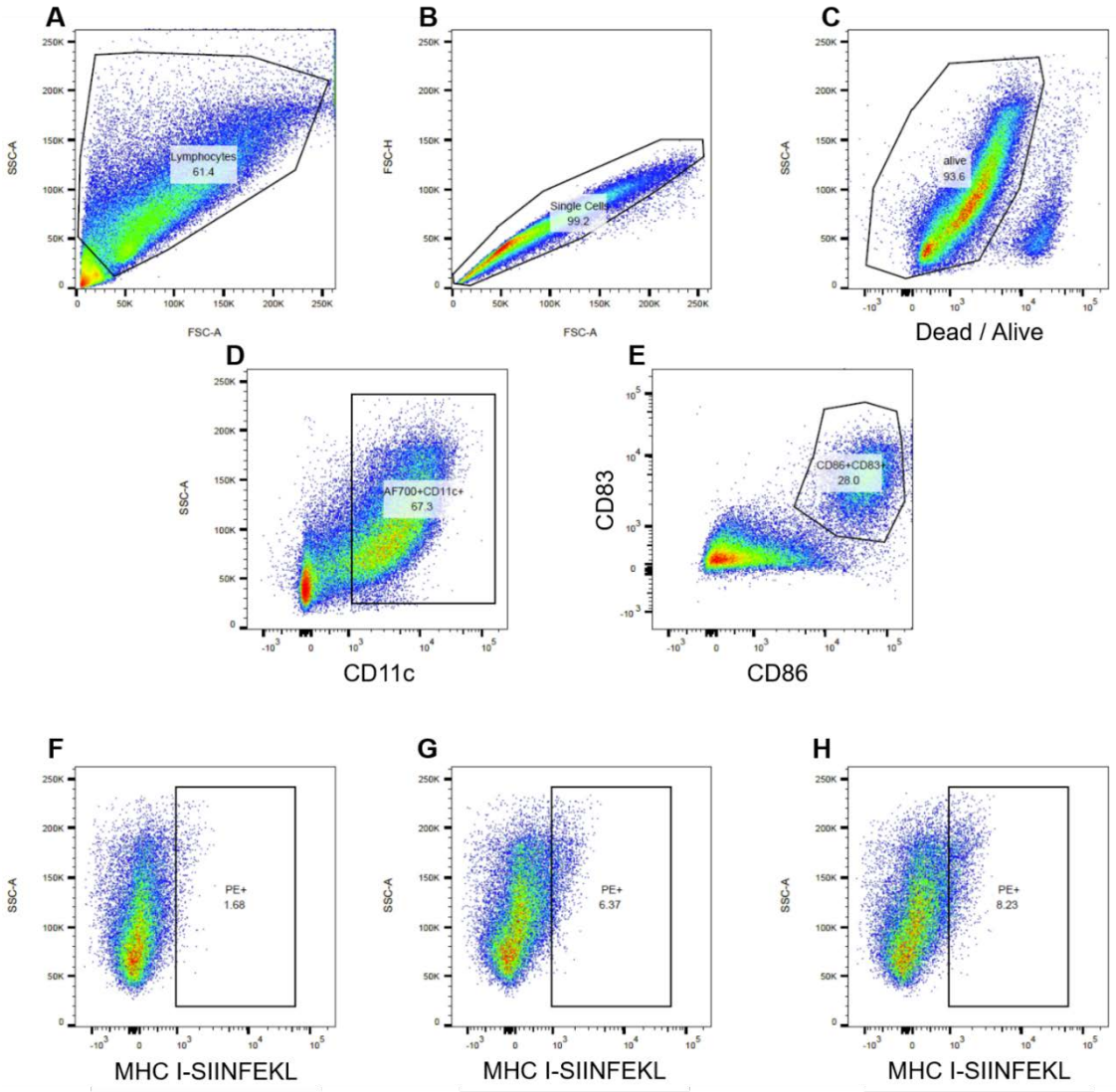

Figure S3. Gating strategy for the flow cytometry analysis of maturation and surface expression of MHC I-SIINFEKL following OVA and OVA-nanogel uptake by BMDCs (see **Figure 5**). Cells were gated from the top left line considering forward and side scatter (FSC and SSC) to define cells from debris (A). Among the cells, single ones were selected (B) and from the single cells the live ones (negative for Zombie Aqua™ Fixable Viability reagent) (C). Among the live single cells, the DCs were then selected by gating $CD11c^+$ cells (D) and the activated $CD83^+$ and $CD86^+$ DCs (E). In panel F, the MHC I-SIINFEKL-associated autofluorescence of BMDCs that have not been treated with OVA is used to define the gating setting for MHC I-SIINFEKL positive BMDCs. Panel F and G, as an example show a flow cytometry scatter plot of BMDCs that have been exposed to 60 µg of OVA or OVA-NG per 1 x 10^6 cells respectively.

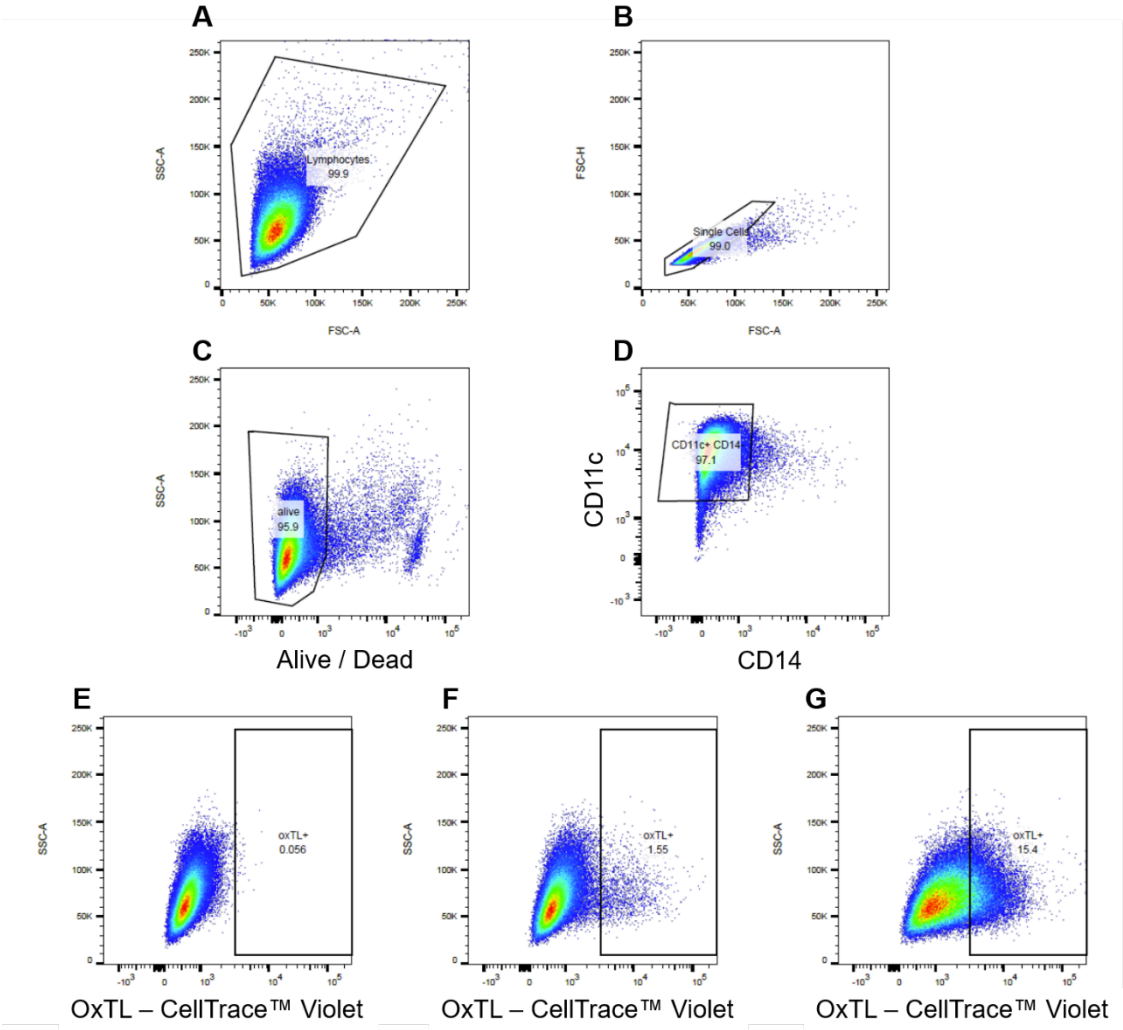

Figure S4. Gating strategy for the flow cytometry analysis of OxTL/OxTL nanogel uptake and mo-iDC viability (see **Figure 8**). Cells were gated from the top left line considering forward and side scatter (FSC and SSC) to define cells from debris (A). Among the cells, single ones were selected (B) and from the single cells the live ones (negative for LIVE/DEAD™ Fixable Near-IR Dead Cell reagent) (C). Among the live single cells, the DCs were then selected by gating $CD11c^{+}$ and $CD14^{-}$ cells (D). In panel E, the OxTL-associated autofluorescence of mo-iDCs that have not been treated with OxTL is used to define the gating setting for OxTL positive mo-iDCs. Panel F and G, as an example shows a flow cytometry scatter plot of mo-iDCs that have been exposed to 20 µg of OxTL or OxTL-NG per 1 x 10^{6} cells, respectively.

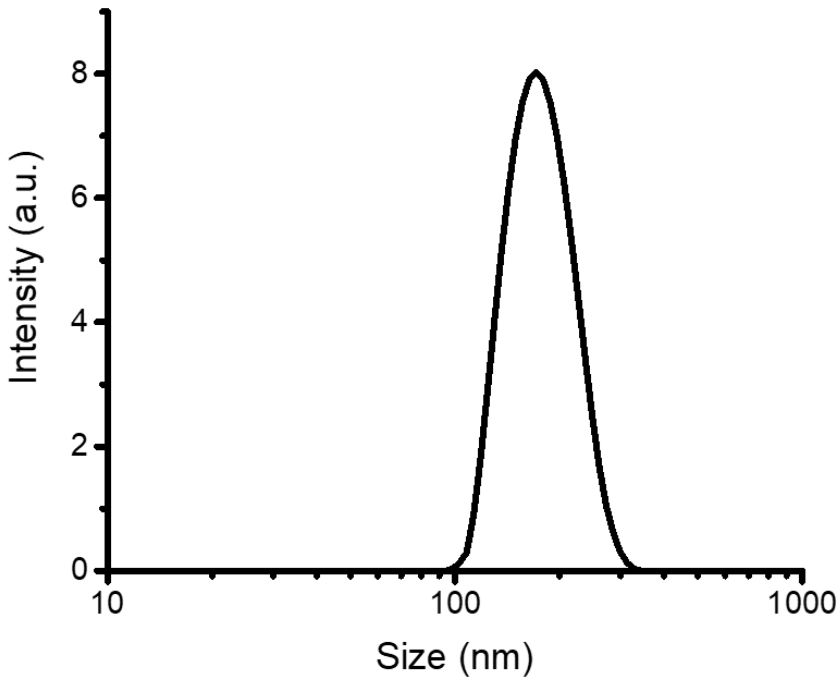

Figure S5. Intensity-average size distribution of nanogels synthetized with OVA and OVA-AF488 mixture, where OVA-AF488 was added at 0.5 wt % (50 µg OVA-AF488 in 10 mg OVA).

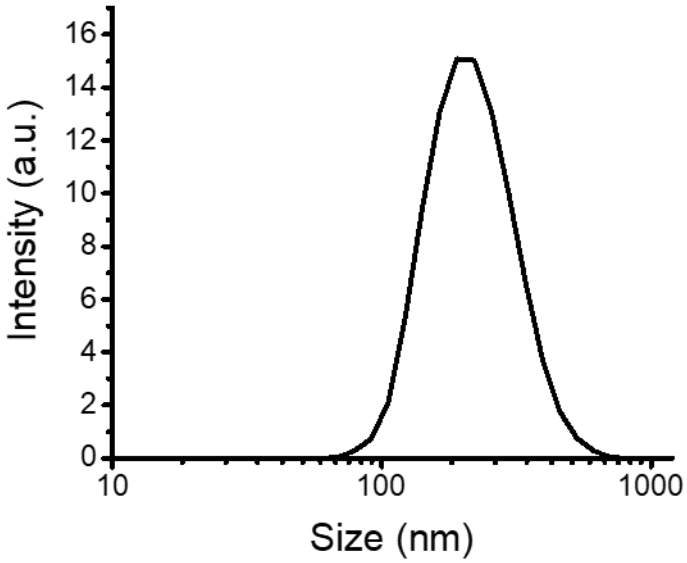

Figure S6. Intensity-average size distribution of nanogels synthetized with CellTrace Violet labelled A375 oxidized tumor Lysate.

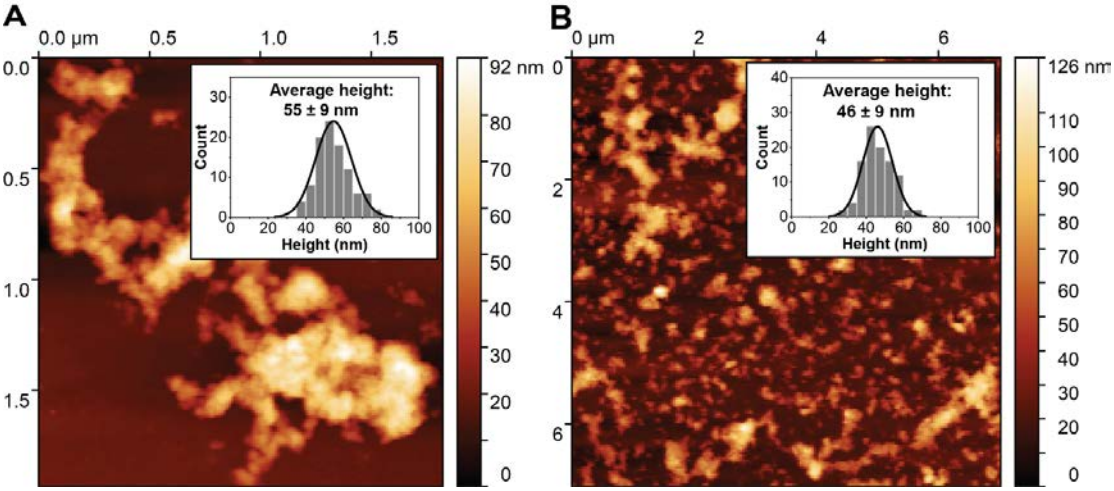

Figure S7. Atomic force microscopy images recorded on (A) dried ovalbumin nanogels and (B) dried oxidized tumor lysate nanogels. The histograms represent the size distribution obtained from the analysis of 100 particles.

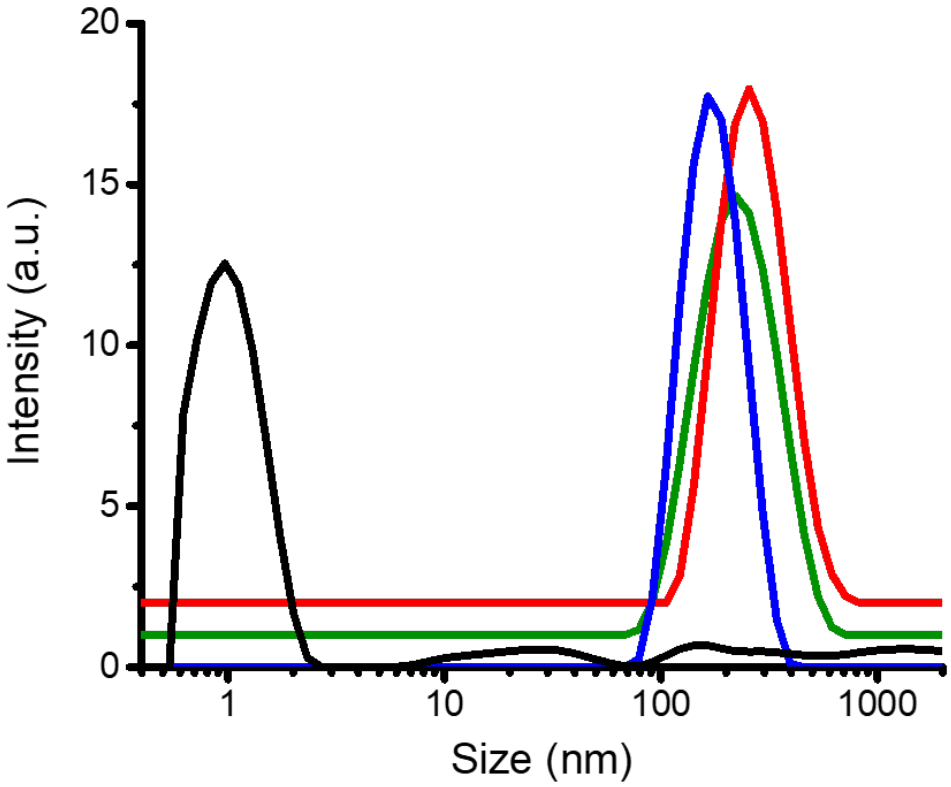

Figure S8. Intensity-average size distribution intensity of nanogels synthetized with CellTrace™ Violet labelled oxidized tumor lysate incubated in water at timepoint 0 hours (green line) and 24 hours (blue line) or in 10 mM GSH solution in Milli-Q Water at timepoint 0 hours (red line) and 24 hours (black line).

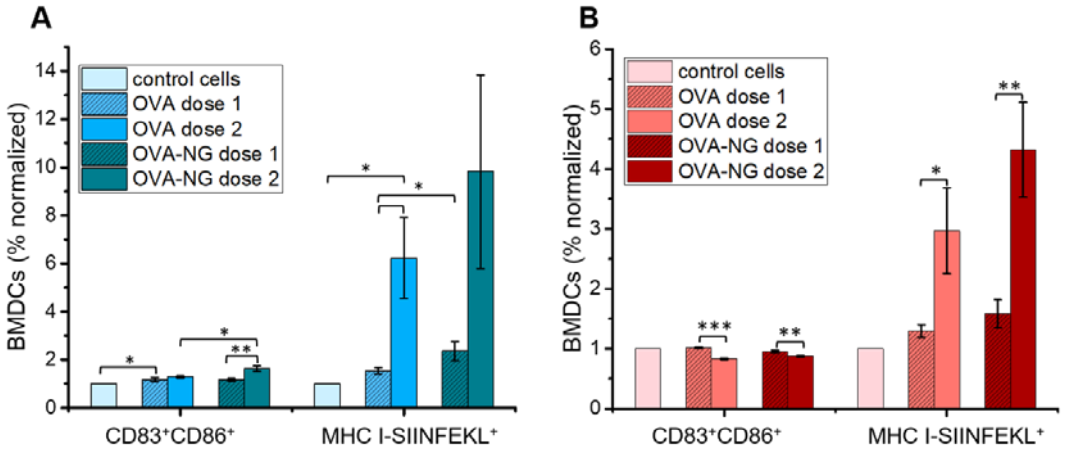

Figure S9. (A) Percentage of CD86/CD83 positive cells and percentage of cells that present MHC I-SIINFEKL for BDMCs challenged with media (control cells, light blue), OVA dose 1 (30 µg/10^6 cells OVA, striped blue) and dose 2 (60 µg/10^6 cells OVA, blue) or OVA nanogels dose 1 (30 µg/10^6 cells OVA-NG, striped dark blue) and dose 2 (60 µg/10^6 cells OVA-NG, dark blue) for 48 h; (B) Percentage of CB86/CD83 positive cells, and percentage of cells that present MHC I-SIINFEKL for BDMCs challenged with media (control cells, pink), OVA dose 1 (30 µg/10^6 cells OVA, striped light red) and dose 2 (60 µg/10^6 cells OVA, light red) or OVA nanogels dose 1 (30 µg/10^6 cells OVA-NG, striped red) and dose 2 (60 µg/10^6 cells OVA-NG, red) for 48 h and that were additionally stimulated by adding LPS and IFN-γ after 24h. Statistical analysis was performed with Student's t-test, *: $p < 0.05$, **: $p < 0.01$, ***: $p < 0.001$.

4. Conclusions and Perspectives

Although approaches like chemotherapy, radiotherapy and biological drugs have offered a treatment for cancer patients, the World Health Organization reports still 10 million deaths in 2020 caused by cancer. Cancer immunotherapy offers a solution for cancers that do not respond to these standard therapies. Current strategies in cancer immunotherapy have been described in **Chapter 1**, with a focus on cancer vaccines and underlying the limitations of this approach. In particular, easier manufacturing solutions and a patient-oriented approach already in pre-clinical setting have been reported as the major limiting factors. Nanoparticles have been suggested as a potential tool for antigen delivery in cancer vaccines, for the possibility to control their size, shape, charge and surface targeting moieties, the ability to protect the antigen and the possibility to co-deliver drugs and adjuvants.

In **Chapter 2** the production of nanoparticles based on PEG-PLGA was described for the delivery of oxidized tumor lysate. The nanoparticles were tested in human donor-derived dendritic cells and have demonstrated low cytotoxicity and increased uptake of the encapsulated oxidized tumor lysate. When evaluating the immune response in autologous T cells, oxidized tumor lysate loaded nanoparticles could induce a specific apoptotic-mediated killing of cancer cells. Additionally, nanoparticles were well-tolerated once tested for therapeutic vaccination in tumor bearing mice, inducing significantly prolonged survival as compared to the control untreated mice.

However, the synthetized PEG-PLGA nanoparticles do not release their cargo intracellularly in a controlled manner and require stabilizers during manufacturing that could pose toxicity issues. Alternatively, protein based nanogels that rely on disulfide cross-linking for stability would offer a high

biocompatible antigen delivery system that degrades in the intracellular reducing environment. **Chapter 3** focuses on the production of such redox-responsive nanogels based on ovalbumin and oxidized tumor lysate. The nanogels degraded in a reducing environment and demonstrated biocompatibility and enhanced antigens uptake in both murine and human primary cell lines. The increased uptake was also confirmed by the specific expression of activation markers on the surface of dendritic cells.

In conclusion, both formulations, either based on synthetic polymers (PEG-PLGA) or natural polymers (proteins), enhanced uptake of the antigen as compared to administration of the soluble format. Using oxidized tumor lysate as antigen source offers a personalized and immunogenic approach which contributes to the efficacy and clinical impact of these nanoformulations, as well as the use of human donor-derived cells. However, the use of human donor-derived cells is a double-edged sword. On one side, it represent the variability commonly encountered in the clinic and therefore offers a more realistic vision of the translation of nanoparticles in patients, as compared to the use of immortalized and murine cell line. On the other side, because of this variability, a larger population would be needed for solid statistic results on efficacy.

Another factor influencing the efficacy of nanoparticles for cancer vaccination is the need for targeted approaches and, as anticipated in **Chapter 1**, for co-delivery of adjuvants and drugs that act on the tumor microenvironment. In fact, reshaping the tumor microenvironment is one of the major challenges in immunotherapy, as the field still unveils the complex and evolving relationship between the immune system and cancer. Therefore, the correct drug combination still needs to be determined and requires a highly personalized and patients-focused approach. This work constitutes therefore the basis for future studies and applications of nanoparticle-encapsulation of tumor material for DC-based vaccination approaches.

Cristiana Berti

Route de Taillepied, 27

1095 Lutry (CH)

+41 78 668 85 67

cristiana.berti@epfl.ch

EDUCATION

Ph.D. Candidate | Material Science and Engineering Nov 2016 – Jun 2021

Laboratory of Polymers

Ecole Polytechnique Fédérale de Lausanne (EPFL), Switzerland

Master of Science | Pharmaceutical Biotechnologies Oct 2014 - Oct 2016

Final grade: 110/110 cum laude

Università degli Studi di Padova, Italy

Bachelor of Science | Molecular Biology Oct 2011 - Jul 2014

Final grade: 108/110

Università degli Studi di Padova, Italy

EXPERIENCE

Nov 2016 – June 2021

PhD Candidate: "Enhancing T-cell response in cancer immunotherapy using nanoparticles"

Laboratory of Polymers

Ecole Polytechnique Fédérale de Lausanne (EPFL), Switzerland

In collaboration with Cancer Vaccine Development Laboratory

University of Lausanne (Unil), Switzerland

Mar 2016 - Aug 2016

Master Thesis Project: “Selection of hFKBP12 binders by phage display for monitoring FK506 in transplant patients”

Laboratory of Therapeutic Peptides and proteins

Ecole Polytechnique Fédérale de Lausanne (EPFL), Switzerland

TECHNICAL SKILLS

Cell biology: Generation, culture, and analysis of Peripheral Blood Mononuclear Cells from healthy human donors; Proliferation and viability assays; Uptake studies; Co-cultures; Cell transfection; Primary murine and human cell lines.

Cell biology techniques: Flow cytometry; Immune assays; Confocal microscopy; Cell killing assay; Phage display; Cell transfection; Protein extraction.

Animal experiments: Generation of bone marrow derived dendritic cells; Tumour inoculation; Vaccination; Tumour growth monitoring and survival studies.

Synthetic skills: Organic synthesis; Nanoparticles and nanogels preparation; Double emulsion method; Desolvating method; Surface modification of nanoparticles; Solid Phase Peptide Synthesis (SPPS).

Analytical techniques: Dynamic light scattering (DLS); UV-Vis spectroscopy; Fluorescence Polarization; Nuclear magnetic resonance (NMR); Electron microscopy; High pressure liquid chromatography (HPLC) Preparatory and Analytical; Mass spectrometry (MS).

IT skills: Flow-Jo; ImageJ; ChemDraw Bio; MestreNova; OriginPro; CorelDRAW; MS Office; REDCap.

PROFESSIONAL CERTIFICATIONS

Good Clinical Practice (R2) Short Course Jun 2019

London School of Hygiene and Tropical Medicine, England

Clinical Trials Administration Jul 2018

Utrecht Summer School and University of California, Netherlands

Management in Innovation and Technology Transfer

Ecole Polytechnique Fédérale de Lausanne (EPFL), Switzerland

Authorization for working *in vivo* (FELASA B)

University of Lausanne (Unil), Switzerland

LANGUAGES

Italian: Native proficiency

English: Full professional proficiency

French: Full professional proficiency

PUBLICATIONS

Graciotti, M., Berti, C., Klok, H. et al. The era of bioengineering: how will this affect the next generation of cancer immunotherapy?. J Transl Med 15, 142 (2017)